EVALUATING THE IMPACT OF AN ENHANCED ENERGY PERFORMANCE STANDARD ON LOAD-BEARING MASONRY DOMESTIC CONSTRUCTION

Partners in Innovation Project: CI 39/3/663

Interim Report Number 7 – Co-heating Tests and Investigation of Party Wall Thermal Bypass

Dr Jez Wingfield, Centre for the Built Environment, Leeds Metropolitan University

Prof Malcolm Bell, Centre for the Built Environment, Leeds Metropolitan University

Dominic Miles-Shenton, Centre for the Built Environment, Leeds Metropolitan University

Prof Bob Lowe, Bartlett School of Graduate Studies, University College London

Tim South, School of Health & Human Sciences, Leeds Metropolitan University

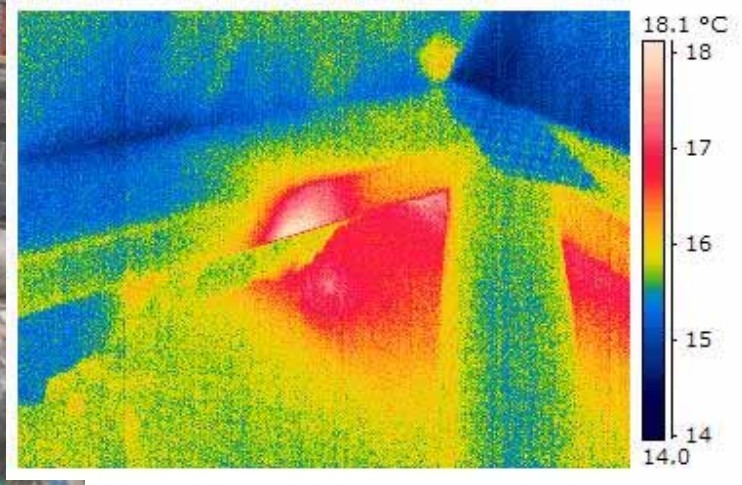

EVALUATING THE IMPACT OF AN ENHANCED ENERGY PERFORMANCE STANDARD ON LOAD-BEARING MASONRY DOMESTIC CONSTRUCTION

Partners in Innovation Project: CI 39/3/663

Milestone number: D7

Report Number 7: Co-heating Tests and Investigation of Party Wall Thermal Bypass

Report prepared by
Name: Dr Jez Wingfield
Organisation: Centre for the Built Environment, School of the Built Environment, Leeds Metropolitan University, The Northern Terrace, Queen Square Court, Leeds LS2 8AJ
Project manager: Prof Malcolm Bell
Signature
Date: May 2007

TABLE OF CONTENTS

Executive Summary

1 This report forms Deliverable 7 of the Stamford Brook PII project and details the results of co-heating tests carried out on four dwellings at Stamford Brook between January and March 2007. These tests were designed to explore the mechanism and magnitude of the thermal bypass via the party wall cavity between semi-detached and terraced dwellings and to investigate methods of blocking the bypass.

2 The heat loss attributable to the party wall cavity was found to range between 20 to 40 W/K. This is the equivalent of an effective *U*-value for the party wall of between 0.50 W/m^{2}K and 0.63 W/m^{2}K. This is in line with the value of 0.6 W/m^{2}K predicted from a theoretical analysis of stack driven air movement in the party wall cavity. This makes the party wall the building element with the second largest *U*-value after that of the windows and doors. The effective *U*-value of the party wall was more than twice the notional *U*-value of the external wall (0.23 W/m^{2}K) and around three times the notional *U*-values of the floor (0.17 W/m^{2}K) and ceiling (0.14 W/m^{2}K). We also have preliminary evidence from thermal imaging and construction observations that the real *U*-values of other elements such as walls, floors and ceilings may be higher than their notional equivalents.

3 A mineral wool-filled cavity sock positioned horizontally in the party wall cavity at the level of the ceiling insulation was partially successful in mitigating the effect of the thermal bypass and reduced the size of the effective *U*-value to between 0.1 to 0.2 W/m^{2}K.

4 Analysis of the heat loss data, cavity temperatures and air flow measurements has shown that the mechanism for heat loss via the party wall is driven by upwards air movement in the cavity. This air movement is generated by thermal stack effects and by pressure differences caused by the action of wind around the dwelling.

5 There is potential for considerable carbon savings for both newly constructed and existing dwellings built with unfilled cavity masonry party walls if measures were implemented to reduce or eliminate the party wall thermal bypass. If it is assumed that a typical cavity party wall has an effective *U*-value of 0.5 W/m^{2}K, then the potential carbon saving if the party wall bypass were eliminated in all new terraced and semi-detached cavity masonry dwellings built in the UK each year would be of the order 20,000 tonnes CO_2 per annum. The possibilities for carbon dioxide savings in the existing stock could be even more significant than that in new dwellings. If the stock of terraced and semi-detached dwellings built after 1965 had improvement measures carried out to eliminate the party wall bypass then the potential carbon saving would be of the order 850,000 tonnes CO_2 per annum. It is interesting to note that, contrary to normal expectations, one of the consequences of the party wall bypass is that terraced and semi-detached dwellings built to 2006 building regulation standards will have carbon emissions higher than that of a similarly sized detached dwelling.

6 It will be necessary to update the *U*-value calculation conventions in BR443 to allow for heat losses via thermal bypasses such as party wall cavities. It will also be necessary to amend SAP 2005 to note the potential for the party wall cavity thermal bypass and other similar bypass mechanisms. The text accompanying the catalogue of Accredited Details should be amended to include information on thermal bypassing and also to remove from the catalogue any details that are likely to give rise to thermal bypasses, such as unfilled party wall cavities.

Introduction

7 Stamford Brook is a development of around 700 cavity masonry dwellings being constructed on part of the National Trust's Dunham Massey Estate near Altrincham in Cheshire. Construction on the site commenced in 2004 and is expected to continue until around 2010. The development is being carried out under a partnership agreement between the land owner, the National Trust, and the two developers Redrow and Bryant. The development partners are also participating in a Partners in Innovation (PII) project with Leeds Metropolitan University (Leeds Met) that is investigating various aspects of the design and construction processes. This report forms Deliverable 7 of the PII project, and details the results of a second series of co-heating tests carried out between January and March 2007. These tests were carried out in response to the results from co-heating tests carried out at Stamford Brook during the winter of 2005-2006, during which a heat loss path involving the party wall cavity was identified (Wingfield, Bell, Bell & Lowe 2006). The aim of this second set of co-heating experiments was to further explore this bypass mechanism.

Background

8 An initial series of co-heating tests were conducted on two separate dwellings (One mid-terrace and one semi-detached) at Stamford Brook between December 2005 and February 2006. The main finding of these experiments was that the measured whole house heat loss coefficients in both cases exceeded the predicted values by between 75% and 103% (Wingfield et al 2006). Further analysis of the data, along with thermal imaging in the loft space and ad-hoc measurement of cavity temperatures in the party wall indicated that a large proportion of the excess heat loss could have arisen due to a thermal bypass associated with bulk air movement up the party wall cavity. A theoretical analysis confirmed that a thermal stack driven bypass in the party wall cavity could potentially give rise to significant heat loss with a magnitude equivalent to an effective single-sided party wall *U*-value in the order of 0.6 W/m^{2}K (Lowe, Wingfield, Bell & Bell 2007 & Appendix 1). The analysis also indicated that the bypass would need to be fed by cold external air entering from the bottom and sides of the cavity. A schematic of the postulated bypass mechanism is illustrated in Figure 1.

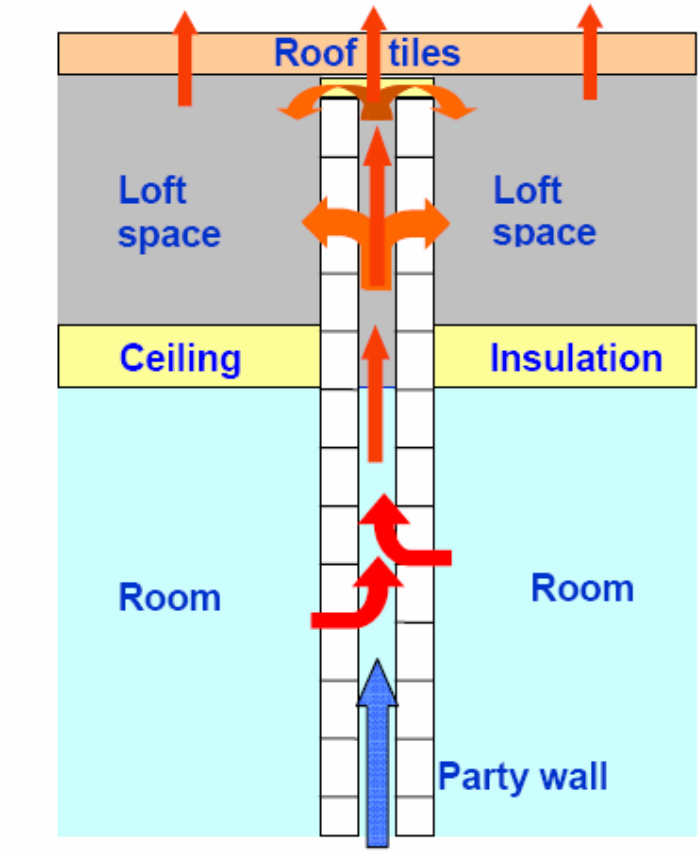

Figure 1 - Schematic of Party Wall Bypass Mechanism

9 Due to the importance of the proposed party wall bypass because of its relative size and the potential implications this could have on UK house design, building regulation and carbon emission calculation conventions, it was agreed with the project steering group to conduct a second series of co-heating tests on further newly constructed dwellings at Stamford Brook during the winter of 2006-2007. The main aim of this second series of tests was to collect more data on temperature and air flow conditions in the party wall cavity so as to establish the extent of the mechanism and to assess the effectiveness of construction techniques designed to reduce or eliminate the bypass effect.

Design of Co-heating Experiments

10 One of the major limitations of the first series of co-heating tests at Stamford Brook was that the experimental protocols were not originally designed to investigate the influence of the party wall. Consequently, heating control in those tests was only available on one side of any party wall. This complicated the analysis of the test results as it was not possible to determine the exact magnitude of the heat loss across the party wall from the test dwelling to the adjacent occupied dwelling(s) (the test dwelling would have been at a higher temperature than any adjacent occupied dwelling) when compared to the size of the heat loss via the party wall cavity bypass. In order to overcome this limitation, both developers were asked to provide a pair of adjacent attached dwellings for the second series of tests so that temperature control was possible from both sides of the party wall.

11 In order to establish the thermal conditions in the party wall cavity during the co-heating tests it was decided to install a series of thermocouples at strategic positions within the party wall cavity. The thermocouples would be placed in the party wall via small holes drilled from one side. The size of the holes also needed to be large enough to accommodate the probe of a hand-held hot-bulb anemometer, which would be used to take spot measurements of air flow within the party wall cavity. It had been hoped to measure air flow on a continuous basis, but the instrumentation costs proved prohibitive.

12 Perhaps the most important aspect of the second set of experiments was to be a demonstration of some form of construction detail built into the party wall and designed to cut-off any thermal bypass via the party wall cavity. The detail would have to be cost effective, easy to install during construction of the party wall and also not be detrimental to other performance criteria such as the acoustic properties of the party wall. The detail would also have to be installed in such a way that it could be removed part way through the co-heating test so that its effectiveness could be determined. A range of design options for the cut-off detail were proposed and discussed with the project advisory group. These options included a layer of insulation material in the cavity in line with the ceiling insulation, an inflatable air barrier or some form of sealing flap operable from outside the cavity. In the end it was decided to use a mineral wool-filled plastic-covered cavity sock of the type normally used to close the vertical junction between the party wall and external wall for fire and acoustic purposes[1]. Such cavity socks were readily available on-site and the masonry construction gangs were already familiar with them. It was proposed that the sock would be inserted in the party cavity wall at ceiling level whilst the block work was being laid. The sock could then be removed when required during the co-heating test by pulling it through openings in the party wall provided by temporarily removing blocks from appropriate locations in the party wall in the attic.

13 A summary of the original test protocols agreed for the second series of co-heating tests is given in Appendix 2. It should be noted that some changes were made to these protocols during the test programme. These changes were normally a result of delays in the build programme or technical issues that cropped up during installation of the test equipment or during the test itself. One of the main limiting factors for the test programme was the need for a reasonably high temperature difference (delta-T) of at least 15 K between the inside of the test properties and the outside temperature. This effectively meant that the co-heating tests had to be completed by the end of March, after which time the external temperatures would have been too high to maintain the required delta-T without resorting to excessive internal temperatures.

[1] A range of acoustic or fire cavity closers are available from the product ranges of all the major UK insulation and building component manufacturers. The important characteristics for this application are that the material should be resistant to the flow of air and the closer is able to conform to the shape of the block work wall so as to provide a reasonable air seal at the edges. It is not the intention of this project to recommend the use of any particular manufacturer's product but rather to demonstrate the potential benefit of sealing the party wall cavity with some form of closer.

Selection of Co-heating Test Dwellings

14 Pairs of test dwellings from each of the two developers were selected from the stock being constructed during 2006 that were scheduled for completion by the end of 2006 or by the start of 2007 at the latest. It was decided to choose pairs of adjacent dwellings that included at least one end terrace. This would mean that at least one dwelling from each pair would have only one party wall with the internal temperature being controlled both sides. In the case of Bryant the houses selected were a pair of 2-storey 3 bed semi-detached dwellings. In the case of Redrow the dwellings were a 3-storey 4 bed end-terrace and the adjacent 3-storey 4 bed mid-terrace. For both pairs of dwellings one house was designated as the test house and one the access house. The designations are given in Table 1, which also summarises the main characteristics of the dwellings. Access to the test houses was limited to very short periods necessary for sensor adjustment and thermal imaging. The access houses were used to conduct the internal experiments during the co-heating tests. The holes in the party walls for the thermocouples were drilled from the access house side. Air flow measurements were conducted from the access houses. The data logger was located in the access houses. Platforms were erected in the lofts of the access houses to enable safe access to the party wall in the loft.

Table 1- Details of Co-heating Test Dwellings

Developer	Plot No.	Access House or Test House Designation	Developer House Type	Form	Gross Floor Area (m^2)	Volume (m^3)	Plan Aspect Ratio	Glazing Ratio (window area/ GFA)	General Orientation of Main Facade
Bryant	116	Test House	Chatsworth	Semi	73	200	1.6	0.17	West Facing
Bryant	117	Access House	Chatsworth	Semi	73	200	1.6	0.17	West Facing
Redrow	110	Access House	Mendip	Mid-terrace	137	356	1.7	0.16	North Facing
Redrow	111	Test House	Mendip (with bay window)	End-terrace	141	365	1.7	0.16	North Facing

15 Photographs of the completed co-heating test houses are illustrated in Figures 2 and 3. Plan, elevation and section drawings for the two different house types are given in Appendix 4.

Figure 2 - Redrow Plots 110 and 111

Figure 3 - Bryant Plots 116 and 117

Summary of Co-heating Test Methodology

16 The co-heating test procedure is described in more detail in Appendix 3. The original specification for the co-heating tests is given in Appendix 2. The sequence of activities for the co-heating tests was as follows:

a) Conduct acoustic test of party wall between the test dwellings. The horizontal cavity sock in the party wall would be in position at this point. (The acoustic test was not actually carried out on the two Bryant properties due to time limitations).

b) Conduct airtightness pressure test of both test dwellings.

c) Drill holes for thermocouples in party wall and install all fan heaters, fans, kWh meters, temperature sensors and datalogger.

d) Conduct first half of co-heating test with horizontal cavity sock in position. Take cavity airflow measurements at regular intervals.

e) Drill out mortar around appropriate blocks in the attic party wall in the attic and remove horizontal cavity sock by pulling through the holes. Replace blocks and fill gaps with mineral wool and tape over the joints.

f) Conduct second half of co-heating test with horizontal cavity sock removed. Take cavity airflow measurements at regular intervals.

g) Remove fan heaters, fans, kWh meters, temperature sensors and datalogger. Plug thermocouple holes in the party wall using wooden dowels.

h) Conduct second acoustic test of party wall between the test dwellings. (Second acoustic test was not actually carried out on the two Bryant properties due to time limitations).

i) Conduct second airtightness pressure test of both test dwellings. (Second pressure test was not actually carried out on Bryant plot 117 due to time limitations).

Location of Internal Temperature and Humidity Sensors

17 The locations of the temperature/humidity sensors used to measure the internal condition of the heated space of the four test dwellings and the also condition in the lofts of the test dwellings are summarised in Table 2.

Table 2 - Location of Internal Temperature/Humidity Sensors

	Bryant Plot 116	**Bryant Plot 117**	**Redrow Plot 110**	**Redrow Plot 111**
Temp/Humidity Sensors in Internal Heated Space	GF Kitchen GF Living Room FF Master Bedroom FF Bedroom 2	GF Kitchen GF Living Room FF Master Bedroom FF Bedroom 2	GF Kitchen FF Living Room FF Bedroom 1 SF Bedroom 2 SF Bedroom 3	GF Kitchen FF Living Room FF Bedroom 1 SF Bedroom 2 SF Bedroom 3
Temp/Humidity Sensors in Loft Space	Next to Loft Hatch 1m above Hatch 2m above Hatch Ridge above Hatch	Next to Loft Hatch 1m above Hatch 2m above Hatch Ridge above Hatch	Next to Loft Hatch 1.5m above Hatch Ridge above Hatch	Next to Loft Hatch 1.5m above Hatch

Thermocouple Locations & Air Flow Measurement Method

18 The temperatures in the party wall cavity during the co-heating test were measured using type-K thermocouples. These were inserted into the party wall via 10 mm holes drilled through the party wall on the access house side. The thermocouples were positioned such that the probe tips were in the centre of the cavity. The thermocouple wires were taped down to stop them moving and the holes were sealed using polyurethane foam stoppers. The locations of the sensors in the walls are

illustrated by the house sections shown in Figures 4 and 5 (locations shown with red X). Some adjustment had to be made to the location of the sensors in the Redrow dwellings compared to that envisaged in the original test specification (Appendix 2). This was due to limitations in placement of the sensors caused by walls, kitchen and bathroom fittings and restrictions due to the length of the thermocouple wires. A photograph showing the holes and thermocouple wires in position in one of the co-heating test houses is illustrated in Figure 6.

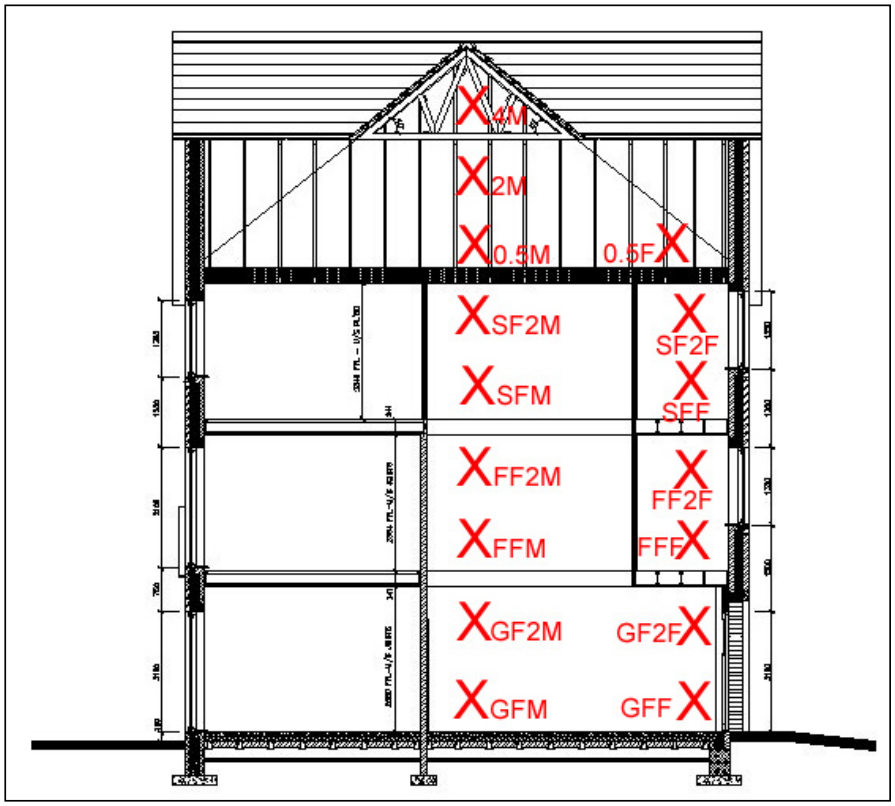

Figure 4 - Thermocouple Locations (X) in Party Wall Cavity Redrow 110-111

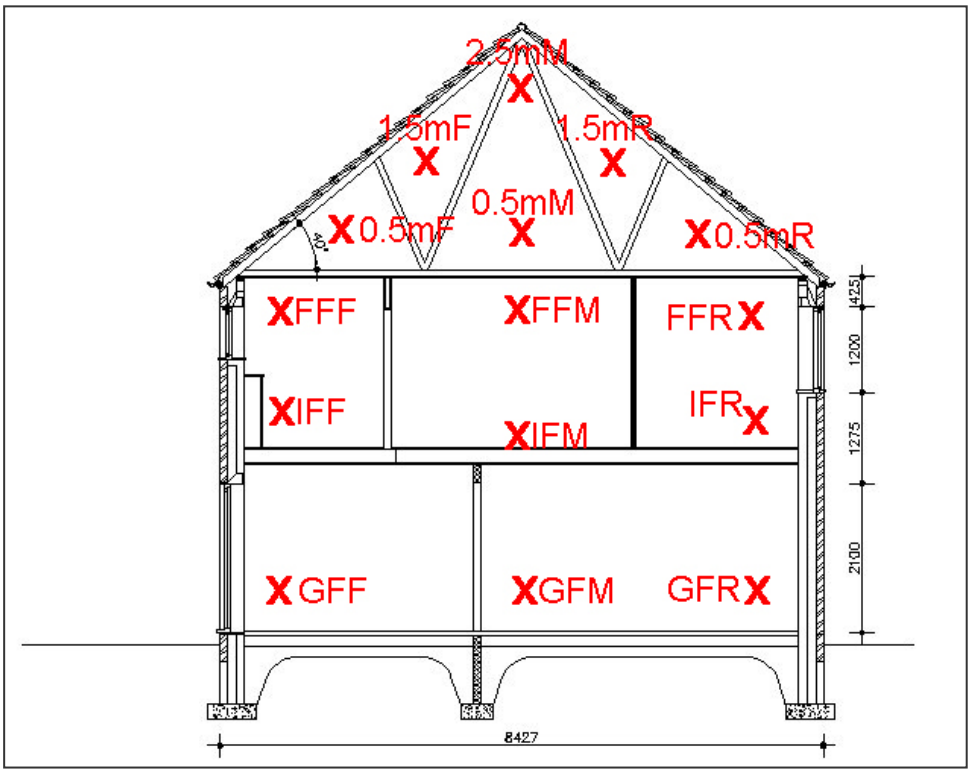

Figure 5 - Thermocouple Locations (X) in Party Wall Cavity Bryant 116-117

19 Air flow measurements in the party wall cavity (in m/s) were taken at regular intervals during the co-heating test using an Airflow TA35 hot bulb anemometer. The thermocouples were temporarily removed from the holes in the party wall and the anemometer probe inserted through the hole and the sensor head positioned so that it was in the centre of the party wall cavity. Maximum and minimum readings over a period of 30 seconds were taken with the anemometer sensor cowl oriented in both the horizontal and vertical planes in order to give air flow measurements horizontally and vertically through the cavity. A photograph of an air flow measurement being undertaken during the Redrow co-heating test is shown in Figure 7.

Figure 6 - Thermocouples in Position in Party Wall

Figure 7 - Researcher Taking Cavity Air Flow Measurements through Hole in Party Wall

Installation of Horizontal Cavity Socks

20 Mineral wool-filled cavity socks were used to seal the horizontal space in the party wall cavity at the level of the ceiling insulation. The location of the sock is illustrated in sections through the Bryant and Redrow co-heating houses shown in Figure 8. The cavity socks were 1.2m long by 240mm wide by 150mm thick. Each sock consisted of two 75mm thick mineral wool batts covered by a green polythene sleeve sealed at both ends. It was necessary to use several socks to completely fill the length of cavity. A photograph of the socks being installed in the Bryant dwellings is given in Figure 9. The socks were closely butted together to minimise any air leakage between them, and

were extended across the ends of the cavity so that they met the vertical acoustic/fire cavity closer, as shown in Figure 10. In the case of the Bryant dwellings, the party wall cavity was 142mm wide which could be easily filled with the sock. The party wall cavity in the Redrow test properties was narrower at 75mm, and it was necessary to remove one of the two mineral wool batts from each sock so that it would fit snugly in the cavity.

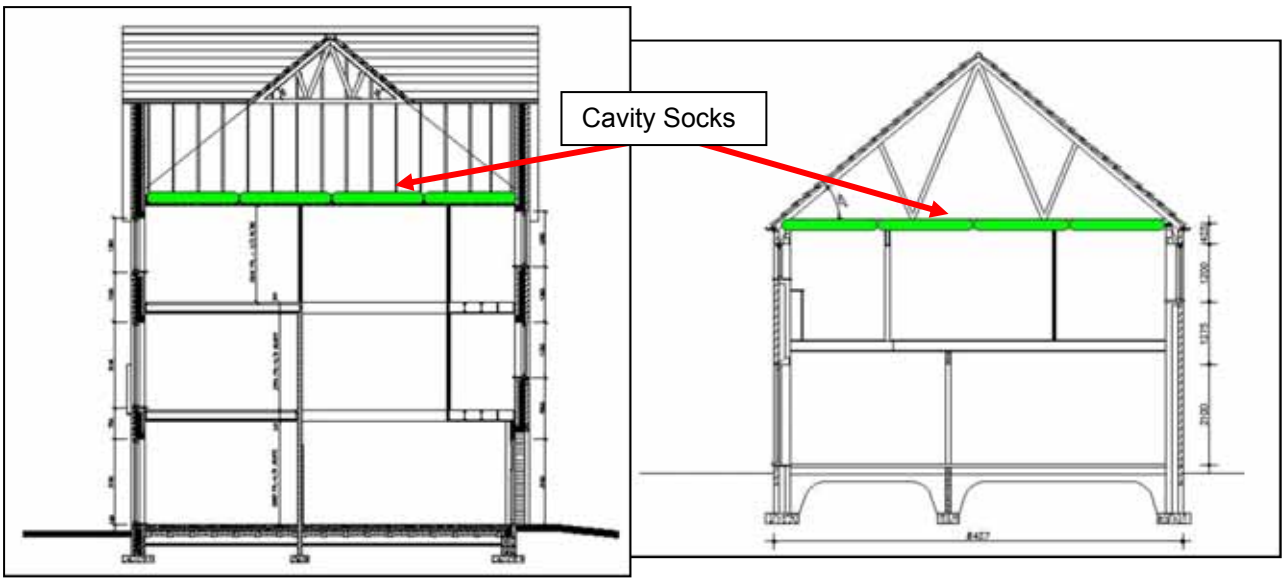

Figure 8 - Sections Showing Location of Horizontal Cavity Socks in Party Wall Cavities

Figure 9 - Installation of Cavity Socks

21 The masonry gangs were asked to protect the top of the horizontal sock from mortar that might be dropped into the cavity as they continued construction of the party wall to the roof line. This was achieved using a wooden board laid over the top of the sock as shown in Figure 11.

Figure 10 - Junctions between Horizontal and Vertical Cavity Socks in Bryant Test Dwellings

22 In order to facilitate easy removal of the socks part way through the co-heating test, a number of blocks in the party wall adjacent to and just above the position of the sock were only partially mortared in. This was in order to minimise the amount of mortar that would need to be removed by drilling. An example of one of these blocks is shown in Figure 12.

Figure 11 - Sock Protected from Mortar Snots

Figure 12 - Removable Block in Party Wall

Removal of Horizontal Cavity Socks

23 The horizontal cavity socks were removed from the party wall cavity halfway through the co-heating test on both pairs of dwellings. The remaining mortar was drilled from around the designated blocks in the party wall in the lofts of the access houses as illustrated in Figure 13. The blocks were

removed from the wall (Figure 14) and the cavity socks were pulled out from the cavity (Figure 15). Following removal of the socks, the blocks were replaced in the party wall, any gaps filled with mineral wool and the joints taped over as shown in Figure 16. The co-heating test was then continued to completion. It should be noted that in the case of both pairs of dwellings it took two sessions over a period of two days to completely remove the socks. This was due to the time taken to drill out the mortar, difficulties in accessing the sock (especially in the narrower Redrow cavity), and problems caused by mortar snots on top of the sock that in effect glued the socks to the walls of the cavity.

Figure 13 - Drilling out Mortar around Block

Figure 14 - Removing Block

Figure 15 - Removing Cavity Sock

Figure 16 - Block Replaced and Joints Taped Over

Results of Co-heating Tests

Internal Temperatures in Test Dwellings

24 Plots of the mean internal temperatures during the co-heating test in Bryant plots 116 and 117 are illustrated in Figure 17 and for Redrow plots 110 and 111 are shown in Figure 18. In both cases the graphs also show the external temperature for comparison. Both plots show that the internal

temperatures of the adjacent test dwellings were very similar and also relatively stable at around 25 to 26 °C in the case of the Bryant properties and around 27-28°C in the case of the Redrow houses. There were some short term spikes in the temperatures of plots 110 and 111. These were associated with solar gain via the windows on the west facing rear façade of the properties in the afternoon which could not be compensated for by the relatively crude temperature control system.

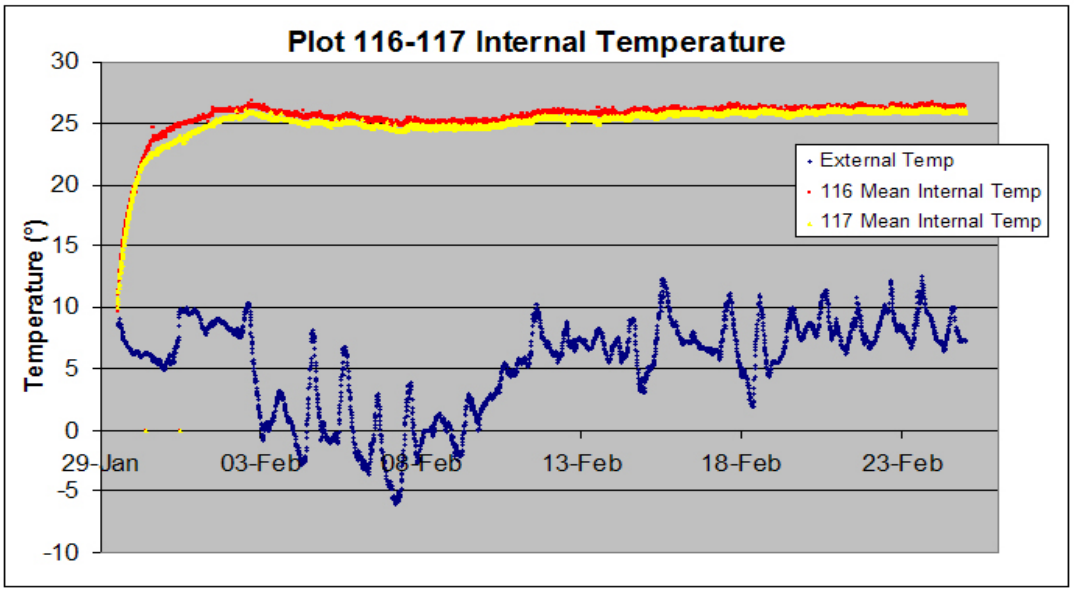

Figure 17 - Internal and External Temperatures during Co-heating Test Bryant Plots 116-117

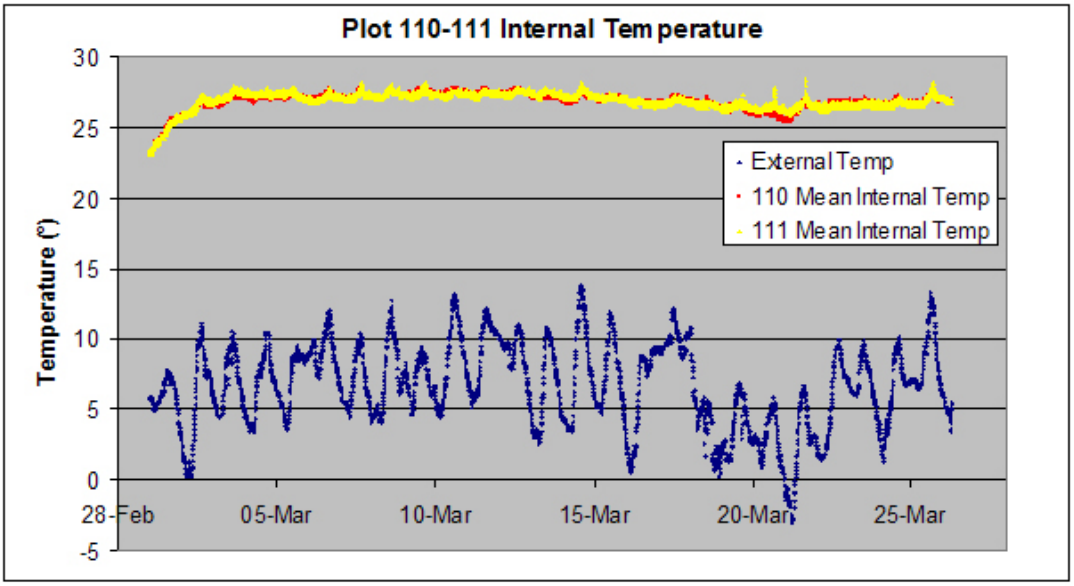

Figure 18 - Internal and External Temperatures during Co-heating Test Redrow Plots 110-111

Temperatures in Party Wall Cavity

25 Plots of the party wall cavity temperatures for Bryant plots 116-117 are shown in Figure 19 for the thermocouple sensors below the level of the ceiling insulation and in Figure 20 for the sensors above the level of ceiling insulation. On each plot an arrow indicates the period during which the horizontal cavity socks were removed from the party wall cavity. It can be seen that in the case of the temperatures below the ceiling before sock removal, those at the top of the cavity were around 23 to 25°C which was almost isothermal with the internal temperature in both dwellings. The temperatures at the bottom of the cavity were much lower at around 20°C and showed a response to fluctuations in external temperature. Following removal of the horizontal sock, all the cavity

temperatures below the ceiling showed a general reduction (the delta-T between cavity and outside decreases from around 20-25 K to around 10-15K) and also become more variable. This indicated that they were responding to changes in external conditions, perhaps due to greater air movement from outside into the cavity. It can also be seen that when the sock was first removed on the 12th February, there was a significant reduction in the temperature at the bottom of the cavity at position GFF. This would suggest that there is a large gap in the vertical cavity sock[2] in the vicinity of this sensor, giving rise to a large flow of cold air from outside.

Figure 19 - Sensor Key

GF-F	Ground Floor Front
GF-M	Ground Floor Middle
GF-R	Ground Floor Rear
IF-F	Intermediate Floor Front
IF-M	Intermediate Floor Middle
IF-R	Intermediate Floor Rear
FF-F	First Floor Front
FF-M	First Floor Middle
FF-R	First Floor Rear

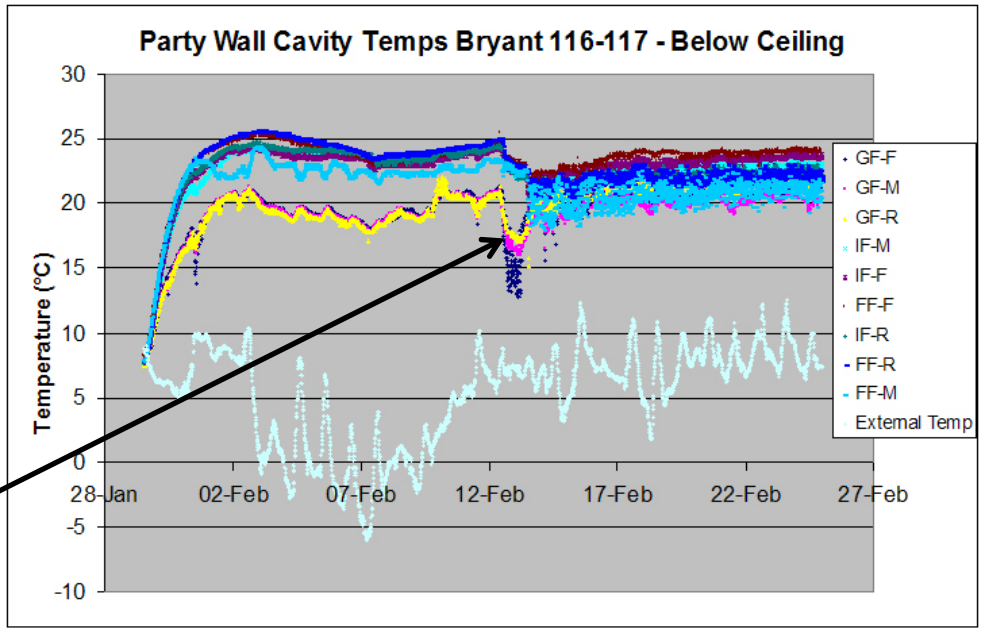

Figure 19 - Party Wall Cavity Temperature below Ceiling Bryant Plots 116-117

26 In the case of the cavity in Bryant 116-117 above the level of the ceiling (Figure 20), the cavity temperatures increased significantly following removal of the horizontal sock. This is indicative of air flow and heat flow upwards from the cavity commencing once the sock barrier had been removed. The temperatures in the cavity above the ceiling after sock removal ranged from around 17 to 21°C, which indicates that the upwards heat flow is significant.

Figure 20 - Sensor Key

Loft 0.5 F	Front 0.5m above ceiling
Loft 0.5 M	Middle 0.5m above ceiling
Loft 0.5 R	Rear 0.5m above ceiling
Loft 1.5 M	Middle 1.5m above ceiling
Loft 1.5 R	Rear 1.5m above ceiling
Loft 2.5 M	Middle 2.5m above ceiling

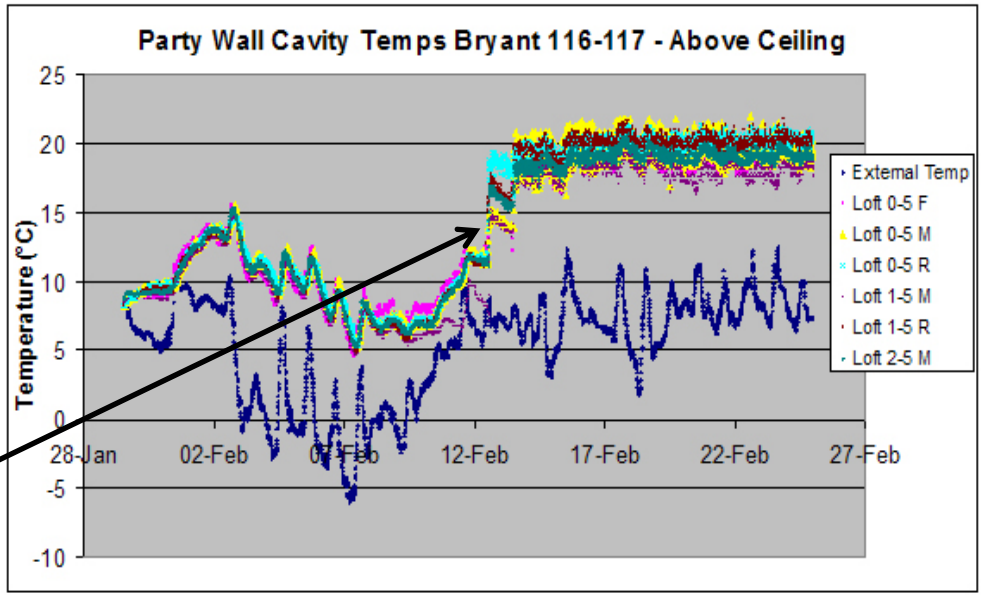

Figure 20 - Party Wall Cavity Temperature above Ceiling Bryant Plots 116-117

[2] A mineral wool filled cavity sock is positioned at the vertical junctions between any party wall cavity and the external cavity. Its purpose is to form a fire barrier between dwellings and to prevent flanking sound transmission between dwellings via the external cavity.

27 Plots of the party wall cavity temperatures for Redrow plots 110-111 are shown in Figure 21 for the thermocouple sensors below the level of the ceiling insulation and in Figure 22 for the sensors above the level of ceiling insulation. Again, on each plot an arrow indicates the period during which the horizontal cavity socks were removed from the party wall cavity.

28 It can be seen in Figure 21 that, after the heat up period and before sock removal, the cavity temperatures below the ceiling ranged from 24 to 27°C. Those towards the top of the cavity are effectively isothermal with the internal dwelling temperatures of 27°C. The fact that there is a stratification of temperatures within the cavity again suggests that there is air flow from outside into the cavity from the sides or the bottom. There will also be some conductive heat loss to the ground at the bottom of the cavity. Following removal of the sock there is a significant reduction in all party wall cavity temperatures. In some cases this fall in temperature is dramatic, as is the case with sensors on the second floor at the front of the dwelling. This drop in temperature indicates a significant change in the air flow conditions within the cavity. It can also be seen that before sock removal the cavity temperatures were relatively stable with respect to fluctuations in external temperature, although there is some indication that those at the bottom of the cavity showed small perturbations that matched the external trend. After sock removal there are significant temperature fluctuations in all cavity temperatures below ceiling level that, in general, follow the external trend.

Figure 21 - Sensor Key

GFM	Ground Floor Middle
GFF	Ground Floor Front
GF2M	Ground Floor Middle 2
GF2F	Ground Floor Front 2
FFM	First Floor Middle
FFF	First Floor Front
FF2M	First Floor Middle 2
FF2F	First Floor Front 2
SFM	Second Floor Middle
SFF	Second Floor Front
SF2M	Second Floor Middle 2
SF2F	Second Floor Front 2

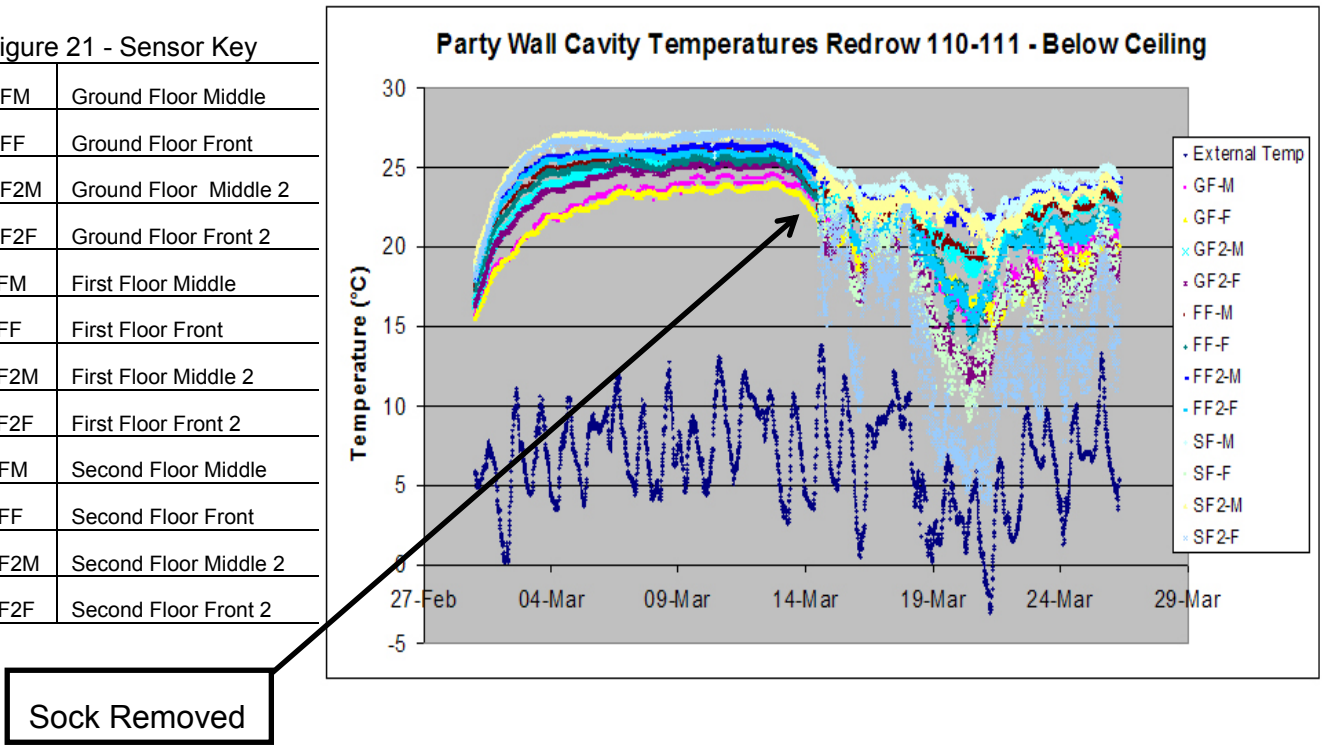

Figure 21 - Party Wall Cavity Temperature below Ceiling Redrow Plots 110-111

29 It can be seen in Figure 22 that the party wall cavity temperatures above the ceiling and before sock removal were only just slightly above external temperature (by between 1 an 5°C depending upon the time of day) and fluctuated in line with the external trend. Upon removal of the horizontal cavity sock the cavity temperatures increased significantly and the difference between the cavity temperatures and external temperatures increased to between 10 and 15°C. Again this is indicative of significant heat flow upwards in the party wall cavity once the horizontal sock had been removed. The heat flow would have to be driven by a temperature difference between the internal spaces either side, and the air in the cavity. This heat would then flow upwards in the cavity and would need to be associated with the flow of cold external air entering the party wall cavity from the bottom or the sides of the cavity. It is also interesting to note that the trend in fluctuation of the cavity temperature above the ceiling and after sock removal is the opposite of the trend in external temperature (i.e. as the external temperature goes down the party wall cavity temperature goes up and visa versa). This is further evidence for heat flow when the sock is removed that is ultimately derived from the heated spaces in the dwellings.

Figure 22 - Sensor Key

Loft 0.5M	Middle 0.5m above ceiling
Loft 0.5F	Front 0.5m above ceiling
Loft 2M	Middle 2m above ceiling
Loft 4M	Middle 4m above ceiling

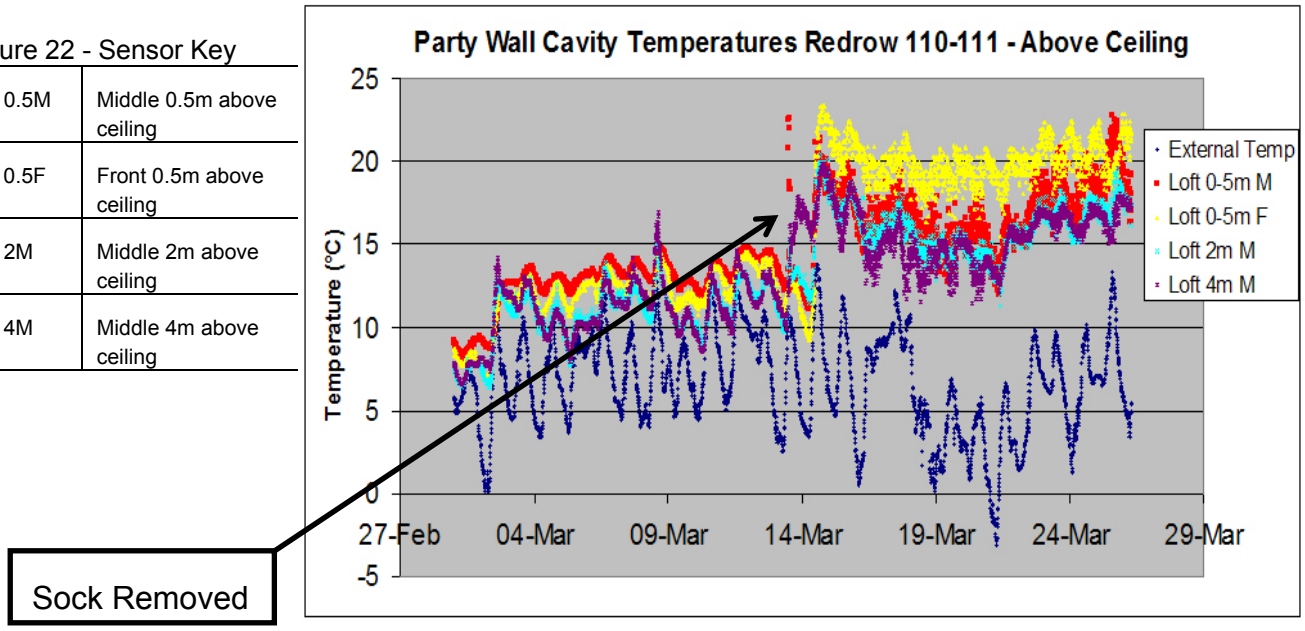

Figure 22 - Party Wall Cavity Temperature above Ceiling Redrow Plots 110-111

Heat Flux into Party Wall Cavity

30 The daily mean heat flux (W) from the inside of the test properties into the party wall cavity below the level of ceiling insulation was calculated for both sides of the party wall for both pairs of dwellings. The flux was calculated from the product of the area of party wall (60 m^2 for the Redrow properties and 39 m^2 for the Bryant plots), the *U*-value of the party wall leaf dividing the internal space from the cavity (2.1 W/m^2K) and the difference between the mean internal temperature and the mean cavity temperature. Plots of daily heat flux over the test period are shown in Figure 23 for Bryant plots 116-117 and in Figure 24 for Redrow plots 110-111. The daily mean external temperatures and sock removal dates are also indicated on the graphs.

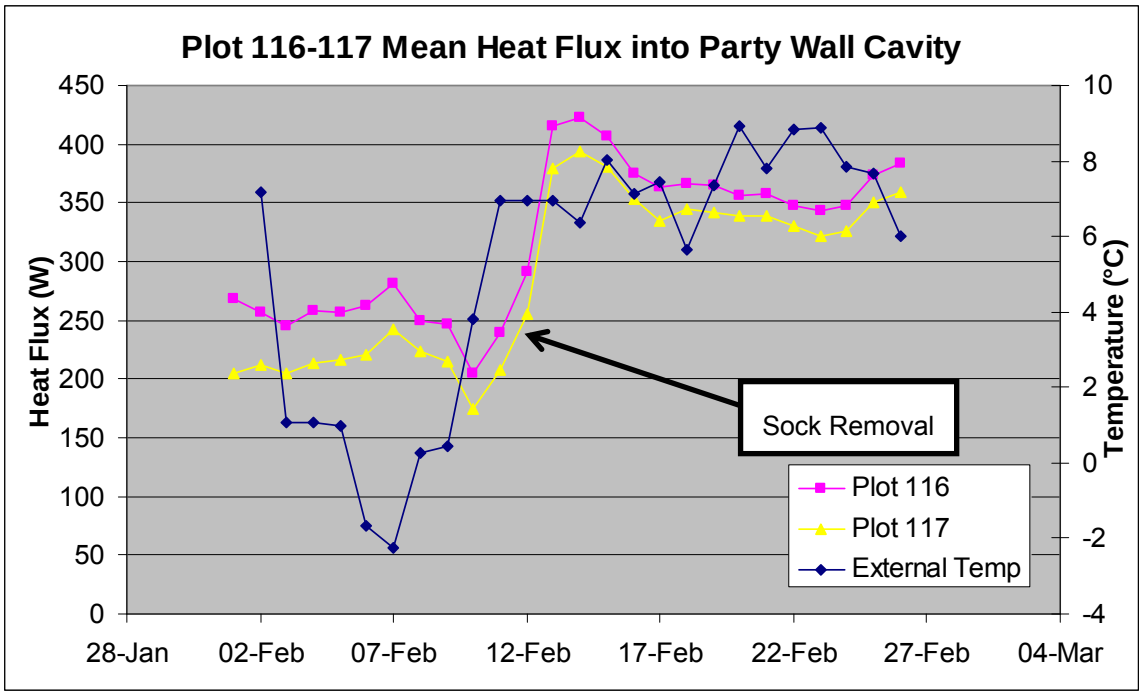

Figure 23 - Daily Mean Heat Flux into Party Wall Cavity - Bryant Plots 116-117

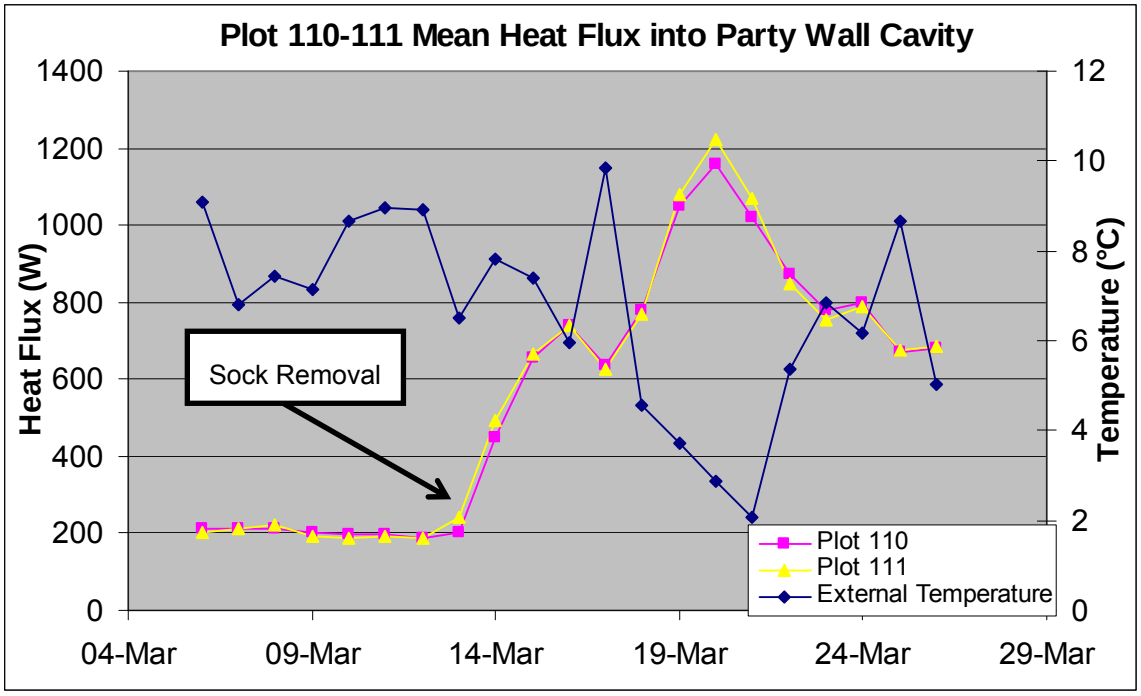

Figure 24 - Daily Mean Heat Flux into Party Wall Cavity - Redrow Plots 110-111

31 It can be seen in Figures 23 and 24 that for both pairs of test dwellings there was a significant increase in heat flux into the party wall cavity after the horizontal cavity sock had been removed. It is also apparent that, following sock removal, the size of heat flux was proportional to the external temperature. This was especially evident in the case of the Redrow houses as illustrated by the scatter plot of daily mean party wall heat loss coefficient versus mean delta-T (internal-external temperature difference) shown in Figure 25. This indicates that heat loss via the party wall cavity is in some way driven by external conditions, for example by wind effects, and that cold air from the outside environment may be entering the cavity at some point.

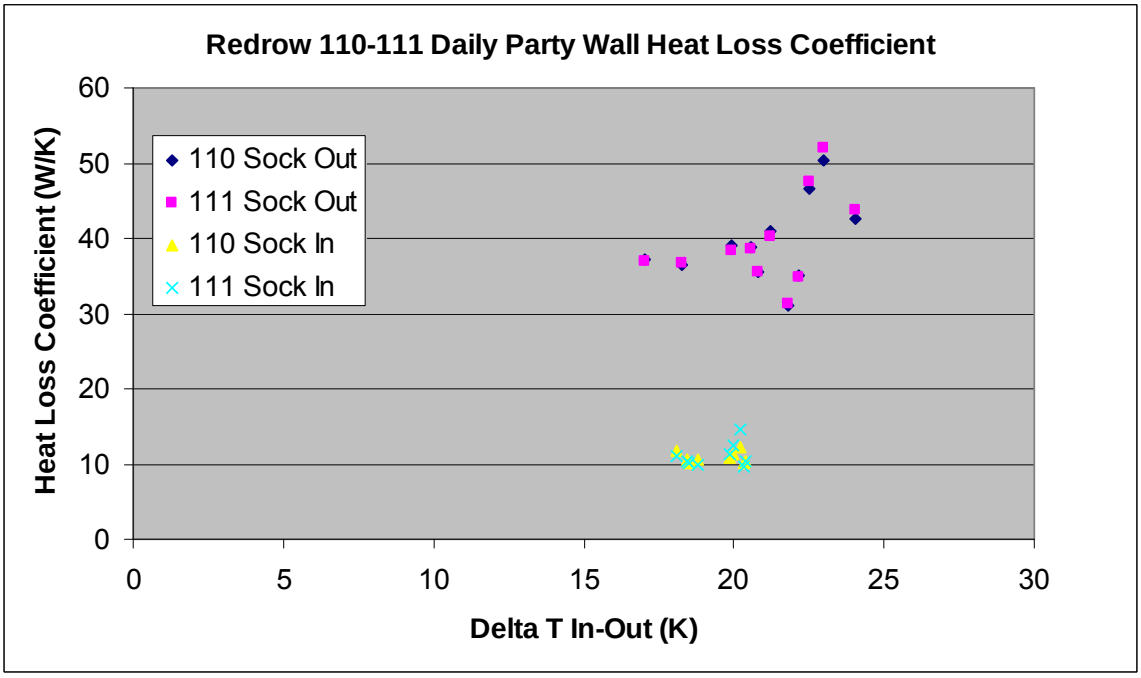

Figure 25 - Scatter Plot of Party Wall Heat Loss Coefficient versus Delta-T

32 The mean single-sided party wall heat loss coefficients (in W/K) were calculated for both pairs of dwellings for the test periods before and after removal of the horizontal cavity sock. The results are shown in Table 3. The overall heat loss for each party wall will actually be twice the value given in the table as it would include heat loss from both sides. The heat loss coefficients were used to calculate an effective single-sided *U*-value for the party wall, taking into account the area of the party walls. These *U*-values are also given in Table 3. It can be seen in both cases that there is a significant increase in the party wall heat loss coefficient upon removal of the horizontal cavity sock by around 100% for the Bryant properties and around 300% for the Redrow dwellings. There is a corresponding increase in the effective *U*-values for the party wall.

Table 3 - Party Wall Heat Loss Coefficients and Effective Party Wall *U*-value

Test Dwellings	**Mean Party Wall Heat Loss Coefficient (W/K)**		**Effective Single-Sided Party Wall *U*-value (W/m^{2}K)**	
	Before Sock Removal	**After Sock Removal**	**Before Sock Removal**	**After Sock Removal**
Bryant 116-117	10.1	19.2	0.26	0.50
Redrow 110-111	10.7	37.9	0.18	0.63

33 Interestingly, with the sock in position the heat loss via the party walls in both cases was still around 10 W/K, showing that the horizontal sock has not completely eliminated heat loss via the party wall. Some of this residual heat loss could still be going via the vertical bypass, for example, if there were gaps at the junctions between the individual socks, gaps at the junction between the horizontal sock and vertical socks or if the edges of the horizontal sock were not fully sealed against the blockwork of the party wall. It is almost certain that there is a conductive heat loss path to the ground via the uninsulated space at the bottom of the cavity. There is also likely to be some heat loss due to horizontal air movement across the party wall cavity resulting from wind induced pressure differences between front and back facades of the adjacent houses. This will occur because the vertical cavity closers do not properly seal the side edges of the party wall cavity at the junction with the cavity in the external wall.

34 The measured effective *U*-value of the party wall at between 0.50 W/m^{2}K and 0.63 W/m^{2}K is in line with the value of 0.6 W/m^{2}K predicted by the authors from a theoretical analysis of stack driven air movement in the party wall cavity (Lowe Wingfield Bell & Bell 2007). The effective *U*-values are also in the range of 0.4 to 0.8 W/m^{2}K suggested by Siviour in his analysis of direct flux measurement and thermal imaging of in-situ party walls (Siviour 1994).

Loft Temperatures

35 The first series of co-heating tests indicated that loft temperatures could be used as an indicator of the party wall bypass. This was possible because solar insolation during the majority of the testing period was negligible due to extended periods of overcast weather and also the external temperatures were generally very low during the winter of 2005-2006. The loft temperatures during the second series of tests in 2006-2007 were influenced to a much greater degree by both solar and wind effects and it proved difficult to identify any trends in loft temperature that might have been caused by any thermal bypass via the party wall cavity.

36 The loft temperature difference ratio (TDR = (loft temp-external temp)/(internal temp-external temp)) was calculated for all the test dwellings and no discernable difference could be identified before and after removal of the horizontal cavity sock. Graphs of daily loft temperature difference ratios during the test period are given for Redrow plot 111 in Figure 26 and for Bryant plot 116 in Figure 27. The date that the horizontal cavity sock was removed is indicated on both graphs. In can be seen that in both cases there is no obvious change in the pattern of the loft temperature difference ratio before and after sock removal and that the general trend in the loft TDR roughly follows that of the magnitude of the solar insolation.

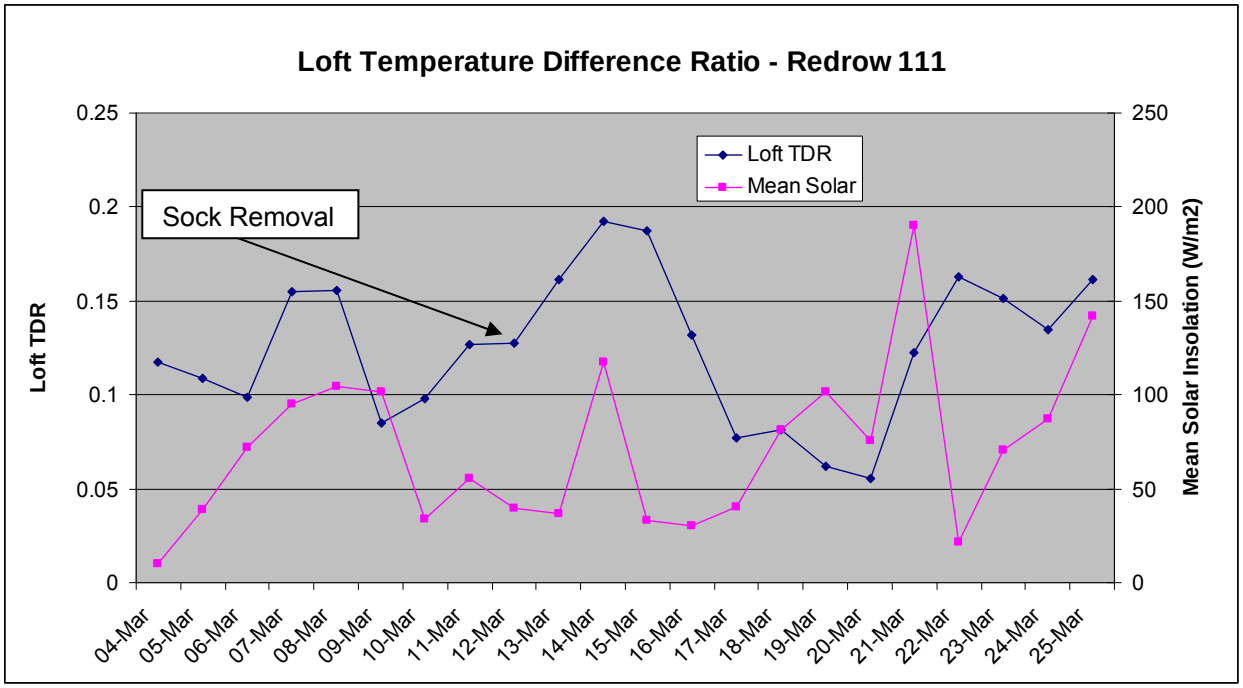

Figure 26 – Loft Temperature Difference Ratio Redrow Plot 111

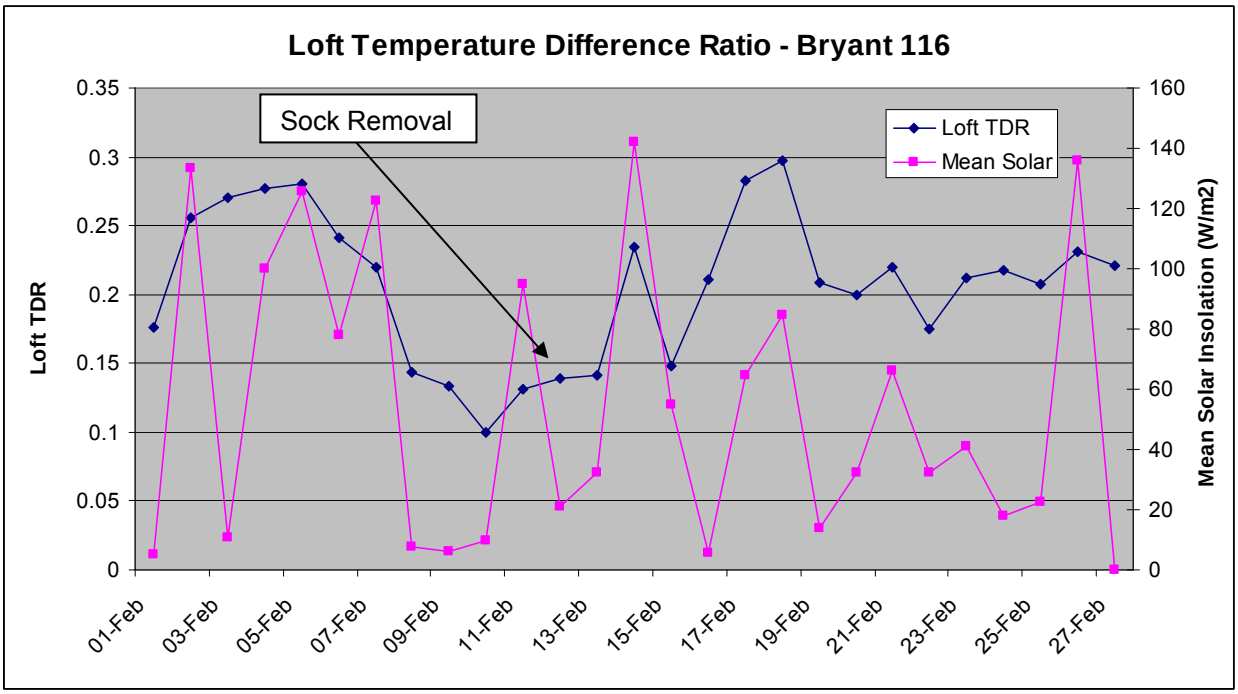

Figure 27 – Loft Temperature Difference Ratio Bryant Plot 116

Heat Loss Measurements

37 It was originally envisaged when setting up the second series of co-heating tests that it should be possible to determine the difference between the whole house heat loss coefficient with the horizontal cavity sock in place and the coefficient with the sock removed. In order to do this, the research team expected that it would be necessary to have two to three weeks worth of heating data either side of the sock removal dates in order to minimise the influence of confounding effects such as solar gain, wind driven ventilation losses and large external temperature fluctuations that might otherwise mask any changes. However, due to delays in the construction programme it was only possible to run the tests for around one and a half weeks either side of the sock removal

dates. The consequence of this is that the whole house heat loss data are much more difficult to interpret.

38 The heat loss coefficients were calculated for all four dwellings on a rolling hourly basis in order to capture heat loss fluctuations across the day in response to external conditions. The data for Bryant plots 116 and 117 are shown in Figure 28 and for Redrow plots 110 and 11 in Figure 29. Also shown on the plots are the removal date for the horizontal cavity sock and the hourly mean wind speed (m/s).

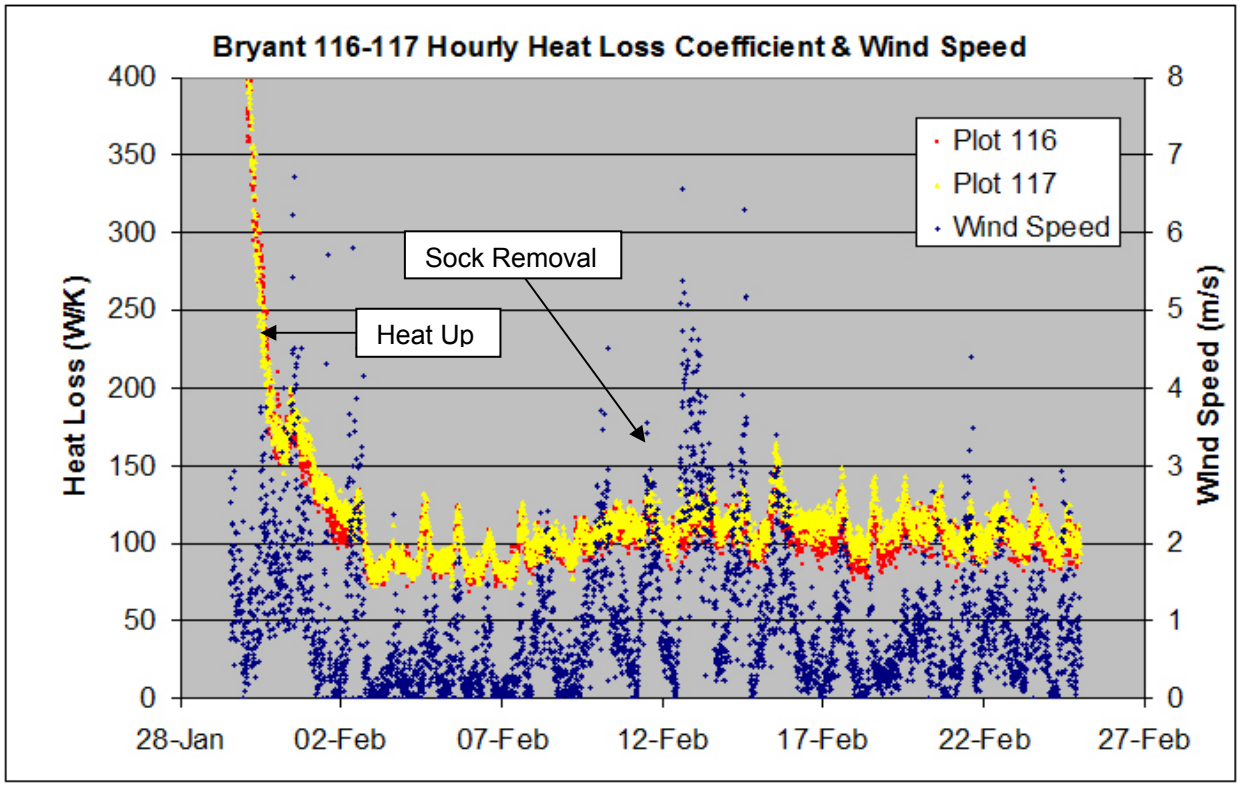

Figure 28 – Hourly Heat Loss Coefficient Bryant Plots 116-117

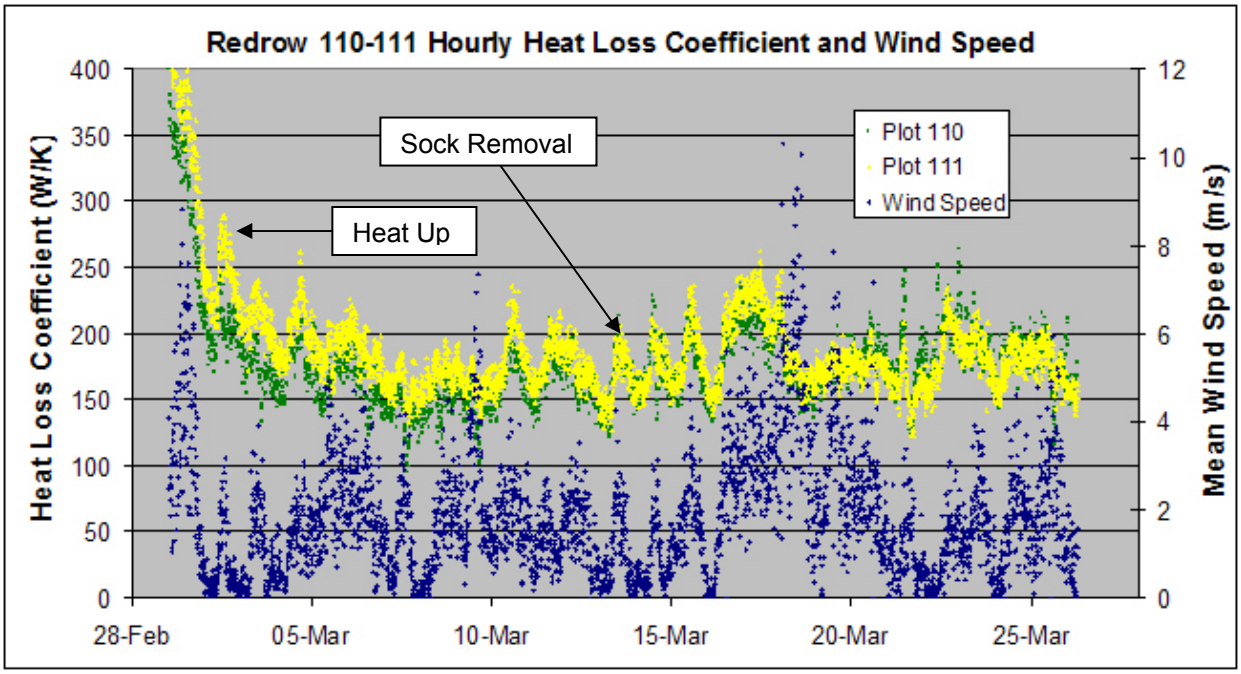

Figure 29 – Hourly Heat Loss Coefficient Redrow Plots 110-111

39 It can be seen from Figures 28 and 29 that the diurnal variation in the whole house heat loss coefficient ranged from around 50 W/K to as much as 100 W/K. The general trend in heat loss matches to a certain degree the trend in wind speed, although there are times when increases in wind speed are not matched with a corresponding increase in heat loss. It would be expected that increased wind speed would give rise to an increase in background ventilation loss. In the case of the two Bryant properties, it is possible to discern a slight increase in heat loss coefficient of around 10 to 20 W/K after the cavity sock had been removed. However, it was much more difficult to identify any change in heat loss following sock removal in the case of the two Redrow dwellings. It is apparent that the external wind effects are overwhelming any differences that might be due to any thermal bypass via the party wall. Part of the problem lies with the relatively high internal temperatures which will exacerbate stack driven ventilation losses. The stack effect will be enhanced even further in the case of the 3-storey Redrow properties. It is also likely that there are wind driven losses, even with the horizontal sock in position, however, the air flow in the cavity wall bypass is probably driven mainly by inside-outside temperature difference.

40 In the first series of co-heating tests a multiple regression analysis was used to allow for the effect of solar gain (Wingfield et al 2006) in the calculation of the mean heat loss coefficient for the dwellings. Similar multiple regression calculations were attempted for the second set of tests to allow for the influence of both solar gain and wind driven ventilation losses. However, the data were such that it was not possible to derive regression terms with a sufficiently high r^2 coefficient of determination that would give confidence in the results. For the pair of Bryant dwellings it was possible to determine heat loss coefficients before and after sock removal using the raw uncorrected power and temperature data as shown in Figures 30 and 31. Least squares trend lines through the raw data (trend lines forced through origin) indicate a difference in the heat loss coefficient before and after horizontal sock removal of between 10 and 15 W/K. This difference is of the same order of magnitude as the difference of 20 W/K calculated from the heat flux into the party wall cavity shown in Table 3.

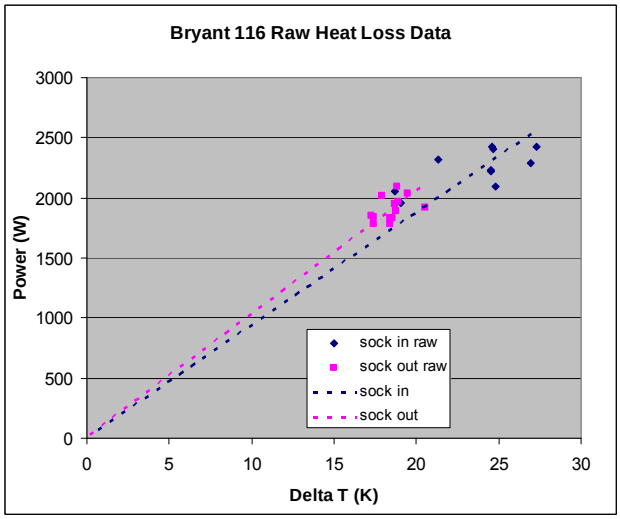

Figure 30 – Power versus Delta-T Bryant 116

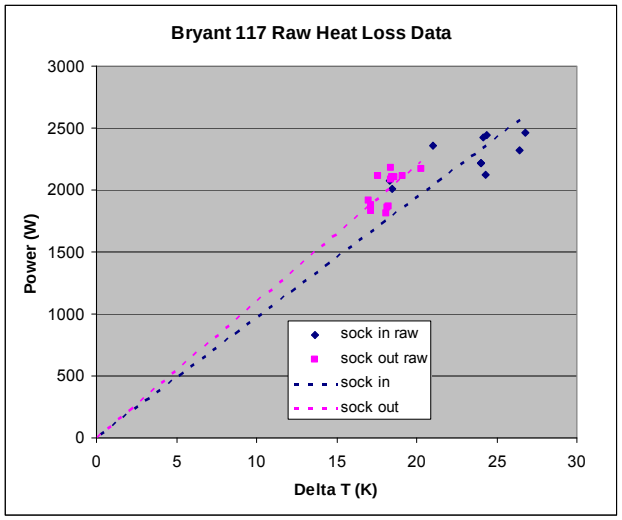

Figure 31 - Power versus Delta-T Bryant 117

41 The magnitude of the raw data heat loss coefficients for Bryant 116 and 117 without the horizontal sock ranged from 102.9 W/K for 116 and 109.9 W/K for 117. These values are reassuringly close to the value the unadjusted heat loss coefficient of 105.4 W/K reported in deliverable 5 for Bryant plot 13 which was constructed using the same Chatsworth semi-detached house design (Wingfield et al 2006). This gives confidence that the co-heating test methodology gives broadly repeatable test results for the same house type with identical designed fabric performance.

Air Flow Measurements

42 Air flow readings in the party wall cavity were found to be extremely variable over the measurement period of around 30 seconds. In general, the measured flow rate appeared to increase in response to increasing external wind speed and would then fall again as external wind speed decreased. The overall air flow rates and the degree of fluctuation were more significant in both pairs of test dwellings during the period when the sock had been removed. Indeed, in some locations in the party wall cavity, air flows in excess of 1 m/s were recorded when the sock had been taken out.

Given the limited amount of data available for the analysis, it was believed that the maximum air flow readings were more likely to give an indication of the overall differences in flow conditions with and without the horizontal cavity sock in position in the party wall cavity. Schematics of the party wall cavity are given in Figures 32 and 33 which compare maximum air flow during periods when the external wind conditions were broadly similar (wind gusting from around 1 to 5 m/s). The air flow maxima are illustrated using different sized arrows at the various measurement points. The size of the arrow relates to the maximum measured flow in the following ranges: 1. No flow, 2. (>0 to <0.1 m/s), 3. (0.1 to <0.25 m/s), 4. (0.25 to <0.5 m/s) and 5. (>0.5 m/s). It can be seen from these diagrams that there was a significant increase in maximum air flow in the party wall cavity in both pairs of dwellings once the horizontal sock had been removed from the cavity. This indicates that the horizontal sock had been partially successful in the intended aim of reducing air flow upwards in the cavity past the line of the ceiling insulation. However, a certain level of both horizontal and vertical air flow could still be measured with the sock in position. This suggests that there were some gaps in the horizontal sock in the party wall cavity and that also there were likely gaps in the vertical socks in the external cavities. The effect of this air movement would be to induce heat losses even with the socks in place, a point reinforced by the heat flux calculations indicated in paragraph 30 above.

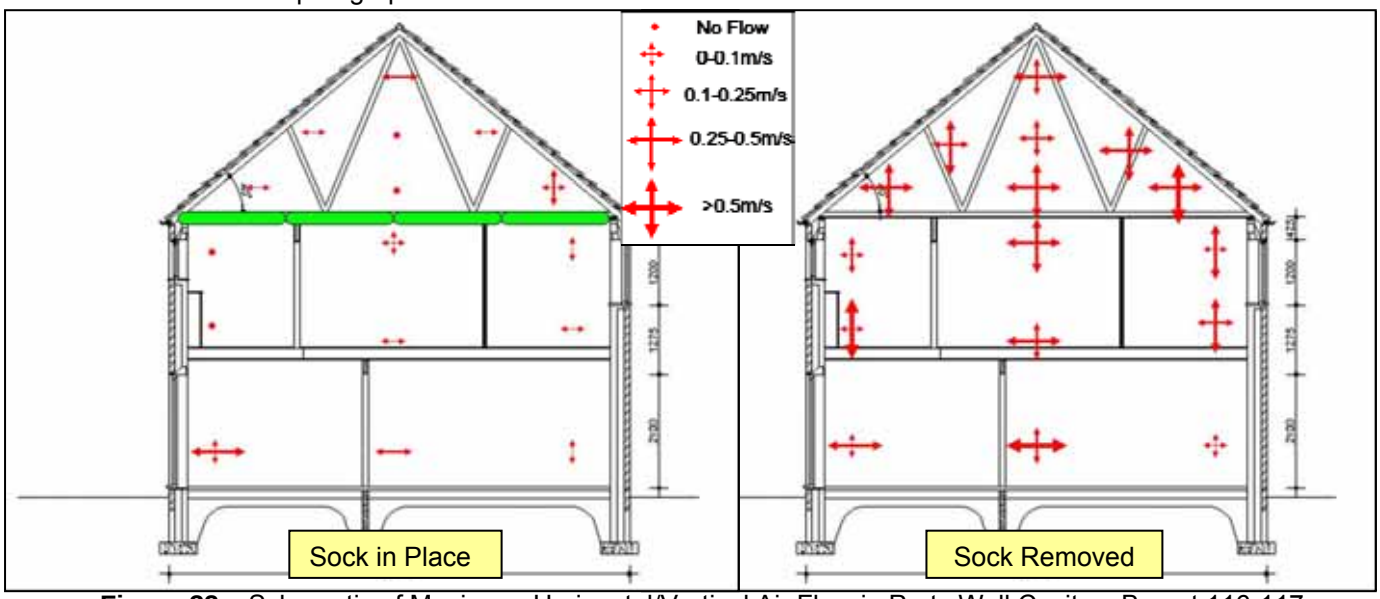

Figure 32 – Schematic of Maximum Horizontal/Vertical Air Flow in Party Wall Cavity – Bryant 116-117

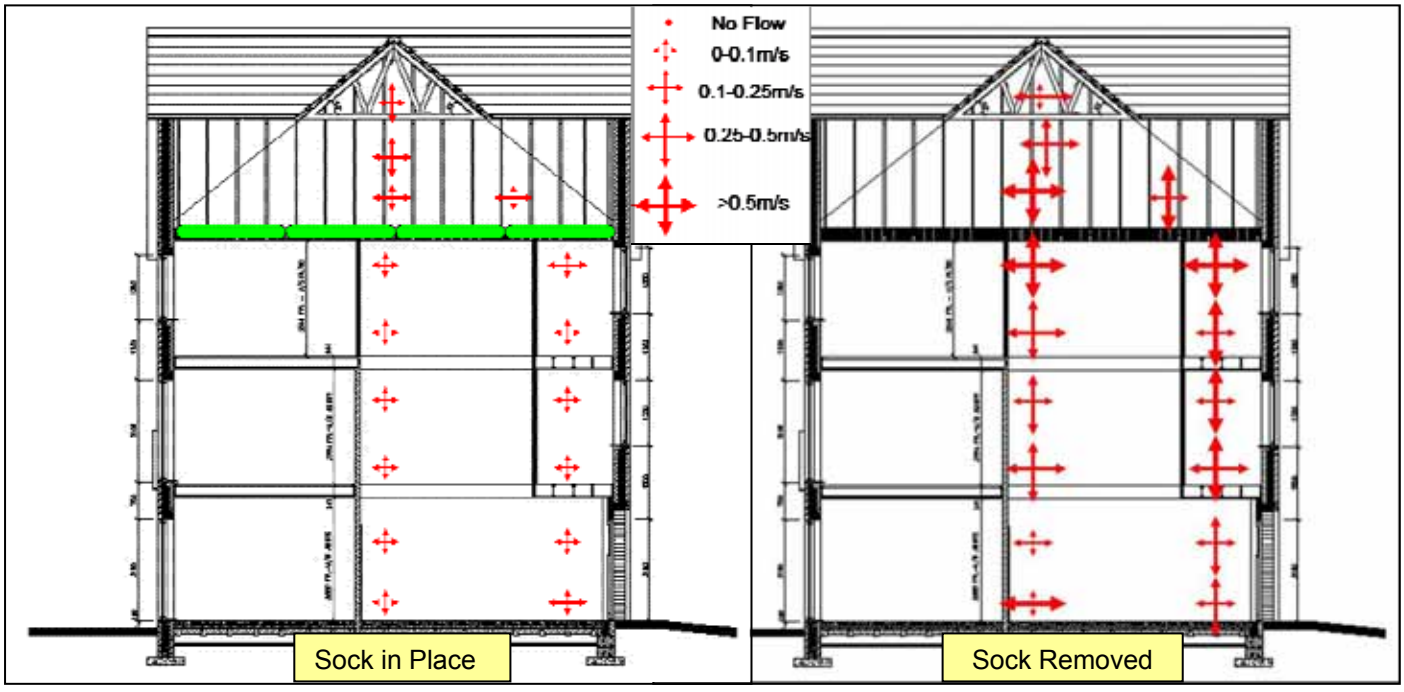

Figure 33 – Schematic of Maximum Horizontal/Vertical Air Flow in Party Wall Cavity – Redrow 110-111

Thermal Imaging

43 Infra-red thermal imaging was conducted using a FLIR Systems Thermacam B4 infra-red camera. The camera was equipped with either a standard 27mm (23°) lens or a 15mm (45°) wide angle lens. Thermal images were taken during both co-heating tests from inside the dwellings and also from outside the dwellings when the external conditions were appropriate.

44 An infra-red image of the block work of the party wall in the loft of Bryant plot with the horizontal cavity sock in position is shown in Figure 34 and with the horizontal cavity sock removed is shown in Figure 35 (Both pictures taken at around midday with the external temperature at around 10°C in both cases). The temperature close to the apex of the party wall was around 10°C with the sock in position. The remainder of the wall was at a similar temperature of around 10°C. In comparison, the infra-red image of the party wall taken when the sock had been removed shows the block work at the apex at a temperature of around 16°C, with the rest of the wall ranging from 14 to 15°C. These pictures are further evidence for vertical flow of warm air up the party wall cavity with the horizontal cavity sock removed. By contrast, the infra-red image in Figure 36 taken of the gable wall in the loft of plot 117 shows the wall at close to external temperatures (taken at the same time as Figure 35). These four images are probably the clearest qualitative demonstration of the bypass mechanism.

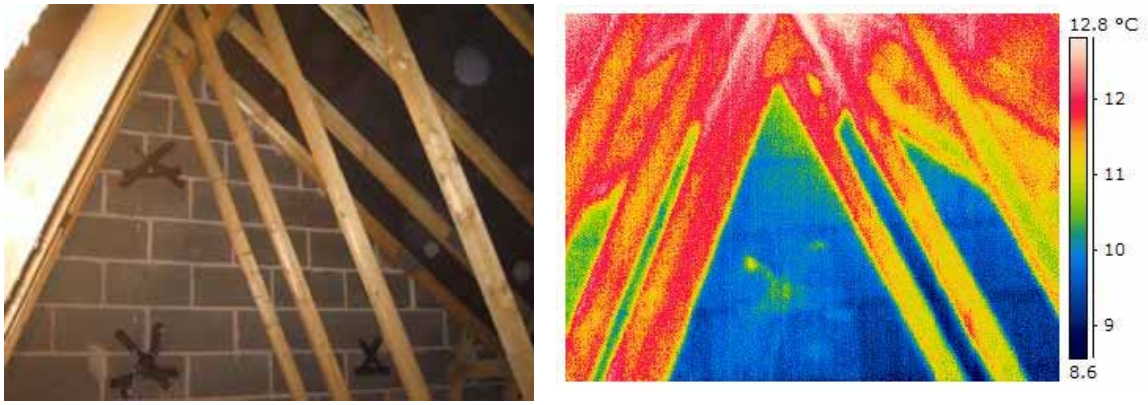

Figure 34 – Photograph and Infra-red Images of Loft Party Wall in Bryant Plot 117 – Sock in Position

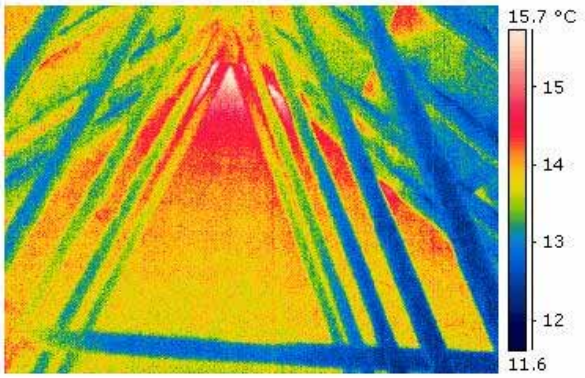

Figure 35 – Infra-red Image of Loft Party Wall in Bryant Plot 117 – Sock Removed

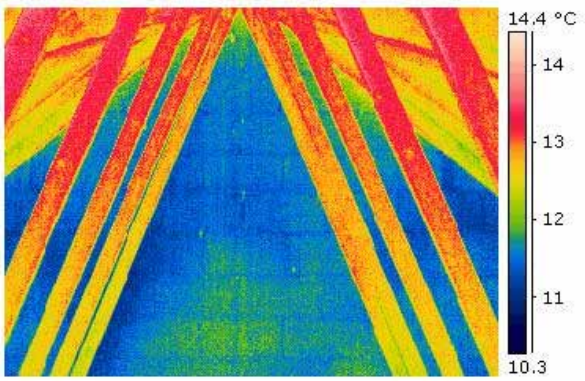

Figure 36 – Infra-red Image of Loft Gable Wall in Bryant Plot 117

45 Further evidence for the flow of warm air over the top of the party wall is shown by Figure 37 which shows a view of the apex of the party wall in Bryant plot 117 when the horizontal cavity sock had been taken out. The infra-red image illustrates the warming effect of the air flow as it passes over a gap in the party wall formed by missing mortar in one of the perpends. It can be seen that an area of the wooden roof truss has been heated to around 18°C. This area coincides with the gap in the perpend, as shown by the red circle in the photograph in Figure 37.

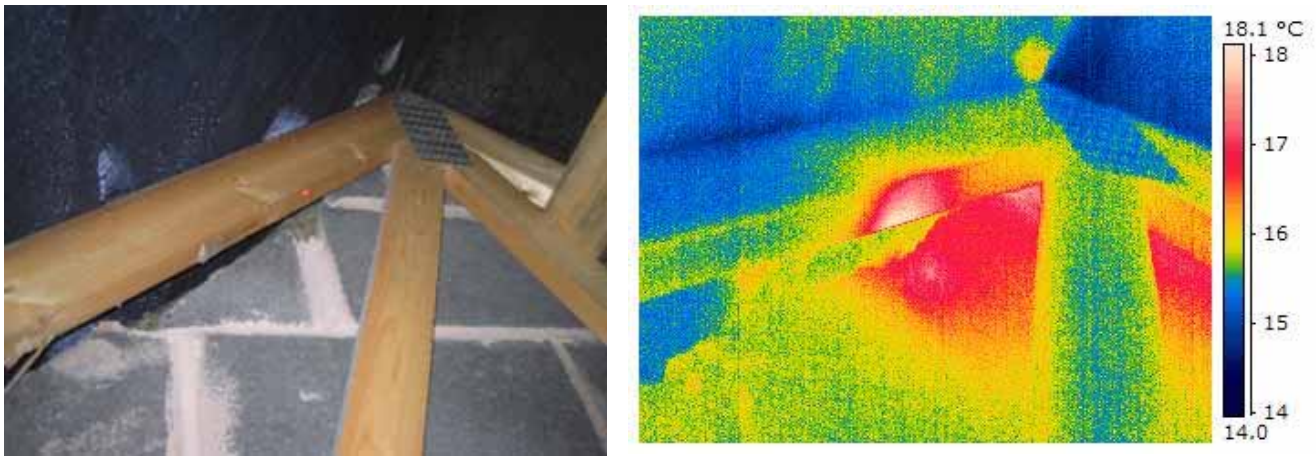

Figure 37 – Heat Loss at Apex of Party Wall in Loft of Bryant 117 – Sock Removed

46 The external walls of the pair of Bryant dwellings exhibited several areas of high heat loss. Of particular interest was a zone at the rear of the houses in between the first floor windows in the vicinity of the party wall as shown in Figure 38. This zone was roughly circular and a 500mm in diameter and there was also less intense zone on the left hand side of the spot that ran along side the window in plot 117. This heat loss pattern was only seen during the test period when the horizontal cavity sock was in position in the party wall and was visible even though the wall was saturated at the time due to a missing gutter downpipe. When the party wall sock was removed the observed thermal image pattern changed completely and the expected pattern due to the saturated wall became apparent as shown in Figure 39. This change is indicative of some change in the direction of heat flow in the cavity behind this part of the external wall that must have occurred as a result of removing the sock. Further investigation was carried out by removing a brick from the wall in order to inspect the condition of the cavity at this point. It was found that the high heat loss zone coincided with an area of missing loose fill mineral wool insulation as shown in Figure 40. This suggests that during the part of the co-heating test when the horizontal sock was in position, the conductive heat loss was higher at this point due to the missing insulation. However, when the sock was removed it is probable that this resulted in increased air flow and associated heat loss from the external cavity into the party wall cavity. This indicates that, in this case, the vertical sock in the external cavity has not provided an effective air seal to the party wall cavity. Given the nature of the construction, it is likely that a much more robust solution would need to be found.

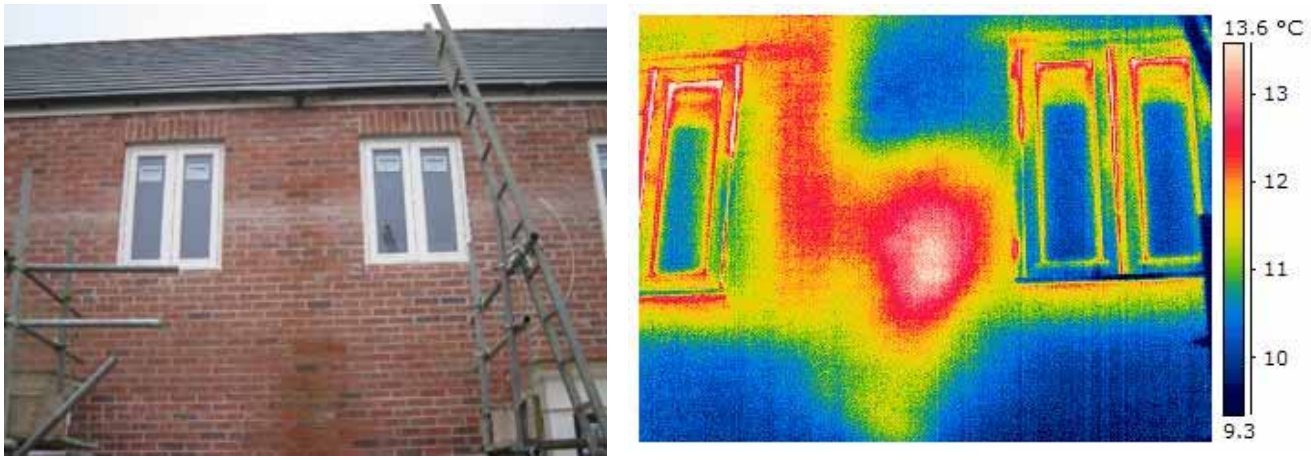

Figure 38 – Heat Loss from Rear Wall of Bryant Plot 116-117 – Horizontal Sock in Position

Figure 39 – Rear Wall of Bryant Plot 116-117 – Horizontal Sock Removed

Figure 40 – Missing Insulation in Cavity of Rear Wall of Bryant Plots 116-117

47 Other areas of high heat loss observable with the thermal camera coincided with known thermal bridges. In particular these included the heads of openings such as the head of the bay window in both the Bryant dwellings (Figure 41) and Redrow dwellings (Figure 43), and the head over external doors as shown in the example in Figure 42. A major thermal bridge in the two Redrow dwellings was at the threshold of the so called Juliet balconies as illustrated in Figure 44. There were two of these details in both Redrow test properties. Another thermal bridge was observed at the junction of the head of the recessed front door porch as shown in Figure 45.

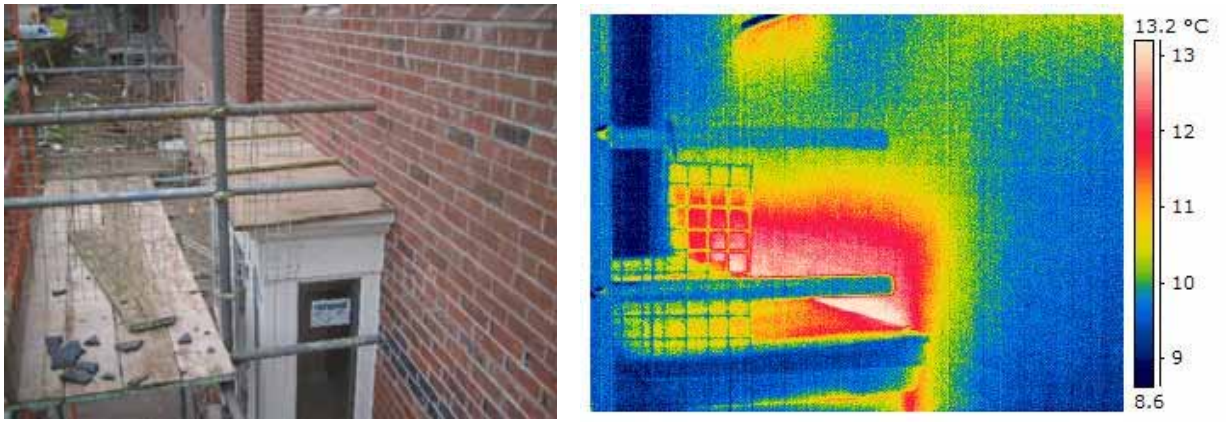

Figure 41 – Thermal Bridge at Bay Window Head (Bryant Plot 117)

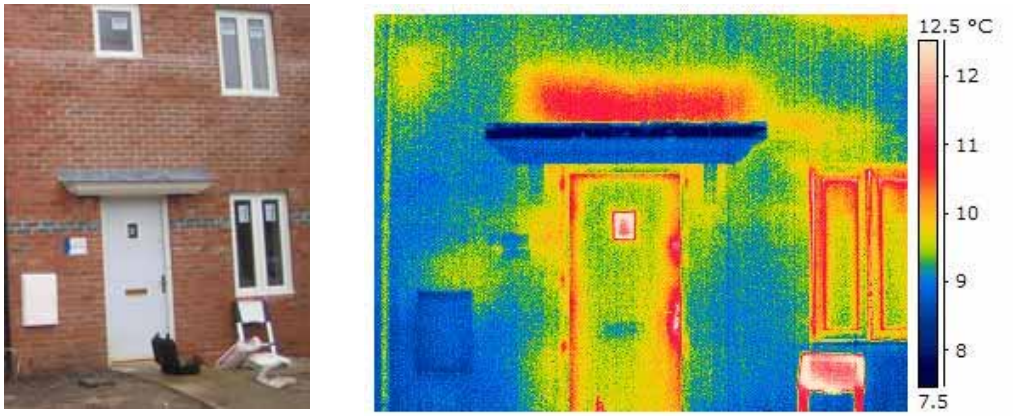

Figure 42 – Thermal Bridge at Door Head (Bryant 116)

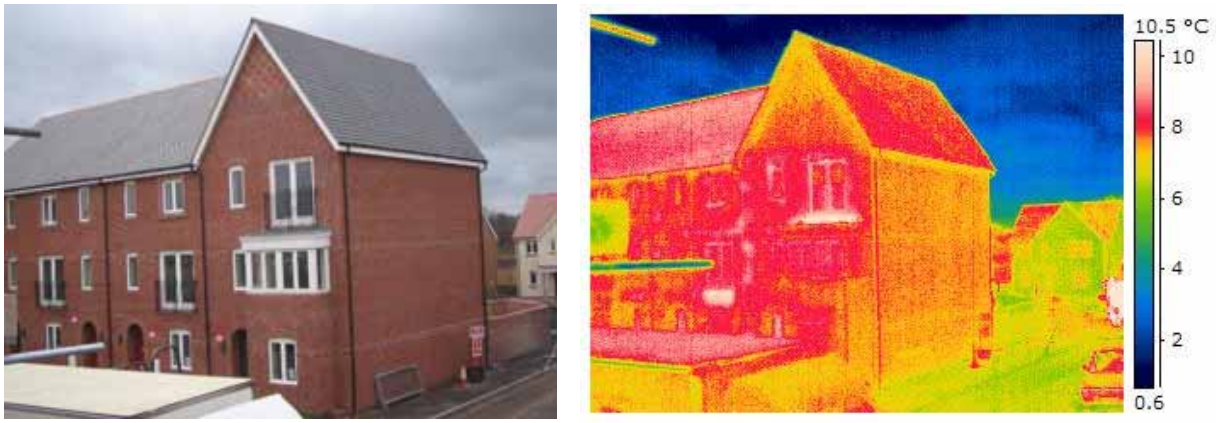

Figure 43 – Thermal Bridge at Balcony Thresholds and Bay Head – Redrow Plots 110-111

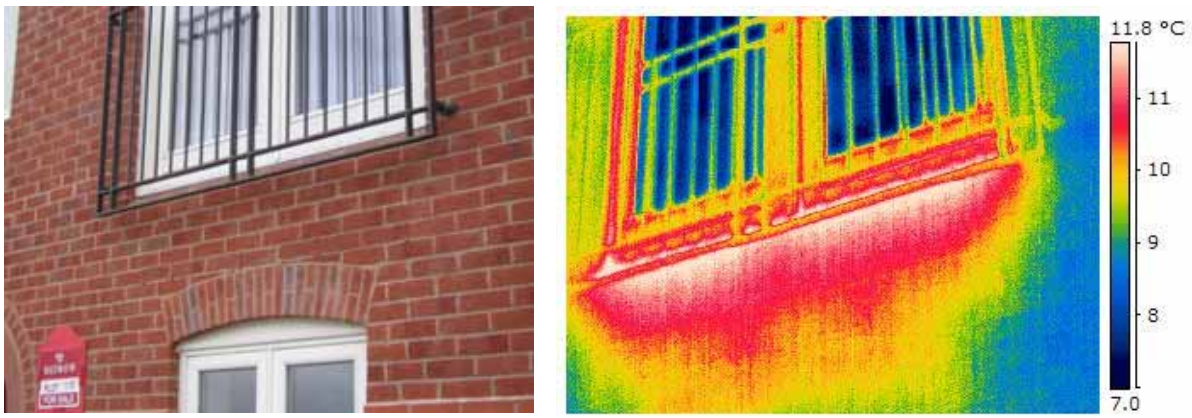

Figure 44 – Thermal Bridge at Juliet Balcony Threshold – Redrow Plots 110

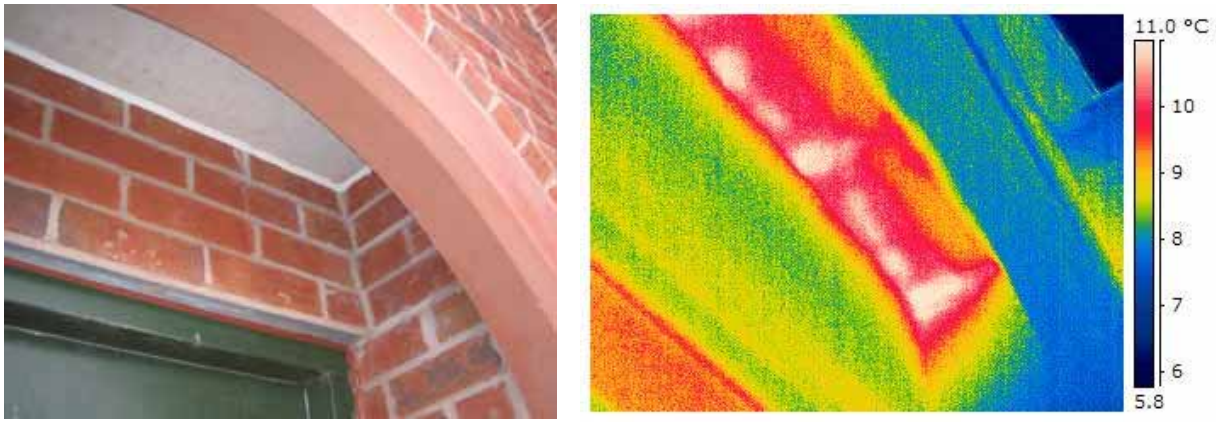

Figure 45 – Thermal Bridge at Front Door Recess – Redrow 110.

48 An internal infra-red image taken at the junction of the party wall with the external wall on the second floor of Redrow plot 110 is shown in Figure 46. This image was taken with the horizontal cavity sock removed. The external wall in this case was the on the windward front façade of the dwelling. It can be seen that there is a very cold zone (shown in blue on the thermal image) with surface temperature at around 21°C at the vertical junction of the external wall with the party wall. This cold zone extends along the cavity wall for about a metre, gradually increasing in temperature along the wall until the temperature matches the internal temperature of around 26°C. The most likely explanation for this effect is the cooling effect of the wind driven cold air from outside, bypassing the vertical sock in the external wall and flowing into the party wall cavity. There is no corresponding cold zone on the external wall confirming that this effect is not associated with air flow in the space between the wall and the plasterboard. The cold zone at the edge of the party wall actually extended up into the party wall in the loft space as can be seen in Figure 47.

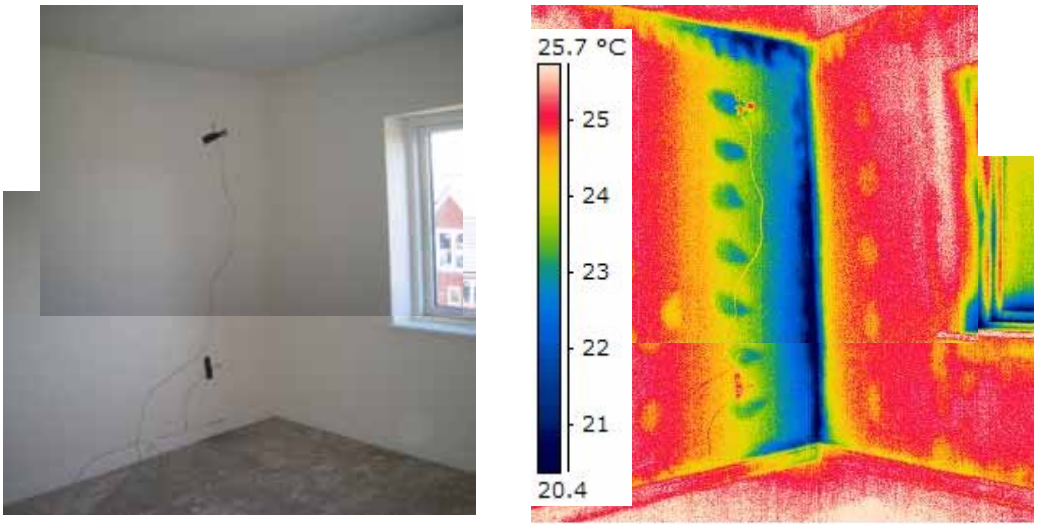

Figure 46 – Internal Junction of Party Wall with External Wall – Redrow Plot 110 – Sock Removed

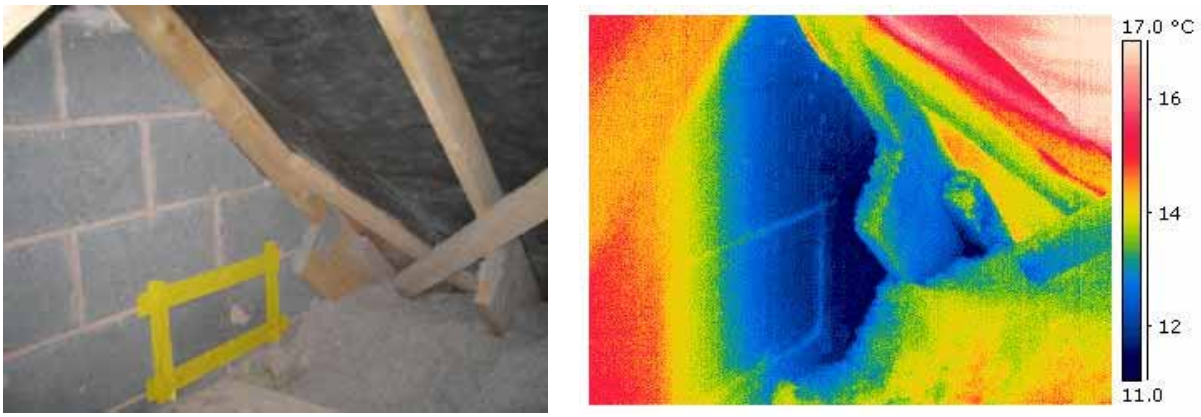

Figure 47 – Junction of Party Wall with Roof in Loft – Redrow Plot 110 – Sock Removed

Observations during Co-heating Tests

49 One of the difficulties encountered when removing the cavity socks in the Redrow test houses was the large amount of mortar snots that had fallen on top of the sock during construction. An example of this can be seen in Figure 48 which shows a layer of mortar approximately 100mm in thickness lying on top of the sock in position in Redrow plot 110. Figure 49 shows a photograph taken along the length of the cavity above the sock showing that this layer of mortar extends the length of the cavity. Part of the problem lies with the height of the party wall in the loft, which is 4m at the ridge. This gives more opportunity for mortar to fall down the cavity. It would have even more difficult to keep the cavity clear during construction in the case of the Redrow houses due to the narrower width (75mm) compared to the Bryant cavity (142mm). Mortar snots in the party wall cavity on top

of the sock have implications for the Part E acoustic regulations because the mortar bridges the two walls.

Figure 48 – Mortar Layer on Top of Sock – Redrow

Figure 49 – Mortar Covered Sock - Redrow

50 One potential issue with the installation of a horizontal sock in any party wall was that it could be damaged by falling debris accidentally dropped down the cavity during construction. One instance of this was observed in the Redrow party wall cavity as shown in Figure 50. When one of the blocks was removed at the half-way stage of the co-heating test, it was found that the sock immediately behind the block had been torn and one side had been pushed downwards by around 200mm. This could have occurred for example if a concrete block or tool had been dropped from above during construction. This small gap would have allowed some air to bypass the sock during the first half of the co-heating test, although this would have been mitigated to some degree by the mortar layer on top of the sock.

51 A photograph (Figure 51) taken inside the party wall cavity when the sock was being removed from the Redrow test houses showed that there would have been a gap of around 200mm between the end of the top of the horizontal sock and the vertical sock in the external cavity. This gap would have provided an unobstructed entrance point for external air into the party wall cavity below the sock during the first half of the co-heating test on the Redrow houses.

Figure 50 – Damaged Sock – Redrow

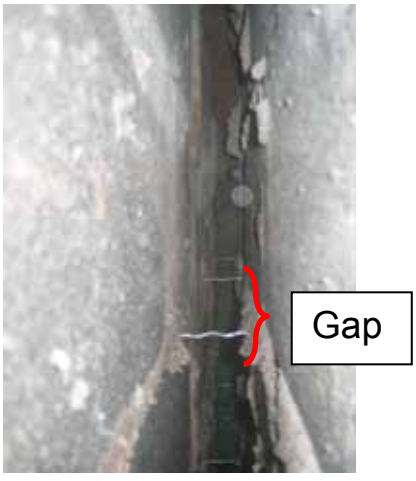

Figure 51 – Gap between Vertical & Horizontal Sock

52 Thermal images taken in the loft of Redrow plot 110 at the start of the co-heating tests showed heat loss where restraint straps entered the party wall at the level of the ceiling. A closer visual inspection showed that the blocks that had been removed for the installation of the straps had not been replaced when the roof was complete. An example of this gap is shown in Figure 52. In order

that these direct paths into the party wall did not influence the co-heating test, all such holes in the party wall in the loft were patched up using blocks and mortar. Thermal images taken after the gaps had been patched confirmed that heat was no longer escaping by these routes.

Figure 52 – Gap in Party Wall in Loft for Restraint Strap - Redrow

Airtightness Tests

53 Pressure tests were conducted on all four co-heating test houses before commencement of the co-heating tests in order to determine the background ventilation rate. Repeat tests were also carried out on completion of the co-heating tests to determine what changes in leakage may have taken place as a result of the high temperatures used in the co-heating test

Pressure Test Equipment & Procedure

54 The equipment used to measure air permeability is summarised in Table 4.

Table 4 - Pressure Test Equipment Specification

Component	Equipment Used	Comment
Blower Door	Energy Conservatory Minneapolis Model 3 Blower Door	Flow Range 25 m^3/h to 10704 m^3/h
Pressure/Flow Gauge	Energy Conservatory DG-700 Digital Pressure Gauge	Gauge calibrated annually
Temperature/Humidity	Rotronic Hygropalm 1 with Hygroclip S3 Sensor	
Anemometer & Barometer	Silva ADC Pro	

55 The pressure tests were conducted according to the methodology described in the ATTMA Technical Standard (ATTMA 2006). Air permeability in m^3 of air at 50 Pa pressure difference per m^2 of external envelope area were calculated using the Leeds Met Permeability Data Spreadsheet (Wingfield 2006). Air permeabilities are given in units of m/h at 50Pa pressure difference. Permeabilities and volumetric air change rates were measured for both pressurisation and depressurisation tests, with the values reported being the mean of the two tests. All tests were conducted from inside the properties with the blower door being located in the front door opening.

56 Pressure tests were conducted before the commencement of the co-heating tests. The pressure tests were then repeated when the co-heating tests were completed and the dwellings had cooled down to normal internal temperatures.

Pressure Test Results

57 The pressure test results are given in Table 5. The measured air permeabilities of all the test dwellings were within the Stamford Brook design target of 5 m/h@50Pa. The three dwellings that were pressure tested after the co-heating test (Redrow 110,111 and Bryant 116) all showed an increase in air permeability. The increase ranged from 0.4 m/h to 0.8 m/h. This difference is of the order associated with the deterioration of secondary sealing around junctions caused by thermal expansion and contraction and adhesive failure of sealants. The effectiveness of secondary sealing

is discussed in more detail in the Stamford Brook report on airtightness (Miles-Shenton, Wingfield & Bell 2007).

Table 5 - Pressure Test Results for Co-heating Test Dwellings

Developer	Test Date	Plot No.	Before/After Co-heating Test Party Wall Cavity Sock in/out	Air Permeability (m/h)	Volumetric Leakage (ach)	r^2 Coefficient	
						Depress	Press
Bryant	22-1-07	116	Before Test Sock In	2.75	3.04	0.992	0.975
Bryant	22-3-07	116	After Test Sock Out	3.57	3.95	0.999	0.998
Bryant	25-1-07	117	Before Test Sock In	3.31	3.66	1.0	1.0
Redrow	27-2-07	110	Before Test Sock In	4.03	3.45	0.981	0.990
Redrow	28-3-07	110	After Test Sock Out	4.78	4.09	1.0	0.998
Redrow	27-2-07	111	Before Test Sock In	2.84	2.46	1.0	0.980
Redrow	29-3-07	111	After Test Sock Out	3.20	2.77	0.998	0.998

58 Background ventilation rates calculated from the mean of the initial and final pressure test results are given in Table 6. Ventilation rates were calculated according to the n/20 rule and adjusted using a shelter factor of 0.85 (Lowe Wingfield Bell & Bell 2007).

Table 6 – Calculated Background Ventilation Rates

Test House	Mean of Air Permeability at Start and End of Co-heating Test (m/h@50Pa)	Calculated Background Ventilation Rate (h^{-1})
Redrow Plot 110	4.41	0.187
Redrow Plot 111	3.02	0.128
Bryant Plot 116	3.16	0.134
Bryant Plot 117	3.31 (Initial Test Only)	0.141

59 Further analysis of the airtightness performance of the dwellings used for the co-heating tests is provided in Stamford Brook project deliverable 6 (Miles-Shenton et al 2007).

Acoustic Tests

60 Acoustics tests of the airborne sound insulation of the party wall were carried out on the two Redrow co-heating test properties only. Construction delays meant that the research team were unable to conduct acoustic tests on the Bryant test dwellings without causing further delays to the

overall test programme. The acoustic tests were conducted on the completed Redrow dwellings immediately prior to commencement of the co-heating tests when the horizontal cavity sock was in position in the party wall cavity. The acoustic tests were then repeated after completion of the co-heating tests with the horizontal cavity sock removed. The acoustic tests were carried out according to the requirements of Appendix B2 of Approved Document E for field testing of the airborne sound insulation of separating walls (ODPM 2004). A photograph of the acoustic test equipment is illustrated in Figure 53, and shows the loudspeaker, power amplifier and frequency analyser. A summary of the test equipment is given in Table 7.

Table 7 - Acoustic Test Equipment

Brűel & Kjær type 2260 frequency analyser, with BZ 7204 Building Acoustics module. Serial number 1772150 (UKAS verification in July 2005)
Brűel & Kjær type 4231 sound level calibrator, serial number 1780811 (UKAS verification in July 2005)
Norsonic type 260 power amplifier, serial number 26983
Norsonic type 250 hemidodecahedron loudspeaker, serial number 23315

Figure 53 - Acoustic Test Equipment

61 The results of the acoustic tests are given in Table 8. It can be seen that the only change in acoustic performance before and after the co-heating test was a small increase in the sound insulation of 3dB on the second floor. This improvement was probably associated with the removal of the bridging mortar layer lying on top of the sock, which was removed at the same time as the horizontal sock was taken out. The important conclusion here is that a mineral wool filled sock itself is unlikely to significantly affect the airborne sound insulation performance of a masonry cavity party wall, assuming that attention is paid during construction to minimise mortar build up on top of the sock. The Robust Details Practice Note (Robust Details Ltd 2006) states in any case that it is good practice to keep the cavity free from mortar droppings and debris. The mean sound insulation for the Redrow party wall before the co-heating test was 55 dB. This compares favourably with the average airborne sound insulation of 53.04 ± 4.06 dB for the 1066 sample national database for the EWM4 masonry cavity wall robust detail (Baker 2007). The EWM4 party wall robust detail (Robust Details Ltd 2005) is identical in construction to the party wall detail used at Stamford Brook. A histogram of the EWM4 robust detail dataset is illustrated in Figure 54 (Baker 2007).

Table 8 – Airborne Sound Acoustic Test Results – Party Wall between Redrow 110 and 111

Location of Test	**Sound Insulation $D_{nT,\ w+Ctr}$ (dB)**		
	Before Co-heating Test	**After Co-heating Test**	**Change in Sound Insulation**
Ground floor, Kitchen to Kitchen	57	57	0
First floor, Lounge to Lounge	55	55	0
Second Floor, Bedroom to Bedroom	53	56	+3

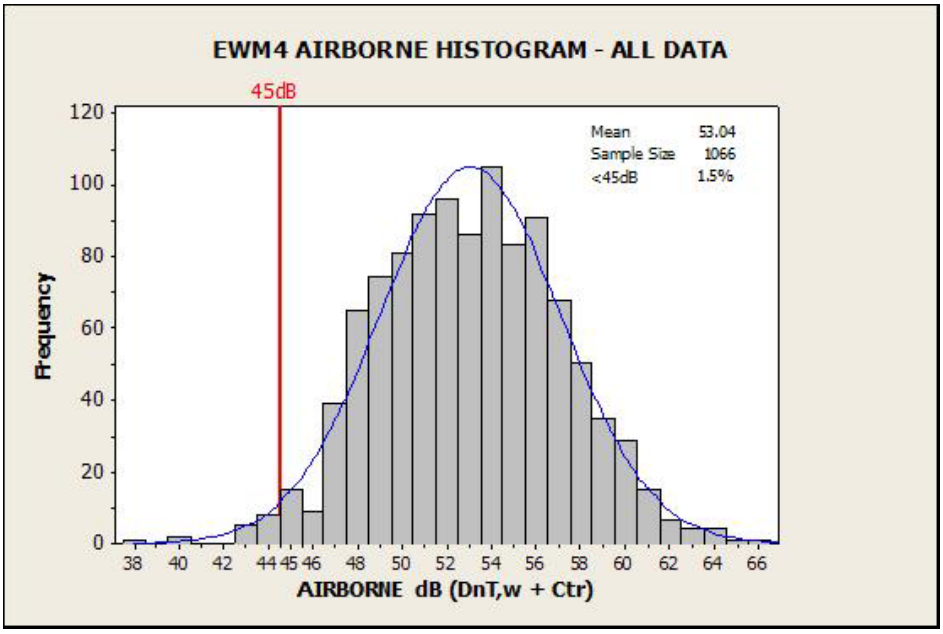

Figure 54 – Histogram of Test Results for EWM4 Party Wall Robust Detail National Dataset (Baker 2007)

Construction Observations

62 Frequent visits were made to the Stamford Brook site during the construction of the four co-heating test dwellings in order to observe critical stages in the construction process. These visits were undertaken at least once per week. A photographic record was kept of the different construction phases, with particular attention focussed on important and difficult to construct details such as junctions and openings. The construction record for Bryant plots 116 and 117 commenced just as the external walls were at wall plate level, whereas Redrow plots 110 and 111 were observed from foundation level onwards. Examples of observed critical defects are described below. Observations relating to airtightness are covered in project deliverable 6 (Miles-Shenton et al 2007).

Vertical Cavity Sock Defects

63 Photographs taken from inside the external cavity (before cavity was filled with mineral wool insulation) and looking towards the vertical cavity sock at the party wall are shown in Figure 55. These show gaps that would readily allow air to enter the party wall cavity from the sides.

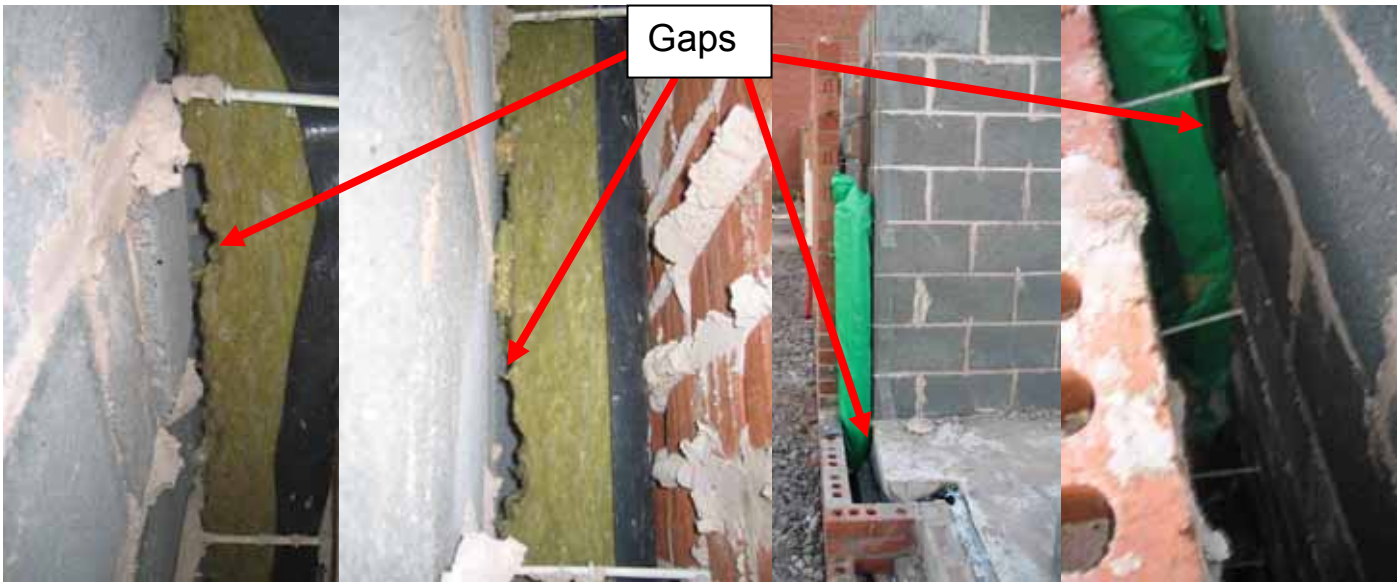

Figure 55 – Gaps between Vertical Sock in External Cavity and Entrance to Party Wall Cavity

64 It was noted that the edge floor slab was not square as shown in Figure 56. This was caused when the DPC membrane was not pushed right into the edges of the former prior to casting the slab. This defect has resulted in a large gap at the bottom of the entrance to the party wall cavity which would be difficult to seal with the vertical cavity sock and would likely allow air to flow from the bottom of the cavity.

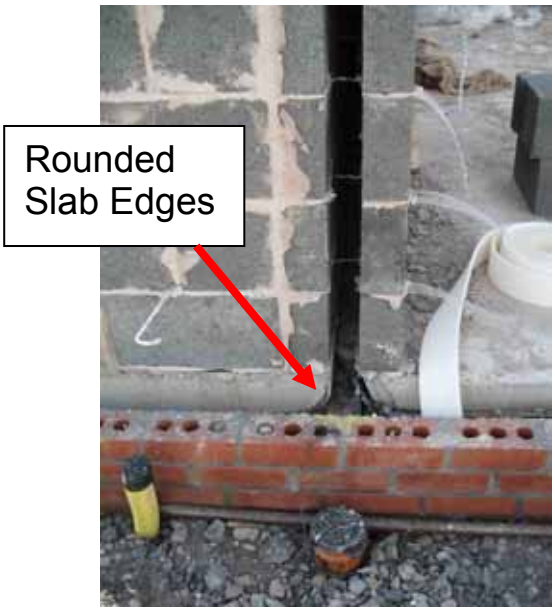

Figure 56 – Imperfect Floor Slab Edges

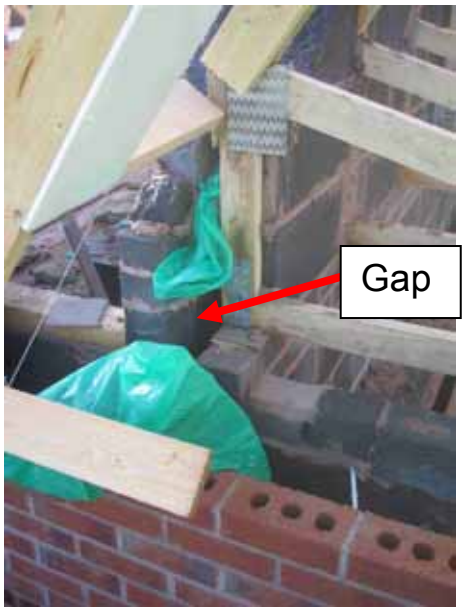

Figure 57 – Gap between Vertical and Horizontal Socks

Cavity Sock Defects

65 Some gaps were observed at the junction between the horizontal sock in the party wall cavity with the vertical sock in the external cavity as illustrated in the photograph in Figure 57. This gap would have allowed air to enter the top of the cavity. In cases where the bricklayers had omitted to install the vertical sock as they were constructing the wall, this would have left opportunities for the top of the sock further down the cavity to become covered in mortar droppings as shown in Figure 58. This could potentially have created a thermal bridge across the cavity. Also, in such circumstances it would have been difficult to properly position the next vertical sock without leaving a gap at the junction between the two socks, which would have given rise to air path into the party wall cavity.

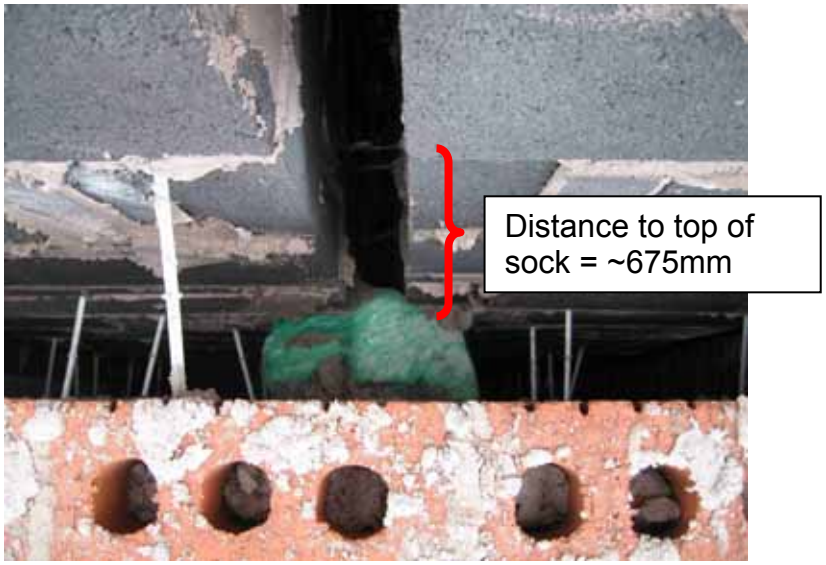

Figure 58 – Vertical Sock in External Cavity

Other Cavity Defects

66 The build up of mortar droppings on top of the DPC membrane used to form the cavity trays was in some instances found to be severe. For example, the photographs in Figure 59 show mortar build up that effectively bridges the external cavity.

Figure 59 – Mortar Build up on Cavity Tray

Defects at Window and Door Heads

67 In order to provide insulation under the plastic cavity trays above window heads, the detailed construction drawings call for mineral wool batts to be installed at this poison as the wall is built up. However, as can be seen in Figure 60, it was often the case that the insulation was inappropriately sized and there were air gaps all the way around the insulation. These gaps would not have been filled when the completed wall cavity was injected with loose fill mineral wool insulation. The effect of these gaps would have been to significantly increase heat loss at window heads compared to the expected losses from these linear thermal bridges. Similar defects have been observed by the Leeds Met research team on other construction sites (Bell Smith and Miles-Shenton 2005).

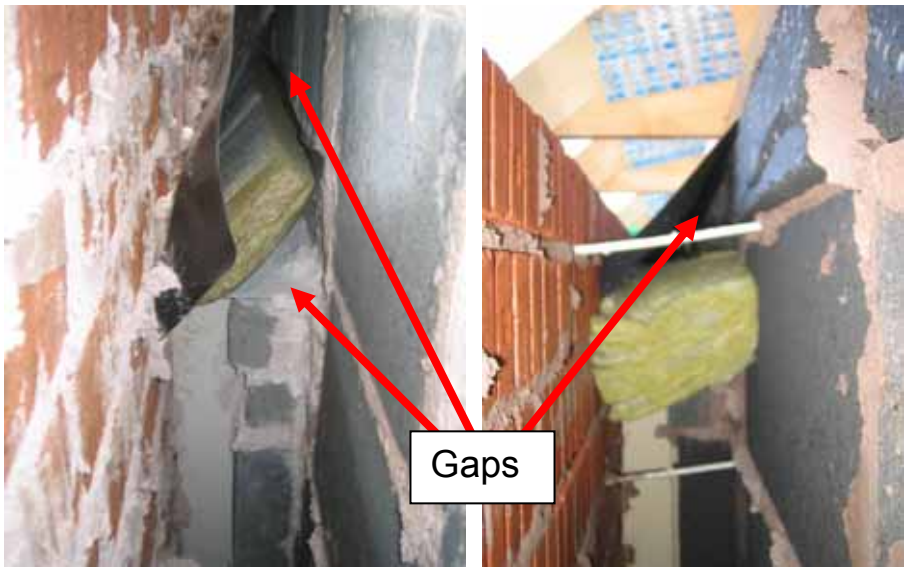

Figure 60 – Insulation underneath Cavity Trays at Window Heads

68 The detailed drawings show the gap between the window lintel on the external wall and the toe of the window lintel on the internal block wall to be 42mm (Figure 61). Measurement of this gap on actual as-built examples on the site indicated that the gap was typically less than this, and as low

as 20mm as shown in Figure 62. It would be expected that there will be some variation in tolerance on as-built details of this nature. The effect of this decrease in gap width would be to increase the thermal bridging value (Ψ) for the window head detail compared to calculated values. This issue is examined in more detail in the discussion section.

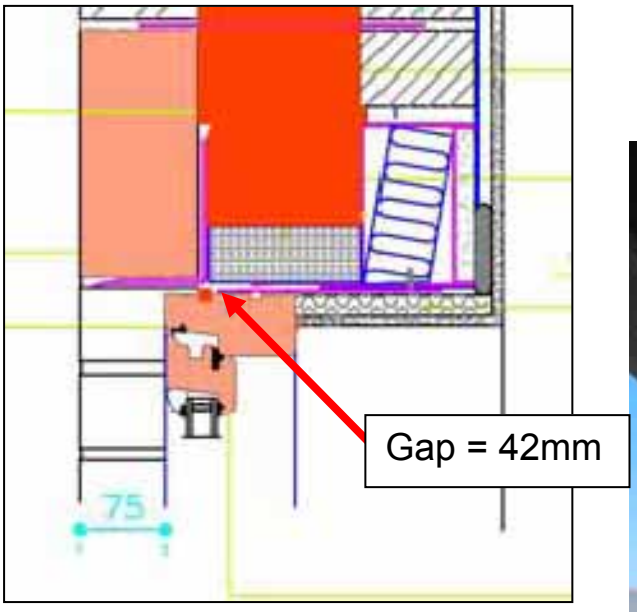

Figure 61 – Window Head - as Designed

Figure 62 –Window Head - as Constructed

69 The gap between the window and door lintels and below the cavity tray was filled with mineral wool insulation batts. In many cases the insulation did not properly fill the gap as illustrated by the three examples shown in Figure 63. In some cases the insulation was found to be sitting too high and in others the insulation did not fully bridge the gap between the lintels. The consequence of this lack of attention to detail would have been to increase the degree of thermal bridging at head details. This would mean that the window and door heads design Ψ values used in the SAP energy calculations for the predicted heat loss will likely underestimate the true value of thermal bridging losses.

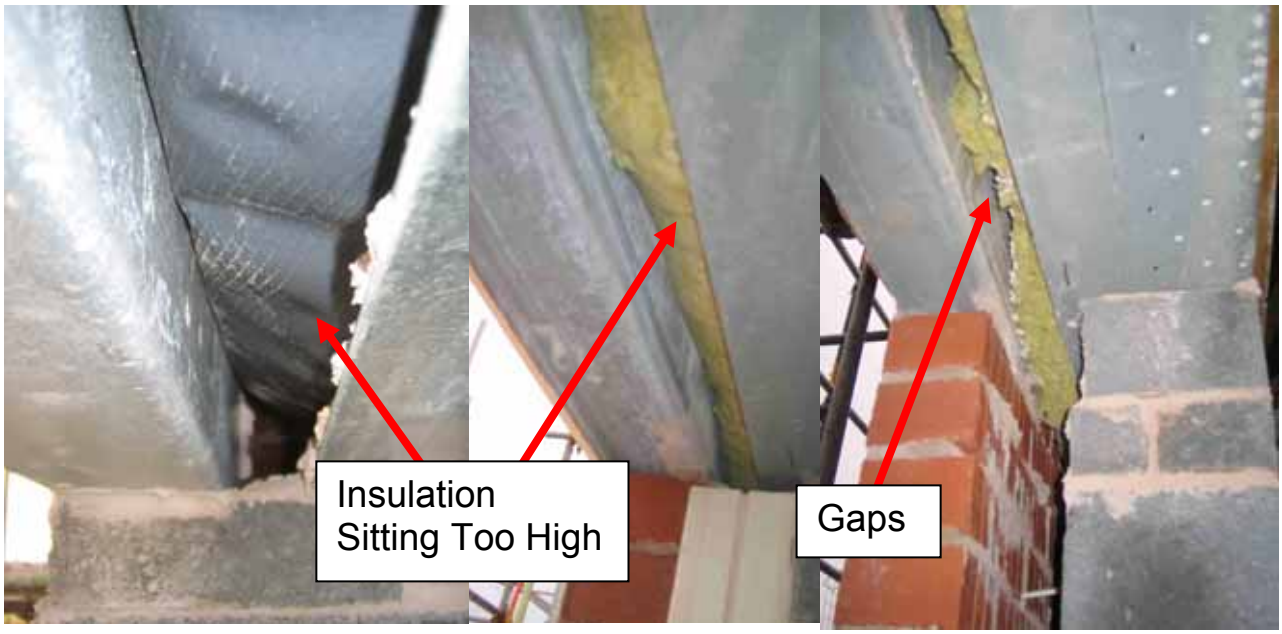

Figure 63 - Insulation between Window Head Lintels

70 The recessed front door used in both Redrow plots 110 and 111 is an example of a complex detail that is both difficult to construct and would give rise to significant thermal bridging over and above that of a standard door head. A photograph of the detail is shown in Figure 64. The main problem here is that the inner lintel supporting the blockwork for the first and second floor will only be covered by a piece of cement board hence creating a significant thermal bridge both vertically downwards and via the junction with the side of the porch as illustrated by the thermal image shown in Figure 45.

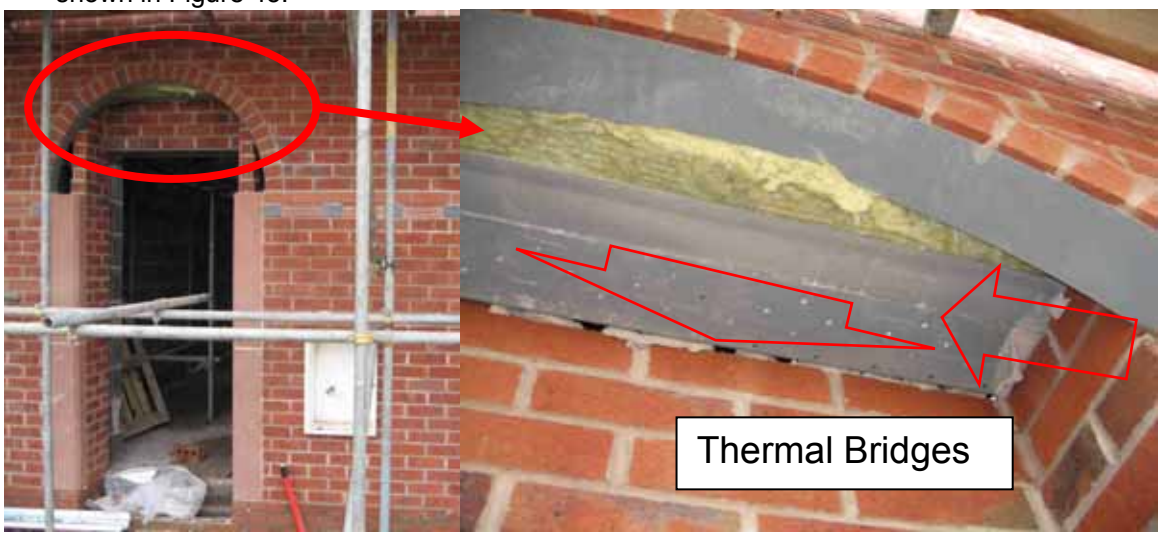

Figure 64 – Recessed Font Door Head Detail

Eaves Junction

71 The length of the overhang of the roof truss over the wall plate is important for maintaining the depth of insulation around the eaves where the ceiling insulation meets the wall insulation. The construction drawings require a 50mm overhang at this point. Measurement of the overhang as constructed on Bryant 116 and 117 showed the actual distance to be only 10mm. This would have the effect of reducing the minimum insulation thickness at the eaves to around 75mm for the detail as constructed instead of around 100mm for the detail as designed. The consequence of this would be to increase thermal bridging at this junction. This discrepancy in the eaves detail was first noticed by the research team and bought to the attention of the site and design teams when the first dwellings were being constructed in 2004 (Roberts Andersson Lowe Bell & Wingfield 2005). However, it appears that no action has been taken since that time to rectify the problem. It is worth noting that the eaves detail as designed already represents a 60% thinning of the roof insulation at this point.

Figure 65 – Roof Truss Overhang at Wall Plate

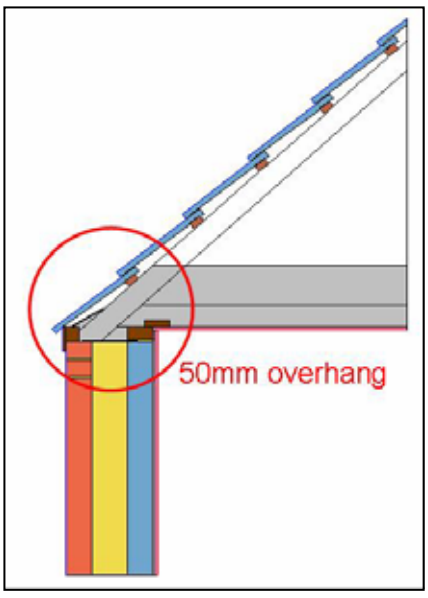

Figure 66 –Truss Overhang as Designed

Defects at Door Thresholds

72 The thresholds of first and second floor patio doors (sometimes called “Juliet” balconies) were found to be a major location of both thermal bridging and air leakage as illustrated by the external infra-red thermal image in Figure 44. Construction of one of these balcony details in Redrow plot 111 is illustrated in Figure 67. It can be seen that the floor boards were left off the threshold for a large part of construction, which would have allowed multiple opportunities for material such as mortar, wood, waste plasterboard and other assorted debris to fall into the cavity. It can also be seen that the insulation does not come right up to the level of the door frame, which would cause considerable thermal bridging at this point. It can also be observed that there would be potential for air leakage between the top of the block work wall and the floor board unless there was very careful sealing at the junction of these components. The consequence of these failings can be seen in the infra red image shown in Figure 68 which was taken during the co-heating test in Redrow plot 110. The thermal image shows significant heat loss around the point of the threshold that is likely a combination of conductive losses and air leakage.

Figure 67 – Construction of Juliet Balcony Threshold Detail

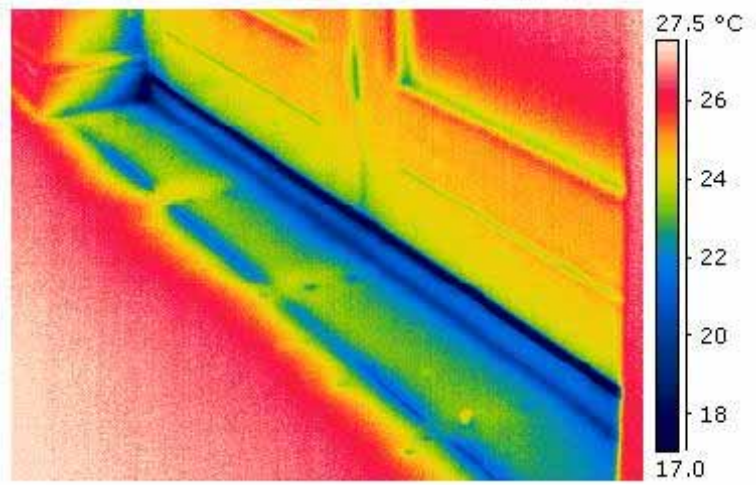

Figure 68 – Thermal Image of Juliet Balcony Threshold during Co-heating Test

Bay Window

73 Both Bryant co-heating test plots and Redrow plot 111 were constructed with bay window details. In all three cases, these were constructed with block work cavity walls and a flat roof constructed from timber with mineral wool insulation. The junction between the timber roof and the wall opening (with steel lintels supporting the wall above the bay) was found to give rise to high thermal losses as shown in the infra-red images taken from outside the dwellings during the co-heating test (Figures 41 and 43). Photographs taken during the construction of the bay window in Bryant plot 116 are shown in Figures 69 and 70. It can be seen that the outer steel lintel supporting the external brick wall above the bay forms a direct thermal bridge into the dwelling. The thermal

losses at this point were observed from inside the dwellings during the co-heating tests as demonstrated by the infra-red thermal image shown in Figure 71. The detailed drawings of the bay window required that the reveal board to the underside of the bay roof be insulated plasterboard with around 25mm of polyurethane insulation. This would have reduced the degree of thermal bridging via the outer lintel. However, the research team observed that uninsulated plasterboard was used in all three co-heating dwellings as illustrated by the installation of the boarding in Redrow plot 116 shown in Figure 73. Given that the inner and outer lintels are separate, it would have been possible to have omitted 2 or 3 courses of bricks behind the bay window roof, to allow the insulation to run continuously from the bay window roof to the wall cavity. As well as eliminating the thermal bridge, this detail would have been slightly cheaper to build than the one actually built, because of the saving of brickwork.

Figure 69 – Bay Window Head before Boarding

Figure 70 – Completed Bay Window

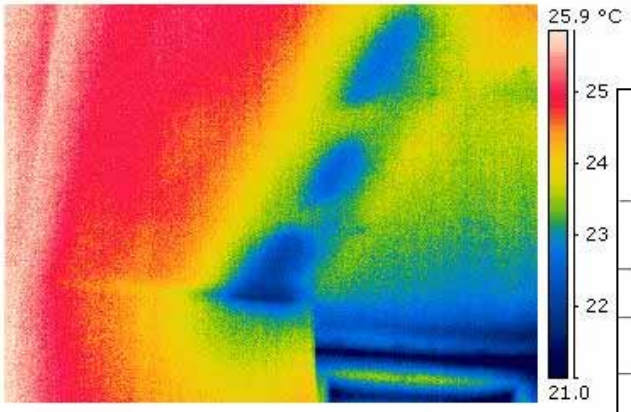

Figure 71 - Thermal Image of Bay Window Head during Co-heating Test

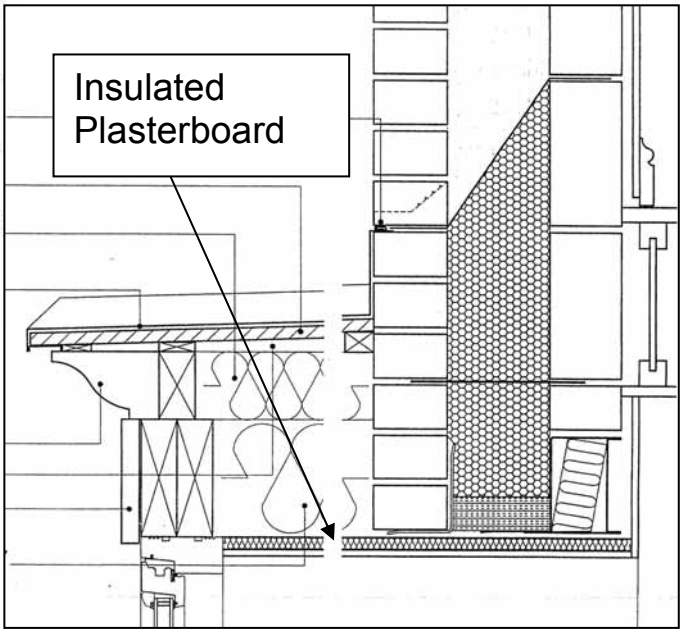

Figure 72 – Detailed Drawing of Bay Window

Figure 73 – Uninsulated Reveal Board in Bay Window

Loft Insulation

74 The loft insulation used in all four co-heating test dwellings was Warmcel recycled newspaper. This was installed as a loose fill material by blowing via hoses into the loft. The required final thickness of loft insulation was 250mm. It was also important to minimise thermal bridging at the eaves, that the insulation was continued right up the eaves board/ventilation stop and down into the external wall cavity.[3] Observations during construction of the co-heating test houses showed that in most cases the insulation did not always continue all the way up to the eaves board, as illustrated by the example in Figure 74. Spot measurements of insulation depth at random locations within the lofts of the co-heating test houses demonstrated that large areas of loft insulation failed to meet the minimum depth requirement of 250mm. This is illustrated by the example in Figure 75 in Redrow plot 111, where the insulation depth is less than 200mm. This would have a significant detrimental effect on the *U*-value of the ceiling. Discussions with the insulation installers revealed that they aim to overfill to around 270mm to allow for some settlement. It is possible that the insulation is settling more than anticipated.

Figure 74 – Loft Insulation at Eaves

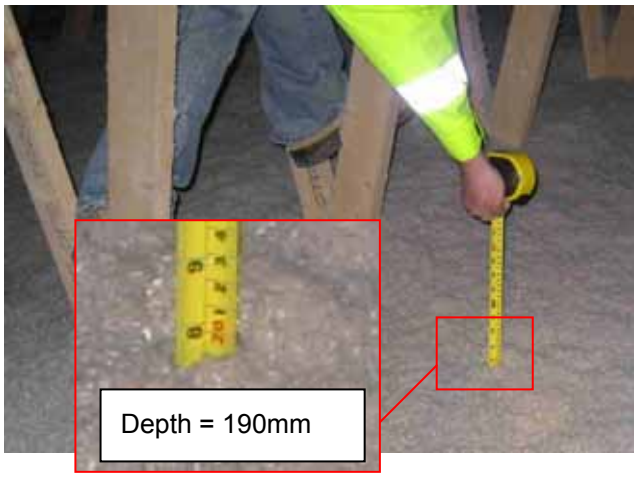

Figure 75 – Loft Insulation Depth

Gable Wall Insulation

75 The Stamford Brook construction specification (Taylor Woodrow Developments & Bryant Homes 2005) states that the cavities of gable walls should be fully filled with insulation right up to the verge. This is also a requirement of insulation manufacturers such as Rockwool, where drilling patterns for gable walls extend into the loft up to the verge as illustrated in Figure 76 (BBA 1998). In the case of Bryant plot 116, the installers omitted to fill the gable cavity. The potential consequence could have been to increase the level of thermal bridging at the junction of the ceiling with the gable wall.

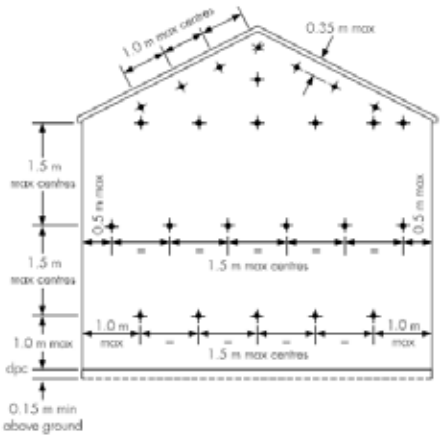

Figure 76 – Gable Wall Drill Pattern for Insulation – 25mm holes (BBA 1998)

[3] It should be noted that Bryant used a cement board cavity closer to seal the top of external wall cavities. This would mean that in this case the loft insulation, if properly installed, would actually rest on top of the cavity closer. In the case of Redrow dwellings no cavity closers were used at the top of the wall cavity, so the loft insulation should actually meet the wall insulation.

Discussion

Effective U-Value of the Party Wall

76 Measurements of heat flux into the party wall cavity taken during the second series of co-heating tests have shown that the magnitude of the effective *U*-value for the party wall without the horizontal cavity sock ranged from 0.50 to 0.63 W/m^{2}K. This makes the party wall the building element with the second largest *U*-value after that of the windows and doors. The effective *U*-value of the party wall was more than twice the *U*-value of the external wall (0.23 W/m^{2}K) and around three times the *U*-values of the floor (0.17 W/m^{2}K) and ceiling (0.14 W/m^{2}K), provided all other elements perform as designed.

77 It is possible that part of the ~0.1 W/m^{2}K difference in effective *U*-value for the 2-storey Bryant dwellings at 0.5 W/m^{2}K and the 3-storey Redrow dwellings at 0.63 W/m^{2}K could be attributed to an enhanced stack effect caused by the taller (7.5m) cavity in the Redrow houses. However, the factors that would influence the stack driven flow of air into and up the party wall cavity are extremely complex and will include such variables as cavity height, cavity width, the location and size of gaps in the vertical cavity closer, surface roughness effects and the resistance to air flow created by the external wall, external wall insulation, and the mineral wool firestopping at the roof-party wall junction. It would be difficult to say for certain which factors are most important for which dwelling type as we simply do not have enough quantitative data to describe each of the different variables. Factors that influence wind induced pressure effects such as the orientation of the dwelling to the prevailing wind and sheltering would further complicate the matter.

78 It is clear from the variation in temperatures across the party wall cavities that the heat loss is not even across the whole party wall. The effective *U*-value for any particular zone of the party wall will actually vary according to the heat flux at that point. Therefore, the magnitude of the calculated effective *U*-obtained during these co-heating tests will depend to a degree on the number and location of temperature sensors in the cavity. We have been careful during these tests to position the sensors evenly across the cavity width and height such that the mean temperature so obtained is representative of the average thermal condition in the cavity. A higher density of temperature sensors would have improved the accuracy of the effective *U*-value but it is believed that the range of around 0.5 to 0.6 W/m2K obtained during these tests is a reasonably accurate estimate of heat loss from a party wall of the type constructed at Stamford Brook.

79 The temperature profiles in the party wall cavities showed temperature stratification from top to bottom, with the higher temperatures generally being towards the top of the cavity and the lowest temperatures at the bottom of the cavity. This stratification was consistent and relatively steady with respect to changes in external temperature when the horizontal sock was in position at the top of the party wall, but became much more variable once the horizontal sock had been removed. It is likely that the stratification in the situation with the sock removed would have been driven by a combination of stack effects and wind effects and would have also been influenced by the positions at which cold external air was entering the sides of the cavity. However, with the horizontal sock in position, stack effects would have been minimised, although not completely eliminated due to the defects in the continuity of the horizontal sock that were observed during the tests.

80 Another possible driver for lower temperatures towards the bottom of the cavity would have been conductive heat flux downwards into the ground, as there was no insulation at the bottom of the party wall cavity. It is also possible that there may have been a cross flow of air through the party wall cavity, with air entering via gaps in the vertical sock on one edge of the party wall cavity and exiting via gaps in the vertical sock on the opposite side of the cavity.

Mechanism of the Party Wall Thermal Bypass

81 The main drivers for the flow of external air into the cavity are likely to be stack effects combined with wind induced pressure effects. We have now collected a wide range of compelling experimental and observational data to support this hypothesis as follows:

a) The measurement data of party wall cavity air flows taken with the horizontal sock removed combined with thermal images of the party wall, as illustrated by the example in Figure 46, show that there can be significant flow of external air into the party wall cavity when there is no barrier to upwards air movement in the cavity past the level of the ceiling.

b) It is apparent that the vertical socks at the junction between the party wall cavity and the external wall cavity do not form an effective air barrier. This is supported by observations during

installation of the vertical socks that showed large gaps that would have allowed the flow of air into the party wall cavity. It is probable that the use of standard mineral wool-filled cavity socks in their current form, and with current installation practice, is unlikely to ever achieve a completely effective air seal to the party wall cavity, although they will reduce the size of the bypass effect.

c) Thermal images taken of the party wall in the loft during the co-heating test when the horizontal cavity sock had been removed (Figures 35 and 37) indicate both that warm air is passing over the top of the party wall and that there is conductive heat flow through the blockwork wall from the party wall cavity into the loft space.

d) Spot measurements were taken using a hot bulb anemometer of air flow coming over the top of the party wall at the ridge in the loft of Redrow plot 110 during the period of the co-heating test when the horizontal sock had been removed. The air flow ranged from 0.5 m/s to 2.0 m/s. A smoke puffer was used to determine the direction of air flow, which was shown to be flowing from the party wall cavity into the loft. Measurements taken in the loft Bryant plot 116 showed a similar flow of air over the top of the party wall and into the loft.

e) Spot measurements were taken using a digital pressure gauge of the pressure difference between the party wall cavity of the Redrow test houses and the outside during the period of the co-heating test when the horizontal sock had been removed. The measurements were taken by positioning the reference hose of the gauge outside and placing the measurement hose of the gauge into the party wall cavity via one of the thermocouple holes on the ground floor of Redrow plot 110. The measurements were taken at a time when there was very little wind (mean wind speed 0.15 m/s). The pressure in the cavity was found to be 4.5 Pa lower than that outside.

f) The observed fluctuation of air flow measurements in the party wall cavity in response to changes in external wind speed is consistent with the notion that air flow in the cavity is partly driven by external wind conditions.

g) The party wall cavity temperatures with the horizontal sock removed responded to external temperature such that the cavity temperature dropped when the external temperature dropped and the cavity temperature increased when the external temperature increased. This indicates that cold air from outside must be entering the cavity at some point.

82 Taking into consideration all these factors we can theorise with some degree of certainty that the mechanism for heat loss via the party wall cavities at Stamford Brook is dominated by a combination of stack driven and wind driven air movement. The postulated mechanism consists of the following stages:

a) A pressure difference will exist between the plenum formed by the party wall cavity and the outside. This pressure difference will in part be caused by the stack effect created by the buoyancy of the warmed air in the cavity and in part by induced pressure differences produced as wind moves around the façade and over the roof of the dwelling.

b) The pressure difference between the party wall cavity and outside will induce cold air from outside to flow through gaps and junctions in the external wall and into the external wall cavity, from where it will flow into the party wall cavity, bypassing the vertical cavity socks.

c) The cold air from outside will mix with the warmer air in the party wall cavity, thus reducing the overall air temperature in the cavity.

d) Heat will move from the heated internal spaces of the dwellings either side of the party wall, through the single blockwork leaves and into the colder cavity, thus raising the temperature of the air in the cavity.

e) Stack and pressure effects will drive the air to move upwards in the cavity, where it will be warmed further by heat flow from the party wall as it rises.

f) The column of warmed air will move upwards to the top of the party wall cavity, therefore bypassing the loft insulation at the level of the ceiling.

g) There will be conductive heat flow from the warm party wall cavity to the cooler loft via the blockwork of the party wall leaves in the loft. The warm air in the cavity will then flow over the top of the party wall where it meets the roof tiles and into the loft. There is a mineral wool fire barrier at the junction between the party wall and the roof, but this would not form an effective air barrier to the movement of air over the top of the party wall.

83 A schematic diagram illustrating the party wall heat loss mechanism that we have proposed is shown in Figure 77.

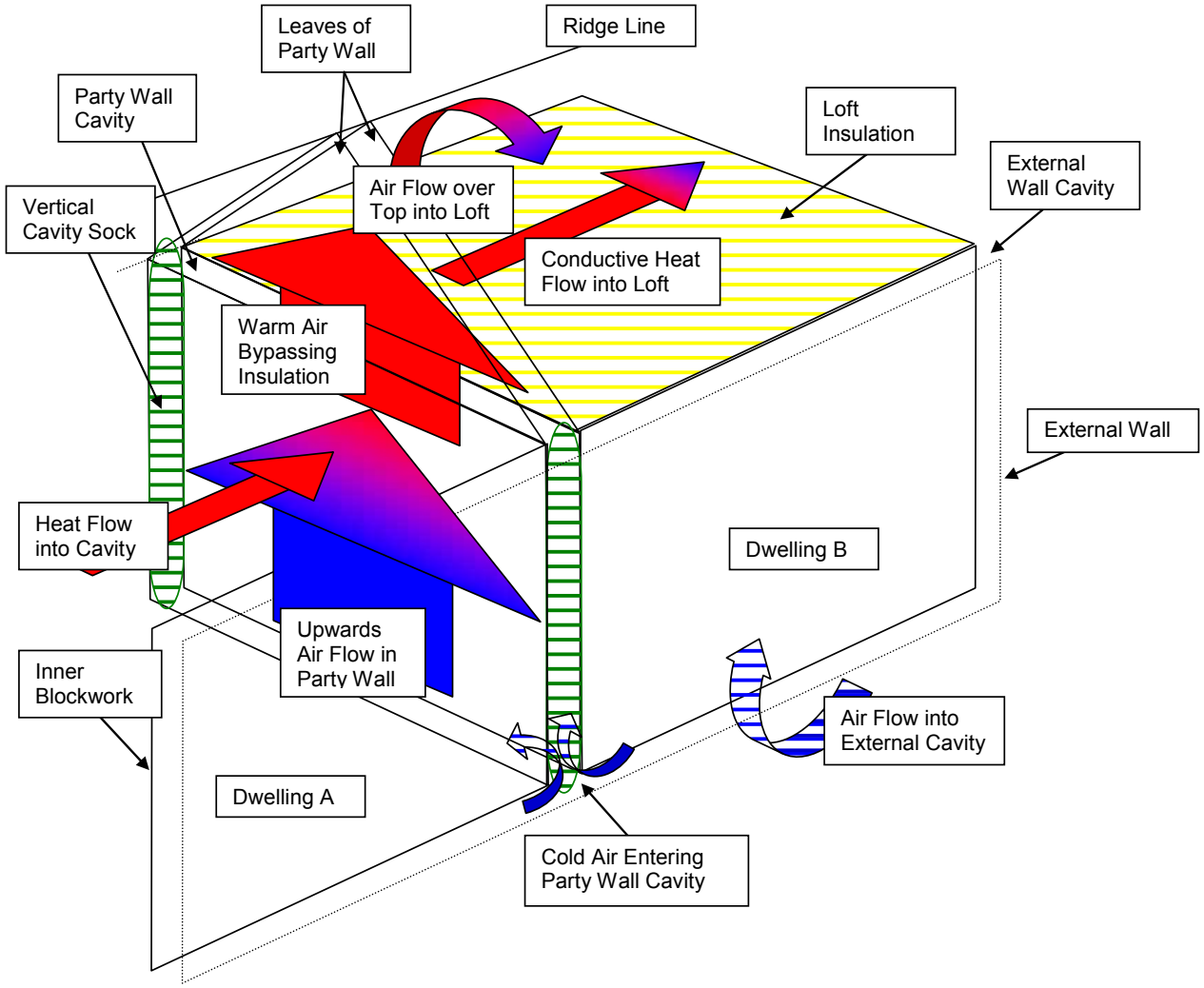

Figure 77 – Schematic Diagram of Party Wall Heat Bypass Mechanism

Effectiveness of the Horizontal Cavity Sock

84 It has been demonstrated that a horizontal cavity sock in the party wall can significantly reduce but not completely eliminate the party wall thermal bypass, whilst at the same time maintaining the acoustic performance of the party wall. The size of the improvement in the heat loss coefficient with the horizontal sock compared to the situation with a clear party wall cavity was between 50% and 75%. Observations of the horizontal sock both during construction and also from within the cavity during the co-heating tests have shown there are likely to be several potential points of leakage around the horizontal sock which would have reduced its effectiveness as a barrier to air movement up the cavity. Possible leakage points could have included:

a) Gaps between individual horizontal socks that had not been tightly butted up against each other.

b) Gaps at the junction between the ends of the horizontal sock in the party wall cavity with the tops of the vertical cavity socks in the external wall cavity.

c) Gaps between the sides of the party wall and the horizontal sock, especially where there were irregular mortar snots that might hold the sock away from the wall and prevent it from forming a good seal with the wall. This was likely to be have been more prevalent in the narrower party wall cavities (75mm) in the Redrow dwellings, where it would have been much more difficult for the bricklayers to reach down into the cavity to strike off any excess bedding mortar. Poor

sealing to the wall might also have occurred in cases where the mineral wool thickness in the sock had been undersized relative to the cavity width. It is thought unlikely that a perfect seal between cavity sock and wall could ever be achieved under real construction conditions.

d) Gaps in the sock caused by falling debris as illustrated in Figure 50.

e) Physical damage to the polythene sleeve that may have occurred during installation, especially where the sleeve had rubbed up against any mortar snots, brick edges or any other sharp protrusions. Any tears or rips in the polythene membrane would have allowed the passage of air directly through the body of the sock.

85 It is also important to bear in mind that, even if it had been possible to completely cut-off air movement upwards in the party wall cavity using the horizontal sock, it is likely that some residual heat loss would have remained, related to conductive losses to the ground via the bottom of the party wall cavity and due to the cross flow of air through the cavity.

Alternative Solutions to Reduce or Eliminate the Party Wall Bypass

86 It is doubtful that the horizontal sock in the form demonstrated at Stamford Brook could ever completely eliminate the party wall thermal bypass. However, it is possible to envisage improvements to the installation process and the configuration and materials used for the sock that might result in further reductions in the size of the thermal bypass. Potential improvements and alternatives might include the following options:

a) A continuous sock of sufficient length to completely fill the cavity width. This would reduce any air flow at junctions between socks. However, a long sock would be difficult to use on site and is more likely to be damaged. Individual socks could be taped together, perhaps using a proprietary jointing sleeve. The vertical and horizontal socks could also be joined together to prevent leakage at that position.

b) The polythene membrane should be comprised of a material grade with sufficient strength and thickness so as to reduce the risk of rips and tears occurring during installation.

c) Improvements could be made to the installation of the vertical cavity socks in the external cavity so that they better seal the entry into the party wall cavity whilst maintaining their original purpose as both acoustic and fire barriers. The air seal could be improved by over sizing the sock so that part of the sock protruded into the party wall cavity. In those cases where the vertical cavity sock comprises a DPC membrane attached to a mineral batt, it may be advantageous to use an adhesive tape to seal the edges of the DPC membrane to the blocks of the internal wall to improve the air seal. There is also scope for improvement in installation practice so that the vertical socks are positioned before both sides of the cavity are complete. This would reduce the risk of snots falling on top of the sock as shown in Figure 58 and would also reduce occasions whereby bricklayers attempt to feed the sock down into the cavity. Both these situations could potentially result in air gaps between socks.

87 The technical solution with perhaps the most potential to eliminate the party wall bypass would be to fully fill the party wall cavity with insulation. This would have the benefit of reducing heat flow into, across and downwards in the cavity and would also restrict air movement around the cavity. Fully filled party wall details are common in construction on the continent as illustrated by the Swedish example shown in Figure 78. The marginal cost to a developer of insulating the party wall would be minimal, comprising mostly of material costs. It would be beneficial to retain the horizontal cavity sock at the level of the ceiling insulation in order to further restrict the potential for upwards air movement. It should be pointed out that the acoustic robust details catalogue (Robust Details Ltd 2005) does not currently include a fully-filled separating wall detail for cavity masonry construction. This would mean that a fully-filled masonry separating party wall detail would need to be submitted to Robust Details Ltd for registration and testing as a proposed new acoustic robust detail, indeed, we understand that such an application is pending. In the interim period prior to approval, it would be necessary for any developer using a fully-filled masonry party wall to conduct post completion acoustic tests in accordance with the provisions of Part E of the building regulations (ODPM 2004). Alternatively, house designers might also consider solid wall constructions for separating walls, as this would completely remove the potential for air movement, although again, careful consideration would have to be given to acoustic performance. One disadvantage of solid party walls is that these would provide little thermal resistance to heat flow between dwellings, whereas insulated party wall cavities would reduce heat flow between adjacent dwellings in addition to mitigating the party wall bypass.

Figure 78 – Fully Filled Party Wall Cavity in Sweden (© R. Lowe and D. Olivier 1980)

Potential Carbon Savings for UK Dwellings

88 There is potential for considerable carbon savings for both newly constructed and existing dwellings built with unfilled cavity masonry party walls if measures were implemented to reduce or eliminate the party wall thermal bypass. It is estimated from the annual NHBC statistics (NHBC 2006) that, of the approximate 200,000[4] dwellings built in the UK every year, around 90% will be of cavity masonry construction. Of these 180,000 masonry dwellings, around 15% (27,000) will be semi-detached properties with one party wall cavity and 20% (36,000) will be terraced dwellings with two party wall cavities. If it is assumed that on average these party walls have an effective *U*-value of 0.5 W/m^{2}K, then the carbon saving if the party wall bypass were eliminated in all new terraced and semi-detached[5] cavity masonry dwellings built each year would be of the order 20,000 tonnes CO_2 per annum. This carbon saving would of course be incremental, with the reduction in CO_2 in the second year following implementation of a solution being 40,000 tonnes CO_2 per annum and so on giving a total saving by 2020 of over 240,000 tonnes.

89 The potential for carbon dioxide savings in the existing stock could be even more significant than that in new dwellings. Of the stock of approximately 20 million dwellings in England, around 40% were built between 1965 and 2006 (DCLG 2006). Nearly all terraced and semi-detached dwellings built after 1965 were likely to have been constructed with some form of party wall cavity. Therefore, if we again assume around 15% (1,320,000) semi-detached properties and 20% (1,760,000) terraced dwellings, and an effective party wall *U*-value of 0.5 W/m^{2}K, then the potential annual carbon saving of rectifying the party wall bypass for all existing dwellings built since 1965 will be of the order 850,000 tonnes CO_2 per annum.

90 It is interesting to note that, contrary to normal expectations, one of the consequences of the party wall bypass is that terraced and semi-detached dwellings built to 2006 standards will have carbon emissions higher than that of a similarly sized detached dwelling. For example, an 80m^2 2006 compliant detached dwelling would have a fabric heat loss coefficient of 98.2 W/K and dwelling emission rate of 24.7 kgCO_2/m^2. In comparison, if we ignore the party wall bypass effect, an 80m^2 mid-terraced dwelling with an aspect ratio of 1.4 would have a fabric heat loss coefficient of 69.7 W/K and a dwelling carbon emission rate of 20.6 kgCO_2/m^2. However, if we include heat loss from the party wall with an effective *U*-value of 0.5 W/m^{2}K, then the fabric heat loss coefficient and dwelling emission rate for the mid-terraced dwelling increase to 107.2 W/K and 26.5 kgCO_2/m^2 respectively. As the detached dwelling has no party wall, we do not have to factor in any additional

[4] The latest published Government target for the rate of construction of new homes in England is 200,000 per year (ODPM 2005). The number of house completions in the UK in 2004 was 203,000 (NHBC 2006).

[5] We used the Leeds Met Parametric SAP spreadsheet (Lowe Wingfield Bell & Roberts 2007) to calculate annual carbon emissions for both a 55m^2 mid-terrace and a 80m^2 semi-detached dwelling with a party wall *U*-value of either zero or 0.5 W/m^{2}K.

bypass loss. This means that an average sized mid-terrace dwelling will have a carbon emission rate around 1.5 $kgCO_2/m^2$ higher than that of an identically sized detached property. The true carbon emissions for a mid-terraced cavity masonry dwelling built to 2006 Building Regulations, but taking into account the party wall cavity bypass, will be typically around 25% higher than expected based on this mechanism alone. The excess would probably be higher if we systematically took account of other common defects. This suggests a powerful case for monitoring of energy use in all new dwellings.

91 As well as masonry terraced and semi-detached dwellings, it is likely that other dwelling forms such as apartments and dwellings constructed using methods other than cavity masonry techniques, will also exhibit an identical or related thermal bypass if they utilise some type of clear separating cavity that bypasses the external insulation layer. For example, the party walls in steel frame dwellings constructed according to Robust Detail E-WS-1 (Robust Details Ltd 2005) consist of two cavities separated by a layer of acoustic insulation as shown in Figure 79. A detailed drawing of a party wall designed according to this detail is shown in Figure 80, and this illustrates the potential for air movement in the two cavities formed by this type of construction, which will allow the air to bypass the ceiling insulation.[6] Similar thermal bypasses are also likely to exist in non-domestic buildings, especially masonry buildings such as small offices that would have been built with very similar construction details to cavity masonry dwellings.

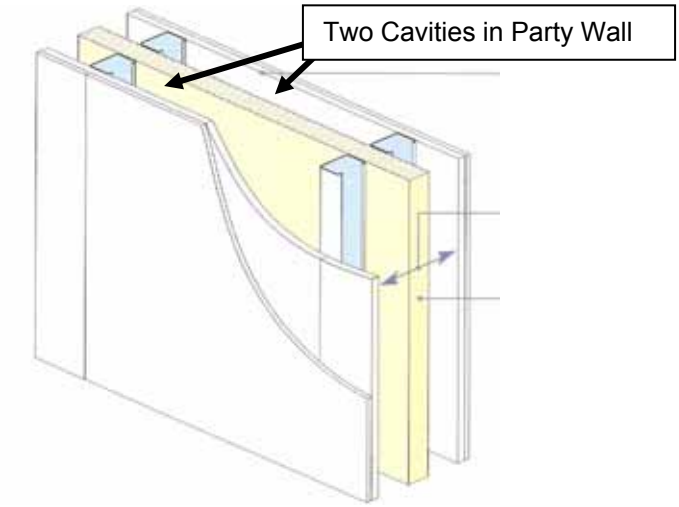

Figure 79 – Robust Detail E-WS-1 Steel Frame Separating Wall (Robust Details Ltd 2005)

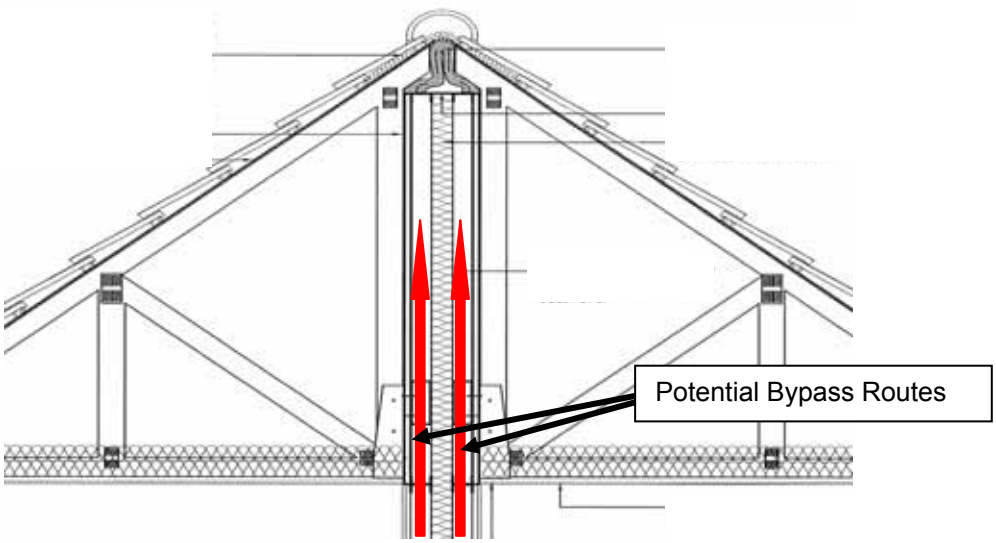

Figure 80 – Party Wall Detail for Steel Framed Dwelling

[6] The horizontal framing elements at the ceiling junction will contain several holes and joints, and as such will not form an effective barrier to air movement up the cavity.

Predicted Heat Loss Coefficients

92 The expected ventilation and fabric heat loss coefficients for the test properties were predicted with the Leeds Met parametric SAP energy model (Lowe Wingfield Bell & Roberts 2007) using the construction details outlined in Table 1 and the measured background ventilation rates from Table 6. The predicted heat loss coefficients so obtained are given in Table 9. These predictions do not include any contribution from the party wall and assume that the thermal bridging is in line with the original design details as described in the project on the design process (Roberts Lowe and Bell 2004).

Table 9 - Predicted Heat Losses of Co-heating Test Dwellings using SAP

Plot	Ventilation Heat Loss Coefficient C_v (W/K)	Fabric Heat Loss Coefficient C_f (W/K)	Thermal Bridging (included in C_f) (W/K)	Total Heat Loss Coefficient $C_v + C_f$ (W/K)
Bryant 116	8.0	50.6	6.0	58.6
Bryant 117	8.5	50.6	6.0	59.1
Redrow 110	23.1	62.7	6.6	85.8
Redrow 111	16.3	81.7	7.5	98.0

93 It is apparent that the predicted whole house heat loss coefficients given in Table 9 differ significantly from the heat loss coefficients measured during the co-heating tests. In the case of the two Bryant dwellings, the measured and uncorrected whole house heat loss coefficients for the co-heating test period without the horizontal sock were of the order 105 W/K. This compares to the predicted value for these dwelling types of around 60 W/K, so there is a discrepancy of around 45 W/K to account for. We have already calculated from the party wall cavity temperatures that the size of the heat loss due to the party wall bypass for the Bryant test dwellings will be of the order 20 W/K (Table 3). This means that a further heat loss of around 25 W/K has still to be accounted for. We know that some of this additional 25 W/K heat loss will be due to additional thermal bridging that we have observed with thermal imaging camera, and that this will be over and above that calculated by theoretical modelling of the junctions as originally designed. If we assume a scenario whereby the actual thermal bridging for Bryant plots 116 and 117 is no better than that expected for accredited construction details as outlined in SAP 2005[7] (BRE 2005), this would give a loss due to thermal bridging of 12 W/K rather than the 6 W/K in Table 9. It is perhaps likely that, given the severity of some of the thermal bridges observed during the co-heating test, that the real thermal bridging may actually be even higher than this. There will also be further additional heat loss over and above the predictions due to other factors such as the observed missing external wall insulation (Figure 40) and mortar snots that bridge the external cavity (Figure 59).

94 It is interesting to note that the heat loss coefficient for the two Bryant properties 116 and 117 were very similar to the identical house type (Plot 13) that was measured during the previous set of co-heating tests (Wingfield et al 2005). However, when thermal imaging was originally conducted on plot 13 during the winter of 2005-2006, no significant thermal bridges were observed. To confirm that this was still the case, the research team carried out additional thermal imaging on plot 13 during February of 2007. This time around, some areas of higher than expected heat loss were observed in plot 13, albeit at different junctions to those observed on Bryant plots 116 and 117. In particular, a significant thermal bridge was seen at the junction between the external wall and the ground floor as illustrated in Figure 81. In order to understand why this might be the case, the photographic records of the early phase of construction at Stamford Brook were reviewed. We were able to ascertain that Bryant plots 13 and 14 were constructed with a floor slab that continued across the external cavity as shown in Figure 82, thus forming a direct thermal bridge. This helps to explain the significant heat loss observed in the infra-red images of this junction.

[7] For dwellings constructed using accredited details, a y factor of 0.08 is used for thermal bridging where $H_{TB} = y \Sigma A_{exp}$. In cases where accredited details have not been used the y factor is 0.15.

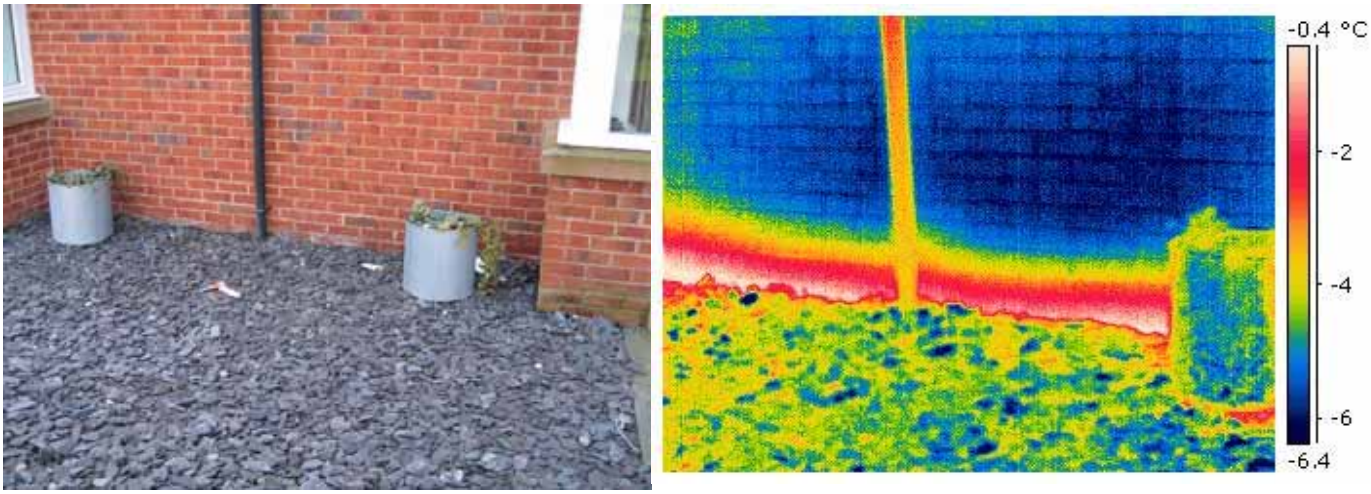

Figure 81 – Heat Loss at Junction between External Wall and Ground Floor - Bryant Plot 13

Figure 82 – Ground Floor of Bryant Plots 13 and 14 under Construction

Technical and Design Implications of the Party Wall Bypass

95 The observed heat loss due to air movement in a party wall cavity is a classic example of a thermal bypass mechanism. These mechanisms are typically found in building designs which incorporate voids, cavities, chimneys, flues, ducts, enclosed service risers or other similar unobstructed passages that could provide potential routes for heat transfer involving the movement of air that can bypass the insulated external envelope.

96 The possibility of significant heat loss from buildings via such thermal bypass mechanisms was first identified in the late 1970s and early 1980s by the Centre for Energy and Environmental Studies at Princeton University (Harrje Dutt & Gadsby 1985). The Princeton research group identified several classes of heat loss mechanism involving air movement in enclosed voids. These included for example, air leakage into loft spaces via hidden paths in internal partitions and convective loops in sealed but uninsulated soffits that allow air movement between the loft and the soffit cavity. A directly comparable bypass to the situation at Stamford Brook was a convective loop mechanism identified by the Princeton research team during the Twin Rivers project (Harrje Dutt & Beyea 1979). This particular heat loss path was found to occur in hollow cinder block party wall constructions and has some similarities with the party wall bypass at Stamford Brook, with the main difference being that the mechanism at Stamford Brook is fed by external air, whereas the heat loss in the party wall at Twin Rivers was a fully convective loop with no mixing of the external air with that in the sealed enclosed cavity formed by the hollow blocks. Schematic diagrams illustrating some of the different bypass mechanisms proposed by the Princeton team are shown in Figure 83.

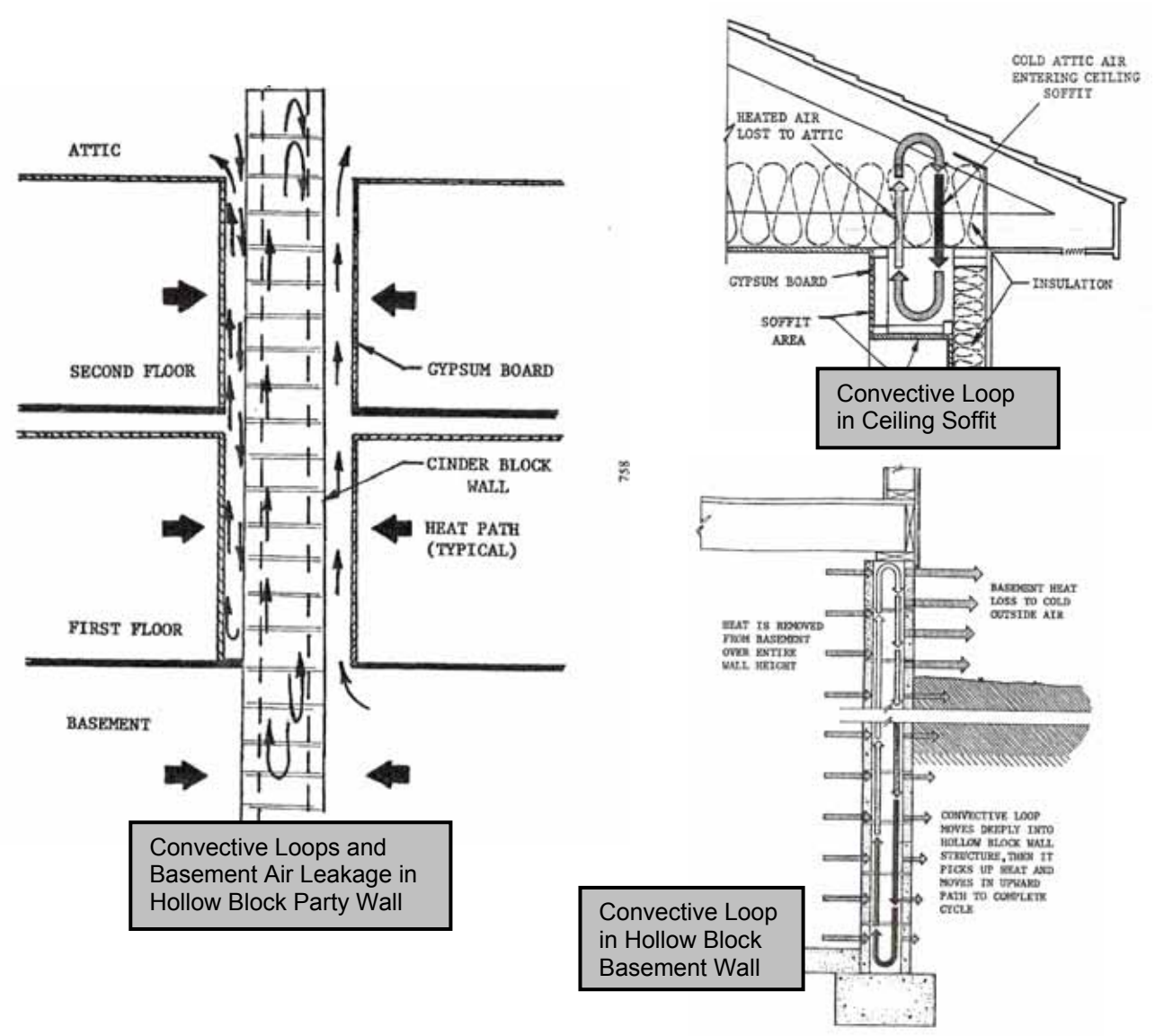

Figure 83 – Examples of Thermal Bypass Mechanisms (Harrje Dutt & Gadsby 1985)

97 It is likely that other potentially significant heat bypass mechanisms will exist in typical UK dwelling designs and that, like the party wall bypass, they would have been routinely omitted from heat loss calculations and not considered when design decisions were made. An example of a common design feature in UK masonry dwellings with the potential to form a convective loop bypass is the boxed-in soil stack that terminates in the loft. Convective loop heat loss could occur in situations where the stack penetration through the ceiling is not properly sealed, as is often the case, and where the service void in the heated space is well sealed both to the wall and any pipe penetrations.

98 As the energy performance of UK houses improves in response to tougher carbon emission performance targets, hitherto overlooked thermal bypass mechanisms, and in particular the party wall bypass, will begin to dominate overall fabric heat loss if action is not taken to minimise their effect in new buildings. It is important that developers and house designers reassess their design portfolios to look for potential bypass routes, in particular for separating walls between dwellings. Designs should be adapted to eliminate or minimise any heat loss by such bypasses. As such, clear design guidance will be needed to help designers identify these problems and also to suggest potential solutions and alternative design strategies.

99 Perhaps the best general design advice to avoid thermal bypassing is to ensure that the thermal insulation layer and air barrier are in close contact and maintained in the same plane around the

external envelope, that there are no discontinuities in the air barrier, and that the air barrier is continued across cavities between dwelling units.

Regulatory Implications of the Party Wall Bypass

100 There are no specific requirements in Part L1A 2006 of the Building Regulations (ODPM 2006) to take account of heat loss by thermal bypasses. Part L1A 2006 requires that the *U*-values should be calculated according to the methods and conventions set out in BR443 (Anderson 2006) and that CO_2 emission rates are calculated using the 2005 edition of the Standard Assessment Procedure (SAP2005) (BRE 2005). The conventions in BR443 do not include any guidance for calculating heat losses via party wall cavities between adjacent heated dwellings, as it is assumed, incorrectly, that these losses would always be negligible. The assumption made in SAP 2005 is also that losses via party walls are insignificant. It states in SAP 2005 that "Losses or gains through party walls to spaces in other dwellings or premises that are normally expected to be heated are assumed to be zero" (BRE 2005). It will therefore be necessary to update both BR443 and SAP 2005 to take account of the potential for the party wall cavity thermal bypass and other similar bypass mechanisms.

101 The most recent edition of the Accredited Details for masonry construction (DCLG 2007) includes guidance on construction of the junctions between a masonry cavity party wall and both the ceiling (detail MCI-IW-02) and external wall (detail MCI-IW-01) as shown in Figure 84. However, the guidance does not include any information on the potential for thermal bypassing via the party wall. It will be necessary to include specific advice in Accredited Details on how to construct separating walls to reduce the thermal losses resulting from the party wall cavity bypass.

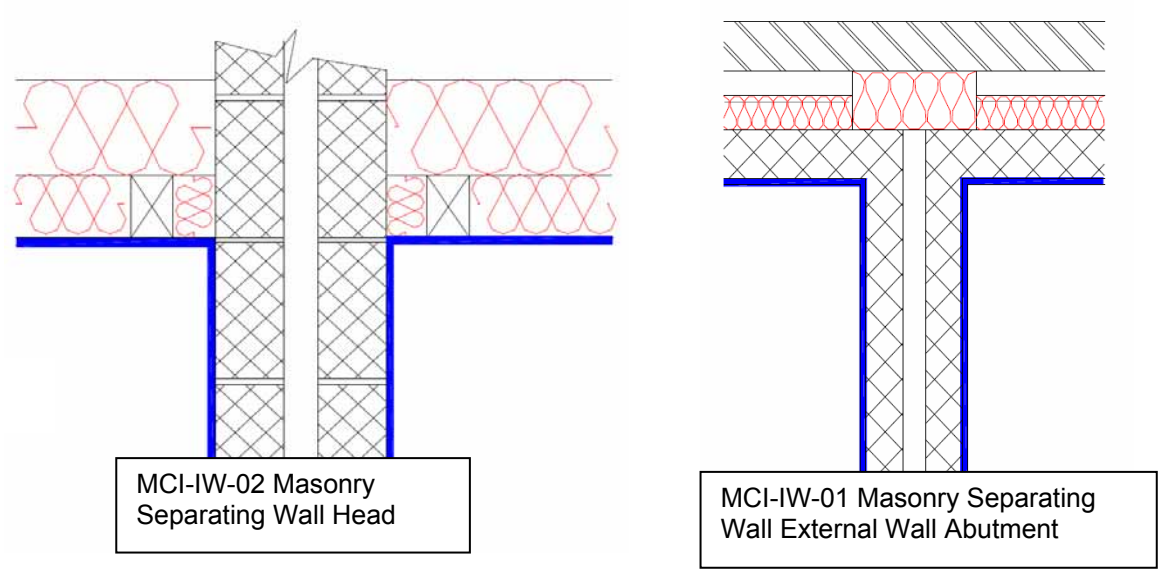

Figure 84 – Accredited Detail Drawings – Masonry Separating Wall (DLCG 2007)

102 It should be noted that the Accredited Detail for the eaves junction of a room-in-roof construction with a pitched roof where the roof insulation is located between the rafters of the roof (MCI-RE-07 (DCLG 2007), does in fact give rise to potential for a thermal loop bypass as shown in Figure 85 which is similar to the soffit bypass shown in Figure 83. This situation arises due to that fact that the insulation layer and air barrier are not in the same plane. This creates a void behind the knee wall in the attic room which is positioned between the insulation layer and the air barrier. Cold air can readily enter this void via the roof structure, where it will be warmed by conduction from the heated internal space via the ceiling below and the knee wall[8]. The warmed air can then leave the void via the roof structure.

[8] One response to this assertion is that, if constructed correctly, the void should not be ventilated and therefore eliminating any bypass. However, even if this could be achieved, the existence of a "sealed" space would exacerbate any potential problems associated with moisture build up. It is inevitable that some ventilation of the space would be necessary but to allow ventilation to the inside would destroy the air barrier and to allow ventilation to the outside would create a bypass route, hence catch 22!

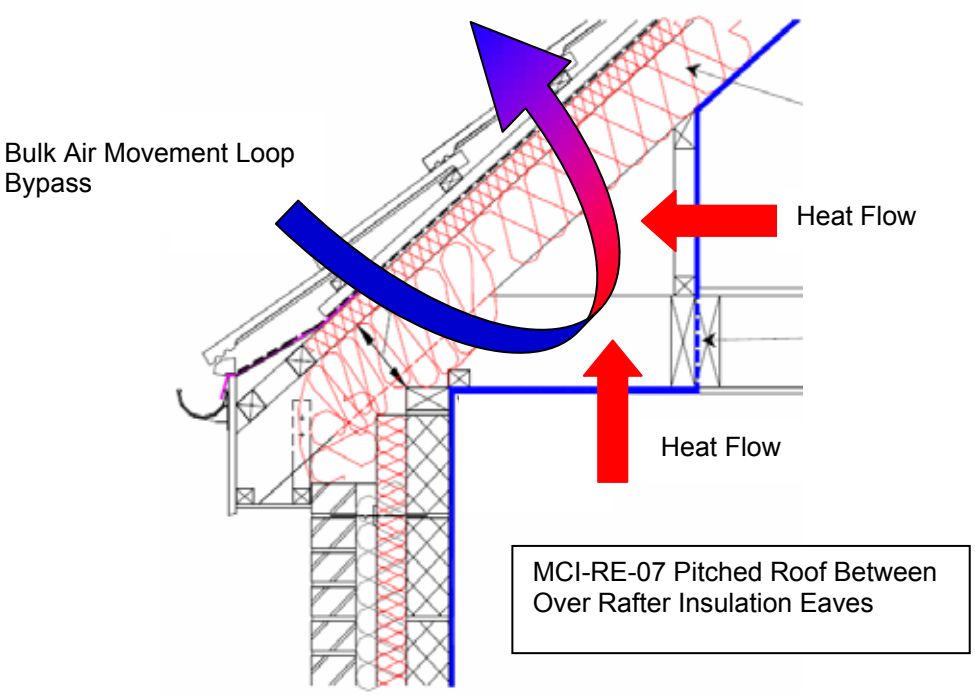

Figure 85 – Loop Thermal Bypass - Accredited Detail MCI-RE-07: Pitched Roof Between Over Rafter Insulation at Eaves

Difference between Designed and Realised Performance

103 It is clear from the measured whole house heat loss coefficients that there was a significant gap between the expected energy performance of the dwellings as designed and the reality of the energy performance as they were constructed. We know from our measurements of party wall cavity temperatures that a large proportion of the difference would have been due to the party wall thermal bypass (see paragraph 25 above). We know, both from our observations during the construction process and testing procedures and also from infra-red thermal imaging of the houses that, after taking into account of the party wall bypass, some of the remaining discrepancy in energy performance will be due to other deficiencies in the building fabric. We expect that actual thermal bridging through linear junctions will be higher than predicted and that the true *U*-values of the floors, walls and ceilings as constructed will also be higher than calculated.

104 The number and variety of defects that were observed and photographed during the construction of the co-heating test houses at Stamford Brook would at first sight seem worrying. However, this should not be considered anything unusual. The Leeds Met research team and the BRE have recorded a similar wide range of construction defects on many housing developments across the UK (Bell Smith & Miles-Shenton 2005, Johnston Miles-Shenton Bell & Wingfield 2004, Johnston Miles-Shenton & Bell 2005, Doran & Carr 2005, Bonshor & Harrison 1982, Harrison 1993). What is clear is that there can be a significant gap between the perfection of construction details as shown on the drawings and as envisaged by the house designer when compared to the reality of the same details as they are actually constructed on site.

105 There could be many reasons for the gap between design intention and realised performance. These issues are not confined to the Stamford Brook development but are common across the UK construction industry and would include the following potential factors:

a) Deliberate design changes made for reasons other than performance such as aesthetic requirements or cost reduction measures.

b) Inadequate quality control procedures.

c) Inadequate training.

d) Lack of understanding of the importance of maintaining construction standards and the possible consequences of failing to meet the required standards.

e) Lack of detailed design information available on site for specific details.

f) Insufficient technical information and construction guidance provided on drawings.

g) Not enough feedback between the design teams and construction teams.

h) Incorrect materials or components delivered or used on site.

i) Inappropriate product substitution.

j) Buildability Issues

k) Sequencing issues.

l) Poor robustness of design or components in relation to the potential for construction or installation errors or faults.

m) Insufficient allowance made in design for construction variability and tolerances.

n) Insufficient focus on the principles of heat loss and their practical application in most courses on building and building design.

o) Unfamiliarity with construction techniques.

p) Commercial time pressures.

q) Poor quality workmanship.

106 In order to illustrate the potential cumulative effect on thermal performance of the various design decisions that are constantly being made and also of the impact of construction variability, we have looked in more detail at the evolution of one specific detail at Stamford Brook. The example chosen for this demonstration is the window head, as it illustrates the combined effect of changes in design, construction tolerances, quality control and workmanship. For this comparison we have modelled the window head in its various forms using the Therm two-dimensional finite element simulation tool (LBNL 2003). Five different models were developed to take account of the various changes in design and the observed construction quality. An example of one of the models is shown in Figure 86. To demonstrate the effect of any changes on thermal performance, the modelled U-factors for each configuration were used to calculate a value of linear thermal transmittance for each situation as given in Table 10. The five models are shown in Figures 87 to 91 with the resultant heat flow patterns shown as a colour flux magnitude (flux in W/m^2)[9].

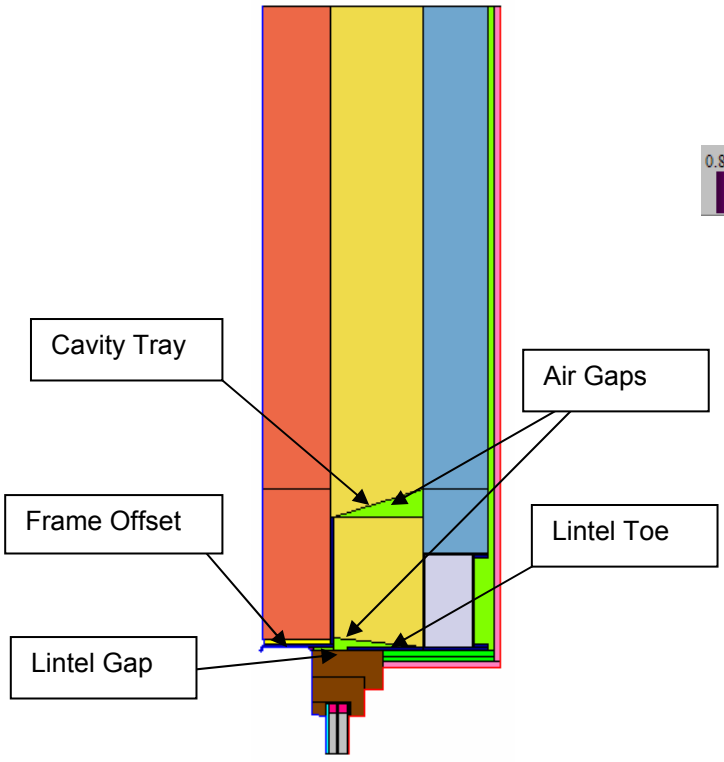

Figure 86 – Therm Model of Window Head as-built Inner Lintel with Toe, 75mm Frame Offset, Air Gaps

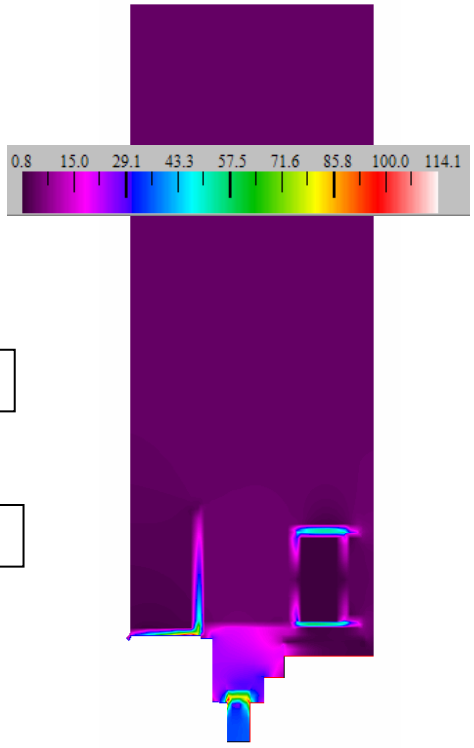

Figure 87 – Colour Flux Magnitude Frame in Line with Insulation

[9] The colour scale of the flux magnitude varies in each model.

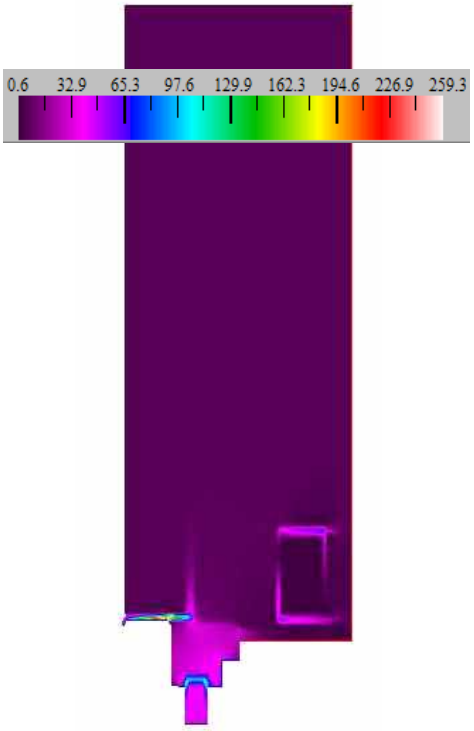

Figure 88 – Colour Flux Magnitude
75mm Frame Offset

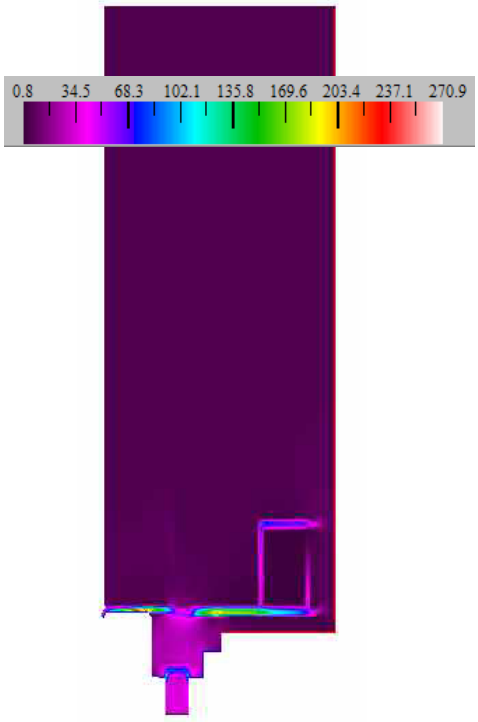

Figure 89 – Colour Flux Magnitude
75mm Frame Offset, Lintel with Toe,
42mm Lintel Gap

Figure 90 – Colour Flux Magnitude
75mm Frame Offset, Lintel with Toe,
20mm Lintel Gap, Air Gaps around Insulation

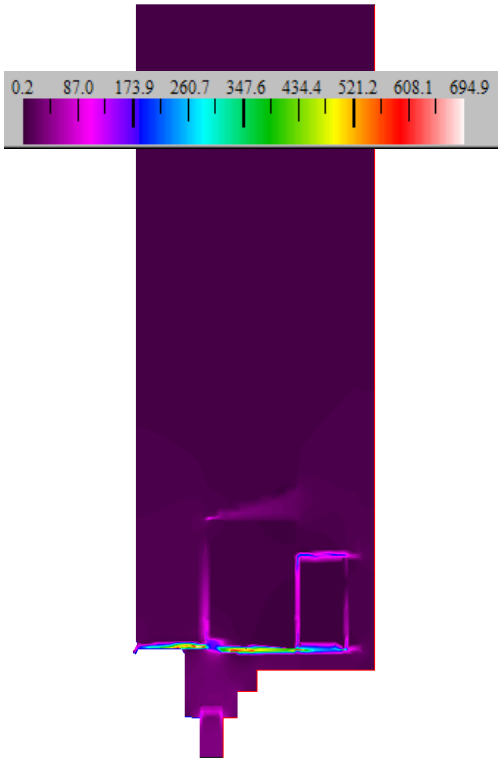

Figure 91 – Colour Flux Magnitude
75mm Frame Offset, Lintel with Toe
20mm Lintel Gap, Air Gaps around Insulation,
Uninsulated Reveal Board

107 The starting point for the window head design is shown in Figure 87. This is the optimum thermal solution with separate lintels, the window frame in line with the cavity insulation and with insulated reveal boards. The Ψ value for this configuration is 0.016 W/mK as given in Table 10. The effect of frame location is discussed in more detail in the Stamford Brook design report (Roberts et al 2004). It can be seen from Figure 87 that the heat flux from the inside of the window to the outside is concentrated at the edge spacer around the window glass.

Table 10 – Window Head Linear Thermal Transmittance and Effect on Total Thermal Bridging and Dwelling Carbon Emission Rate (DER)

Description of Window Head Detail	Ψ value (W/mK)	Total Thermal Bridging (W/K)	Bryant Chatsworth Dwelling Emission Rate DER ($kgCO_2/m^2$)
Plain Twin Lintels – Optimum design with window frame position in line with insulation	0.016	5.98	18.07
Plain Twin Lintels – 75mm frame offset	0.019	6.00	18.07
Inner Lintel with Toe – 75mm frame offset – modelled as drawing with 42mm lintel gap	0.068	6.44	18.13
Inner Lintel with Toe – 75mm frame offset – modelled as observed with 20mm lintel gap & air spaces above lintel	0.181	7.43	18.26
Inner Lintel with Toe – 75mm frame offset – modelled as observed with 20mm lintel gap & air spaces above lintel, no insulated reveal board	0.203	7.63	18.28
Combined Lintel – Table K1 value from SAP 2005 (BRE 2005)	0.300	8.48	18.39

108 The initial decisions to make changes to the optimised window head design were made by the developers' designers following construction of test walls. Firstly, it was decided to position the frame so that it overlapped the external brick wall by 27mm, instead of being completely in line with the insulation. The intention here was to make it easier to fit the frame into the window opening. Secondly, the decision was made to change the simple internal steel lintel to one with a 100mm long protruding toe, with the intention that the toe would provide a support to affix the reveal plasterboard (Roberts et al 2004). This had the consequence of reducing the effective gap between the lintels over the window opening from 142mm to 42mm. The combined effect of these two changes was to increase the Ψ value from 0.016 W/mK to 0.068 W/mK (Table 10). Observations during construction showed that in a typical window installation the gap between the two lintels could actually be as low as 20mm not 42mm (Figure 62) and that there were air gaps around the mineral wool insulation batts between the lintels. When these defects were modelled (Figure 90) the Ψ value more than doubled to 0.181 W/mK. The final factor to be taken into account was the discovery that plain plasterboard had been used instead of reveal board lined with polyurethane insulation. This was apparently a decision taken on site for aesthetic reasons, as there was concern that the insulated reveal board covered up too much of the window frame. The consequence of this change was that the Ψ value has now increased to 0.203 W/mK. It can be seen in Figure 91 that the flux density is now concentrated along the bottom of the lintels and at the gap between the two lintels. The final Ψ value of 0.203 W/mK is more than 10 times the original design conception of 0.016 W/mK and is getting very close to the value of 0.3 W/mK for a single combined lintel given in Table K1 of Appendix K in SAP 2005 (BRE 2005). In the case of the Bryant Chatsworth house design (Plots 116 and 117), the consequence of these increases in the thermal bridging at the window head would be to increase the predicted dwelling carbon emission rate from 18.1 $kgCO_2/m^2$ to 18.4 $kgCO_2/m^2$, an increase of 1.7%.

109 The use of retro-filled mineral wool insulation for the external wall at Stamford Brook instead of building the insulation in with mineral wool batts has resulted in several problems. We have observed large accumulations of mortar snots at the bottom of cavities, on top of cavity trays and on top of cavity socks. We have identified several areas of missing insulation where the filling process has not completely filled the cavity, as for example the zone of missing insulation between Bryant plots 116 and 117. We have also observed that sometimes the insulation does not always fill right up to the top of a cavity, as for example in the case of the threshold of Juliet balconies. All these factors would have reduced the effective *U*-value of the external walls. One advantage often stated for retro-filling is that it is more likely to stop air flow in the cavity and thus avoid any potential

problems with bypassing caused by air circulation via gaps around improperly installed mineral wool batts. However, we have shown with the party wall mechanism that there can still be significant air flows in retro-filled cavities. It is probable that the cold external air flowing into the party wall cavity will be warmed as it passes through the insulated external cavity. This would mean that the effective *U*-value of the external wall would be higher than expected.

110 Using built-in mineral wool batts would have reduced the occurrence of mortar snot accumulations. It would also be easier to visually inspect, monitor and control the installation of built-in insulation during the construction process compared to retro-filling. This overcomes the biggest problem with retro-filling where it is much more difficult to check whether the installation has been carried out properly, as the entire process is hidden from view. More fundamentally, the approach to construction of cavity trays in cavity masonry walls makes these walls almost impossible to insulate properly. The design of cavity trays and lintels has developed over the decades incrementally, with little empirical feedback on the aspects of performance that these elements of construction are supposed to ensure, and with none on aspects of performance that may be compromised by them. It is hard to resist the conclusion that a root and branch reassessment of the detailing of masonry cavity walls is needed.

Training Implications

111 It is almost certain that most house designers have not been taught about and do not understand the potential for heat loss by these obscure but potentially significant bypass mechanisms. There is therefore a need to improve understanding of these issues across the industry, especially in house design. Potential routes to get this information across might include the following:

a) There is currently no mention of thermal bypassing in any of the design advice given by the Energy Saving Trust in the Energy Efficiency Best Practice in Housing series of guides. These guides could be updated to include information on thermal bypassing, ideally with the addition of a new guidance note specifically on this issue.

b) Given that the majority of new dwellings in the UK are constructed under a building control inspection regime administered by the NHBC, there is an opportunity for the NHBC to both provide guidance and also to monitor the adoption of new construction methods to minimise thermal bypassing.

112 There would also be a need for building control authorities to ensure that building inspectors are aware of the potential for thermal bypassing.

Supply Chain Implications

113 There are opportunities for the construction product supply chain to develop new products, components and materials that will assist house builders to eliminate heat loss via party wall cavities, reduce general construction variability, especially at junctions, and to minimise the potential for sequencing errors and poor workmanship. Products could be developed that would make it easier to achieve the desired low levels of thermal bridging at openings without requiring high levels of accuracy in component placement. An example of a potential new product would be a solution to the need for separate steel lintels at window and door heads in preference to the combined lintels more commonly used in the UK. It is possible to imagine a product that combines two lintels with insulation between and a cavity tray above as shown in Figure 92. In this case, both lintels are directly bonded to a foam insulant which separates the lintels by the correct distance. The foam insulant is formed with the appropriate slope to create the shape of the cavity tray and is covered by and possibly even bonded to a plastic moulding that connects all the components. Such a product would overcome problems with missing insulation, close the cavity, maintain the correct gap between lintels and also provide a surface to which the reveal boards can be attached. Similar products to the one outlined are already available on the UK market that could be readily be modified to suit as illustrated by the example of an insulated cavity tray product shown in Figure 93. This product is designed for use at the bottom of a cavity (hence the additional edge insulation for the slab) but small adaptations by the manufacturer would make it suitable for use with separate lintels at a window head.

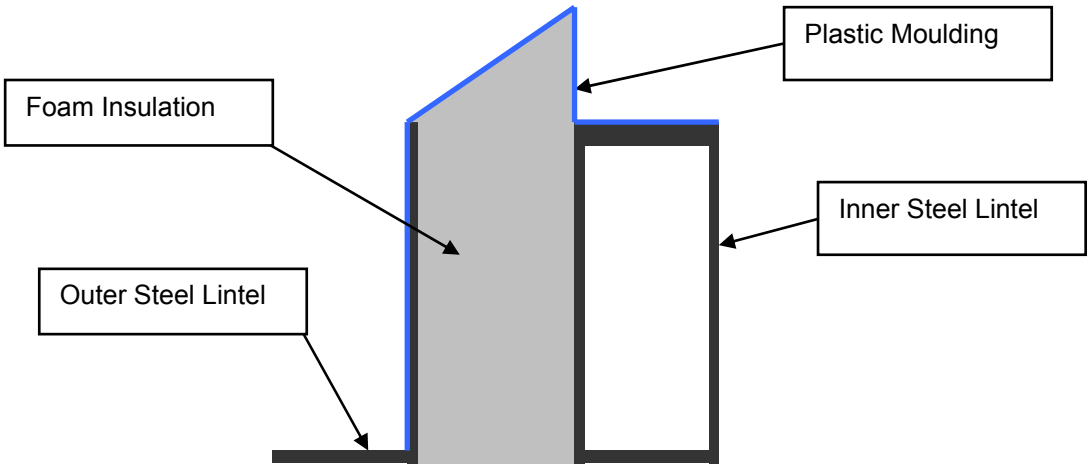

Figure 92 – Separate Window Head Lintels with Insulation Spacer and Cavity Tray

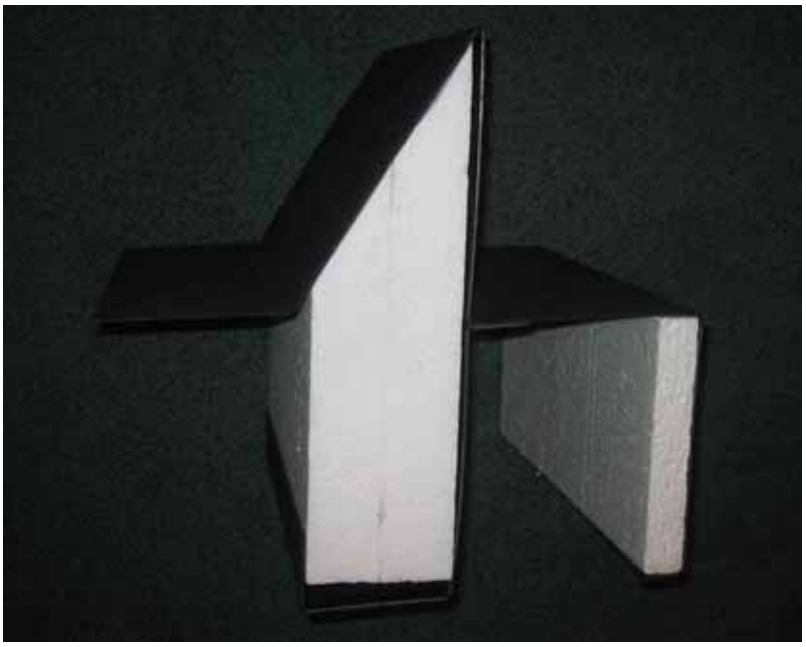

Figure 93 – Commercially Available Insulated Cavity Tray Product

Co-heating Test Methodology

114 The co-heating test has been shown to be a useful method for determining actual fabric heat loss from dwellings. There would be significant benefits if the construction industry encouraged wider adoption of this technique for assessing the real performance of low carbon housing designs, especially if used in conjunction with long term monitoring of energy in use of occupied dwellings. The co-heating test would be an invaluable tool to assess the impact of regulatory changes to energy legislation.

115 There remain concerns about the possible effects of the elevated internal temperatures on ventilation heat loss. It is possible that at internal temperatures of 25°C to 27°C, background ventilation due to stack effects may be higher than we have predicted from our ventilation model (Lowe 2006), especially if ventilation loss is dominated by exfiltration into the loft space. Pressure measurements taken during the co-heating test in the 3-storey Redrow plot 110 indicated that the neutral plane is adjacent to the ceiling, and that the ceiling is depressurised with respect to the inside heated space[10]. This would make the whole area of floor and walls the infiltration zone and

[10] The position of the neutral plane should not be a function of temperature or temperature difference.

the whole of the ceiling the exfiltration zone. It is suggested that in future co-heating tests the set point for the internal temperature is reduced to a level closer to that typically found in occupied dwellings. Temperatures of between 21°C and 23°C would seem a reasonable compromise.

116 Ideally, the heat loss coefficients obtained from a co-heating test should be corrected for uncontrolled external influences such as solar gain and wind. We were not able to do this with any statistical validity for most of the data collected during these co-heating tests, mainly due to the short experimental periods and insufficient range of delta-T. However, in the case of Bryant plots 116 and 117 with the horizontal sock in the cavity, the data were good enough for a multiple regression analysis with power input (W) as the dependent variable and daily mean solar insolation (W/m^2), daily delta-T (K) and daily mean wind speed (m/s) as the independent variables. The calculated regression coefficients are given in Table 11. The raw and corrected heat loss data are plotted in Figure 94. Using these data, the whole house heat loss coefficient corrected for both wind speed and solar gain is around 85 W/K with an r^2 coefficient of determination of around 0.9. This compares to the uncorrected heat loss coefficient of around 105 W/K as discussed in paragraph 41 above. The difference between raw and corrected heat loss is mostly due to the wind correction. However, corrections for wind speed are theoretically complex and by adjusting for wind we are removing an unknown proportion of the party wall bypass loss and an unknown proportion of the background ventilation loss. The solar aperture for these dwellings is numerically equivalent to the solar regression coefficient, which would give an area of between 0.2 to $0.3m^2$, which is perhaps less than we would have expected given the physical area of glazing in these dwellings, even corrected for g, although this is partly due to the east-west orientation of the glazed facades.

Table 11 – Multiple Regression Data – Bryant 116-117 – Horizontal Sock in Position
Dependent Variable = Power (Watts)

	Bryant Plot 116			Bryant Plot 117		
	Coefficient	**Error**	**t-statistic**	**Coefficient**	**Error**	**t-statistic**
y intercept	0	-	-	0	-	-
Solar Insolation Variable	-0.297	0.401	-0.741	-0.186	0.300	-0.621
Delta-T Variable	84.337	1.837	45.914	85.984	1.399	61.476
Wind Speed Variable	373.944	42.673	8.763	396.289	31.981	12.391
r^2 coefficient of determination	0.868	-	-	0.922	-	-

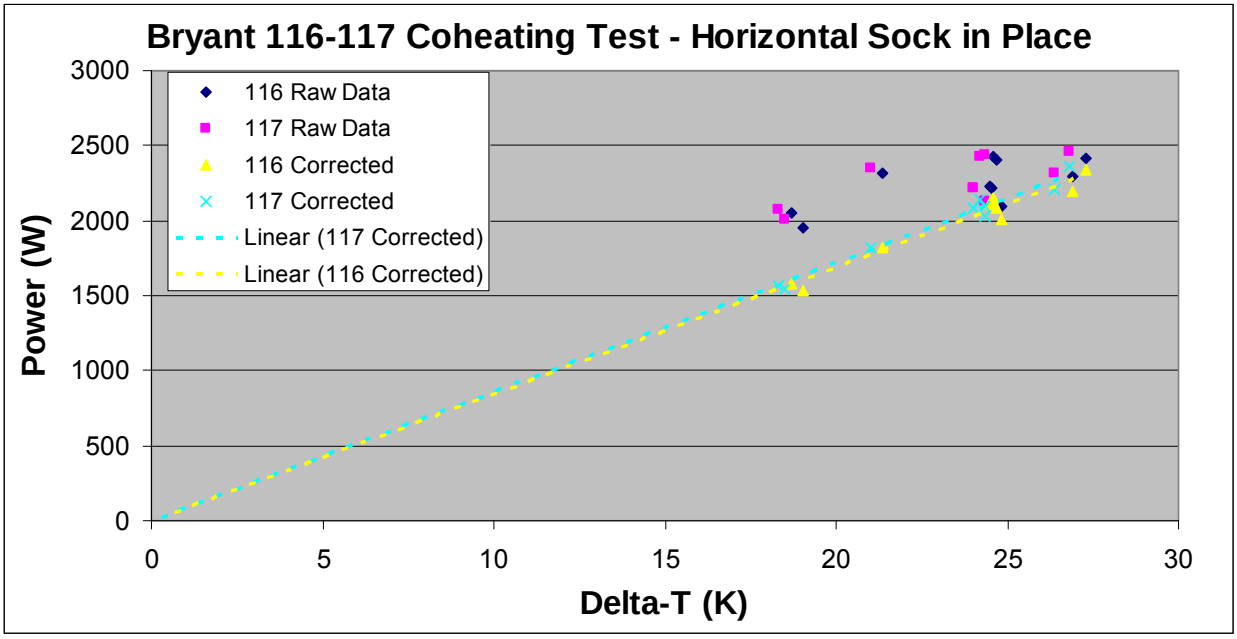

Figure 94 – Bryant Plot 116 & 117 – Co-heating Test with Horizontal Sock - Raw and Corrected Data

Conclusions & Recommendations

117 We have shown that heat loss via a party wall bypass in cavity masonry construction can be significant. Party wall bypass losses will have been present in a large proportion of semi-detached and terraced dwellings with cavity party walls built in the UK since the 1960's[11], and up until now these heat losses have been overlooked in technical guidance and thermal modelling conventions. It will be necessary to update SAP 2005, BR443 and the Part L Accredited Details to take account of the potential for heat loss via party wall cavities and other similar bypass mechanisms. It is recommended that a desk study is undertaken to identify other classes of bypass mechanism that may be present in the design of common UK house types or that may be related to specific construction methods and technologies used in the UK.

118 Experiments to mitigate the party wall bypass by placing a mineral wool-filled cavity sock positioned horizontally in the party wall cavity were only partially successful, and reduced the effective *U*-value of the party wall from around 0.5 W/m^{2}K to between 0.1 to 0.2 W/m^{2}K. Acoustic testing showed that the horizontal sock was not detrimental to the acoustic performance of the party wall. Further work will be required to develop improvements to this method of controlling the party wall bypass, by for example better air sealing of the vertical socks, and also to investigate alternative methods such as fully filling the party wall cavity with insulation.

119 Analysis of the heat loss data, cavity temperatures and air flow measurements has shown that the mechanism for heat loss via the party wall is driven by upwards air movement in the cavity. This air movement is generated by thermal stack effects and by pressure differences caused by the action of wind moving across the dwelling. Heat transfer from the internal conditioned spaces occurs by conduction through the single leaves of the party wall into the party wall cavity.

120 Improved design guidance will be required to assist UK house designers to incorporate measures in the design of new buildings and also to adapt their existing dwelling design portfolios to take account of bypasses such as the party wall cavity bypass.

121 There is potential for significant carbon savings for both newly constructed and existing dwellings built with unfilled cavity masonry party walls if measures were implemented to reduce or eliminate the party wall thermal bypass. If it is assumed that a typical cavity party wall has an effective *U*-value of 0.5 W/m^{2}K, then the potential carbon saving if the party wall bypass were eliminated in all new terraced and semi-detached cavity masonry dwellings built in the UK each year would be of the order 20,000 tonnes CO_2 per annum. The potential for carbon dioxide savings in the existing stock could be even more significant than that in new dwellings. If the stock of terraced and semi-detached dwellings built after 1965 had improvement measures carried out to eliminate the party wall bypass then the potential carbon saving would be of the order 850,000 tonnes CO_2 per annum. It is interesting to note that, contrary to normal expectations, one of the consequences of the party wall bypass is that terraced and semi-detached dwellings built to 2006 building regulation standards will have carbon emissions higher than that of a similarly sized detached dwelling.

122 It is suggested that Bryant and Redrow strongly consider adapting their party wall designs for the dwellings that remain to be constructed during the later phases at Stamford Brook so as to minimise heat loss by the party wall bypass mechanism. This could involve using the horizontal cavity sock as described in this report or by fully insulating the party wall cavity.

123 It is recommended that co-heating tests are used much more frequently in energy performance studies of new housing developments. They have been shown to be an effective and invaluable tool in understanding heat loss characteristics of dwellings.

124 We have demonstrated that infra-red thermal imaging, when used under appropriate conditions, is an extremely effective technique for diagnosing building heat loss effects. We have also found it useful in the identification of hidden air leakage paths during depressurisation tests (Miles-Shenton et al 2007). It is suggested that greater use of thermal imaging, especially when used in conjunction with co-heating tests, would provide enhanced information of the thermal performance of energy demonstration projects.

125 In addition to the party wall cavity bypass, we have identified several other important factors that gave rise to higher than expected heat loss from the test dwellings. These included for example

[11] Many walls in the earlier part of this period were built with cavities below loft floor level only, with solid walls above the loft floor. In addition, some cavities would have been closed at junctions with external walls.

higher than predicted thermal bridging, missing insulation and other construction defects. It is recommended that improvements to quality control procedures would help eliminate some of theses issues. It is also suggested that the use of built-in mineral wool batts instead of retro-filled blown fibre insulation would improve the thermal performance of the external walls. It should also be borne in mind that many of the buildability and quality issues observed at Stamford Brook are inherent in cavity masonry construction and would likely be avoided or minimised in other construction forms such as externally insulated masonry or factory insulated panel systems.

Acknowledgements

The Stamford Brook project is funded/resourced by the Department for Communities and Local Government (under Partners In Innovation project - CI 39/3/663), the National Trust (land owners) and the developers (Redrow Homes and Bryant Homes) with contributions from The National House Building Council, the Concrete Block Association, Vent-Axia, and Construction Skills. The contribution from all partners is gratefully acknowledged.

The research is led by the Buildings and Sustainability Group in the Centre for the Built Environment at Leeds Metropolitan University in collaboration with the Bartlett School of Graduate Studies at University College London.

The authors wish to thank the National Trust, Bryant and Redrow and all project partners for their continued support.

We would especially like to thank the site management and construction teams from Bryant and Redrow for their help and continued tolerance during the co-heating tests.

References

ANDERSON, B.R. (2006) *Conventions for U-value Calculations*, BR443, 2nd Edition, BRE, Garston, Watford

ATTMA (2006) *Technical Standard 1 - Measuring Air Permeability of Building Envelopes*, downloaded from http://www.attma.org/ATTMA_TS1_Issue_1_March_06.pdf on 12/4/07

BAKER, D. (2007) *Personal Communication,* D. Baker, Chief Executive, Robust Details Ltd., Milton Keynes

BELL, M., SMITH, M. & MILES-SHENTON, D. (2005) *Condensation Risk – Impact of Improvements to Part L And Robust Details On Part C - Interim Report Number 7: Final Report on Project Fieldwork*, Report to the ODPM Building Regulations Division under the Building Operational Performance Framework - Project Reference Number CI 71/6/16 (BD2414), Leeds Metropolitan University, Leeds, UK

BBA (1998) *Agrément Certificate No 89/2396 – Rockwool Cavity Wall Insulation – 4th Issue*, British Board of Agrément, Garston, Watford

BRE (2005) *The Government's Standard Assessment Procedure for Energy Rating of Dwellings – 2005 Edition – v9.8*, BRE, Garston, Watford

BRE (2007) *Best Practice Construction Details – Numerical Modelling Results*, Client Report Number 232185, BRE Scotland, East Kilbride

BONSHOR, R.B. & HARRISON, H.W. (1982) *Quality in Traditional Housing Volume 1: An Investigation into Faults and their Avoidance*, Building Research Establishment Report, London, TSO

DCLG (2006) *Live Tables on Stock - Table 110 Dwelling Stock: Year Built, by Region*, downloaded from http://www.communities.gov.uk/pub/16/Table110_id1156016.xls on 14/5/07

DCLG (2007) *Accredited Details – Masonry Cavity Wall Insulation Illustrations*, downloaded from http://www.planningportal.gov.uk/uploads/br/masonry_cavity_wall_insulation_illustrations.pdf on 16/5/07

DORAN, S.M. & CARR, B.D. (2005) *On Site Inspections and Thermal Insulation Performance*, BRE Client Report Number 15921, BRE Scotland, East Kilbride

HARRISON, H.W. (1993) *Quality in New Build Housing*. BRE Information Paper IP 3/93, Building Research Establishment, Garston, Watford

HARRJE, D.T., DUTT, G.S. & BEYEA, J. (1979) *Locating and Eliminating Obscure but Major Energy Losses in Residential Housing*, ASHRAE Transactions, Volume 85, Part 2, pp 521-534

HARRJE, D.T., DUTT, G.S. & GADSBY, K.J. (1985) *Convective Loop Heat Losses in Buildings*, in Proceedings of Thermal Performance of the Exterior Envelopes of Buildings III, Clearwater Beach, Florida, 1985, ASHRAE, pp 751-760

JOHNSTON, D., MILES-SHENTON, D., BELL, M. & WINGFIELD, J. (2004) *Airtightness of Buildings: Towards Higher Performance - Interim Report Number 5: Site Assessments & Feedback Material*, Report to the ODPM Building Regulations Division under the Building Operational Performance Framework - Project Reference Number CI 61/6/16 (BD2429), Leeds Metropolitan University, Leeds, UK

JOHNSTON, D., MILES-SHENTON, D., & BELL, M. (2005) *Airtightness of Buildings: Towards Higher Performance - Interim Report Number 8: Site Assessments & Test Results*, Report to the ODPM Building Regulations Division under the Building Operational Performance Framework - Project Reference Number CI 61/6/16 (BD2429), Leeds Metropolitan University, Leeds, UK

LBNL (2003) *THERM 5.2 Finite Element Simulator - Version 5.2.14*, Lawrence Berkeley National Laboratory, Berkeley, California, USA, downloaded from http://windows.lbl.gov/software/therm/therm.html on 5/4/06

LOWE, R.J. (2006) *Domestic Ventilation Model Spreadsheet v3*, Bartlett School of Graduate Studies, University College London, London

LOWE, R.J., WINGFIELD, J., BELL, M. & BELL, J.M. (2007) *Evidence for Heat Losses via Party Wall Cavities in Masonry Construction*, Building Services Engineering Research & Technology, Volume 28, Part 2, pp 161-181

LOWE, R.J., WINGFIELD, J., BELL, M. & ROBERTS, D. (2007) *Parametric Domestic Energy Model – Version 15.1*, Leeds Metropolitan University, Leeds

MILES-SHENTON, D., WINGFIELD, J. & BELL, M. (2007) *Evaluating the Impact of an Enhanced Energy Performance Standard on Load-Bearing Masonry Construction – Interim Report Number 6 – Airtightness Monitoring, Qualitative Design and Construction Assessments*, PII Project CI 39/3/663, Leeds Metropolitan University, Leeds

NHBC (2006) *New House Building Statistics - 2006 Quarter 3*, NHBC, Amersham, Bucks

ODPM (2004) *The Building Regulations 2000 & The Building (Approved Inspectors etc) Regulations 2000 - Approved Document Part E: Resistance to the Passage of Sound (2003 Edition incorporating 2004 amendments),* Office of the Deputy Prime Minister, London, TSO

ODPM (2005) *Summary Outlining the Barker Response: Factsheet 1*, Office of the Deputy Prime Minister, London, TSO, downloaded from http://www.communities.gov.uk/pub/154/Factsheet1SummaryoutliningtheBarkerresponsePDF44Kb_id1162154.pdf on 23/5/07

ODPM (2006) *The Building Regulations 2000 - Approved Document Part L1A: Conservation of Fuel and Power (New Dwellings) (2006 Edition),* Office of the Deputy Prime Minister, London, TSO

ROBERTS, D., BELL, M. & LOWE, R.J. (2004) *Evaluating the Impact of an Enhanced Energy Performance Standard on Load-Bearing Masonry Construction – Interim Report Number 2 – Design Process*, PII Project CI 39/3/663, Leeds Metropolitan University, Leeds

ROBERTS, D., ANDERSSON, M., LOWE, R.J, BELL, M. & WINGFIELD, J. (2005) *Evaluating the Impact of an Enhanced Energy Performance Standard on Load-Bearing Masonry Construction – Interim Report Number 4 – Construction Process*, PII Project CI 39/3/663, Leeds Metropolitan University, Leeds

ROBUST DETAILS LTD (2005) *Robust Details Part E – Resistance to the Passage of Sound*, Edition 2, Robust Details Ltd, Milton Keynes

ROBUST DETAILS LTD (2006) *Practice Note 1 - Separating Wall - Cavity Masonry*, Robust Details Ltd, Milton Keynes, downloaded from http://www.robustdetails.com/PDFs/Practice_Notes.pdf on 16/4/07

SIVIOUR, J.B. (1994) *Experimental U-Values of Some House Walls*, Building Services Engineering Research & Technology, Volume 15, Part 1, pp 35-36

TAYLOR WOODROW DEVELOPMENTS & BRYANT HOMES (2005) *Construction Specification for Load-Bearing Masonry Homes at Stamford Brook v16*

WINGFIELD, J. (2006) *Minneapolis Blower Door Data Input and Calculation Spreadsheet v15a*, Leeds Metropolitan University, Leeds

WINGFIELD, J., BELL, M., BELL, J. & LOWE, R.J. (2006) *Evaluating the Impact of an Enhanced Energy Performance Standard on Load-Bearing Masonry Construction – Interim Report Number 5 – Post Construction Testing and Envelope Performance*, PII Project CI 39/3/663, Leeds Metropolitan University, Leeds

Appendix 1 - Pre-Publication Draft of BSERT Paper on Party Wall Bypass

(Paper Accepted by Building Services Engineering Research & Technology and published in Volume 28, Part 2, pp 161-181)

Evidence for heat losses via party wall cavities in masonry construction

RJ Lowe[12] MA PhD, **J Wingfield**[b] BSc DPhil MIMMM CEng, **M Bell**[b] DipSurv MSc, **JM Bell**[b] MSci(Phys)

[a]Complex Built Environment Systems Group, University College London, London, UK

[b]Buildings and Sustainability Group, Leeds Metropolitan University, Leeds, UK

Abstract

This paper presents empirical evidence and analysis that supports the existence of a significant heat loss mechanism resulting from air movement through cavities in party walls in masonry construction. A range of heat loss experiments were undertaken as part of the Stamford Brook housing field trial in Altrincham in the United Kingdom. Co-heating tests showed a large discrepancy between the predicted and measured whole house heat loss coefficients. Analysis of the co-heating results, along with internal temperature data, thermal imaging and a theoretical analysis indicated that the most likely explanation for the discrepancy was bypassing of the thermal insulation via the uninsulated party wall cavities. The data show that such a bypass mechanism is potentially the largest single contributor to heat loss in terraced dwellings built to the 2006 revision of the Building Regulations. A comparable convective heat bypass associated with masonry party walls was identified in the late 1970s during the course of the Twin Rivers Project in the United States, albeit in a somewhat different construction from that used at Stamford Brook. A similar effect was also reported in the United Kingdom in the mid 1990s. However, it appears that no action was taken at that time either to confirm the results, to develop any technical solutions, or to amend standards for calculating heat losses from buildings. Current conventions for heat loss calculations in the United Kingdom do not take account of heat losses associated with party walls and it is suggested by the authors that such conventions may need to be updated to take account of the effect described in this paper. In the final part of the paper, the authors propose straightforward solutions to prevent bypassing of roof insulation via party walls by for example filling the cavity of the party wall with mineral fibre insulation, or by inserting a cavity closer across the cavity in the plane of the roof insulation.

Practical Application

The heat bypass mechanism described in this paper is believed by the authors to contribute to a significant proportion of heat loss from buildings in the UK constructed with clear cavities such as those found in separating walls between cavity masonry dwellings. It is proposed that relatively simple design changes could be undertaken to eliminate such heat loss pathways from new buildings. In addition, simple and cost effective measures are envisaged that could be used to minimise or eliminate the bypass from existing buildings. Such an approach could give rise to a significant reduction in carbon emissions from UK housing.

List of Symbols

A_{roof}	*plan area of roof [m^2]*
c_f	*dwelling fabric heat loss coefficient [WK^{-1}]*
c_p	*heat capacity air at constant pressure ≈1000 $Jkg^{-1}K^{-1}$*
c_v	*dwelling ventilation heat loss coefficient [WK^{-1}]*
d	*dwelling plan depth [m]*

[12] Address for correspondence: R Lowe, The Bartlett School of Graduate Studies, 1-19 Torrington Place, University College London, Gower Street, London, WC1E 6BT, UK. Telephone: +44(0)20-76795916, E-mail: robert.lowe@ucl.ac.uk

D_h	*hydraulic diameter [m]*
f	*friction factor*
g	*acceleration due to gravity [ms^{-2}]*
H	*height of cavity [m]*
$h_{loft\ floor}$	*thermal conductance of loft floor [$Wm^{-2}K^{-1}$]*
$h_{roof\ covering}$	*thermal conductance of roof covering [$Wm^{-2}K^{-1}$]*
l_{eave}	*length of eaves [m]*
$l_{party\ wall}$	*length of party walls [m]*
L_{bypass}	*loft bypass heat transfer coefficient [WK^{-1}]*
$L_{loft\ edges}$	*loft edge heat transfer coefficient [WK^{-1}]*
$L_{loft\ floor}$	*loft floor heat transfer coefficient [WK^{-1}]*
$L_{roof\ covering}$	*roof covering heat transfer coefficient [WK^{-1}]*
n	*background ventilation rate [air changes h^{-1}]*
Q	*daily mean heating power [W]*
Q'	*corrected daily mean heating power [W]*
q_{50}	*dwelling air permeability [$m^3/(h.m^2)$ @ 50 Pa]*
R	*effective solar aperture [m^2]*
Re	*Reynolds number*
S	*solar insolation [Wm^{-2}]*
T_{cavity}	*party wall cavity temperature [°C]*
T_{in}	*internal temperature [°C]*
T_{loft}	*loft temperature [°C]*
T_{out}	*external temperature [°C]*
$U_{cavity\text{-}loft}$	*conductance from party wall cavity into loft [$Wm^{-2}K^{-1}$]*
$U_{roof\ effective}$	*effective U-value of roof [$Wm^{-2}K^{-1}$]*
$U_{roof\ notional}$	*notional U-value of roof [$Wm^{-2}K^{-1}$]*
v	*upward speed of air in party wall cavity [ms^{-1}]*
w_{cavity}	*width of party wall cavity [m]*
ΔP_f	*pressure drop due to friction in party wall cavity [Pa]*
ΔP_{stack}	*stack pressure difference [Pa]*
ΔT	*inside-outside temperature difference [K]*
ε	*absolute roughness of party wall cavity [m]*
ρ	*density of air ≈ 1.2 kgm^{-3}*
Ψ_{eave}	*linear thermal transmittance eaves [$Wm^{-1}K^{-1}$]*
$\Psi_{party\ wall}$	*linear thermal transmittance party wall [$Wm^{-1}K^{-1}$]*

1 Introduction

The work described herein was undertaken as part of the Stamford Brook Housing Field Trial[(1)], involving the construction of some 700 dwellings on a site close to Manchester in the North West of England. The Stamford Brook Field Trial has been undertaken as an action research project in a partnership that includes two large housebuilders, Redrow Homes and Bryant Homes (a subsidiary of Taylor Woodrow), the National Trust and Leeds Metropolitan University Buildings and Sustainability Group, with support

from the DCLG[13] and DTI - the departments of state responsible for energy and industrial policy in the UK. The first phase of the project was built to a comprehensive Environmental Performance Standard, developed by the project partners over a period of two years. This resulted in houses with predicted annual CO_2 emissions 5-10% lower than dwellings compliant with the 2006 revision of the Building Regulations for England & Wales[(2,3)].

The houses at Stamford Brook were built in load-bearing masonry construction, with the first dwellings being completed and occupied early in 2005. The monitoring programme began in the autumn of 2005. As well as long term monitoring of occupied dwellings, the test programme included co-heating and pressurisation tests in unoccupied dwellings[14]. The results presented in this paper are based on co-heating tests[15] carried out on two houses in November 2005 and from December 2005 to March 2006. Measurements of temperature in the loft of the first of these houses provided evidence of heat loss significantly in excess of predictions, and measurements of the surface temperature of the party wall provided an initial indication that this discrepancy was associated with the party walls. A review of these initial indications by the Project Advisory Group led to the extension of the second co-heating test.

Results from this second extended test form the core of this paper. The slightly unusual structure of this paper broadly follows the chronology of the empirical and analytical work that was done in uncovering this heat loss mechanism. A full report on the post construction testing is provided in the Stamford Brook project interim report number 5[(4)].

2 Dwelling form and construction

The Stamford Brook development consists of a mix of single storey apartments and two and three storey houses, with the latter predominantly arranged in short terraces. A detailed description of the dwellings is contained in interim reports on the design and construction process[(5,6)]. This section of the paper presents a short summary of the main features of the construction. The two dwellings used during this study were designated as houses A and E[16].

2.1 Walls including party walls

As noted above, walls were load-bearing masonry, with an inner leaf of 100 mm thick medium density blockwork (1400 kgm^{-3}), a 142 mm cavity fully-filled with mineral fibre and an outer leaf of 100 mm thick brickwork. Inner and outer leaves were connected structurally using glass-filled polyester wall ties. The *U* value calculated for this construction[(4)] is approximately 0.23 $Wm^{-2}K^{-1}$.

The primary air barrier in the walls consisted of a sprayed and hand-applied parging layer, approximately 5 mm thick of cementitious material[(7)]. This layer was applied directly to the inside surface of the blockwork before the application of the final surface finish of plasterboard[(7)]. The parging layer was applied to all walls, including party wall and internal masonry partitions. Parging, together with improved detailing throughout the thermal envelope, training and site supervision has led to air permeabilities in the range 1.7 to 9.7 $m^3/(h.m^2)$ @ 50 Pa with a mean of 4.9 ± 1.8. This is less than half the leakage of typical domestic masonry construction in the UK[(8,9)].

Party wall construction is a variant of external wall construction. The party walls consisted of two leaves of blockwork, parged and plasterboarded as described above, separated by a clear, unfilled cavity. This cavity was 142 mm wide in the Bryant houses and 75 mm in the Redrow houses. Its primary purpose is to prevent sound transmission, particularly impact sound transmission across the wall[(10)]. This requires the cavity to be continuous and unbridged. The guidance provided in support of Part L of the Building Regulations for England & Wales[(2,11)] recommends that heat loss across a party wall should be assumed

[13] The Department for Communities and Local Government, previously the Office of the Deputy Prime Minister, ODPM. References produced before the change of name are listed under ODPM.

[14] Difficulties in the recruitment of households have delayed the long term monitoring programme to 2007 but, fortuitously, this has provided the capacity for a more detailed investigation of the party wall heat loss issues discussed in this paper with further co-heating tests (incorporating a more detailed measurements) planned for the winter of 2006/07.

[15] A co-heating test involves electrically heating the inside of a house to a constant temperature over a period of several weeks. Correlation of the measured electrical heat input with external temperature and solar insolation then allows an estimation of the total dwelling heat loss coefficient.

[16] House A is an end-of-terrace house with one adjacent house. House E is a mid-terrace house with two adjacent houses, D and F.

to be zero[17]. This is based on the assumption that the temperatures of adjacent dwellings will be similar. The guidance makes no reference to limiting the flow of external air though the cavity[18]. External and party wall constructions at Stamford Brook are shown in Figure1.

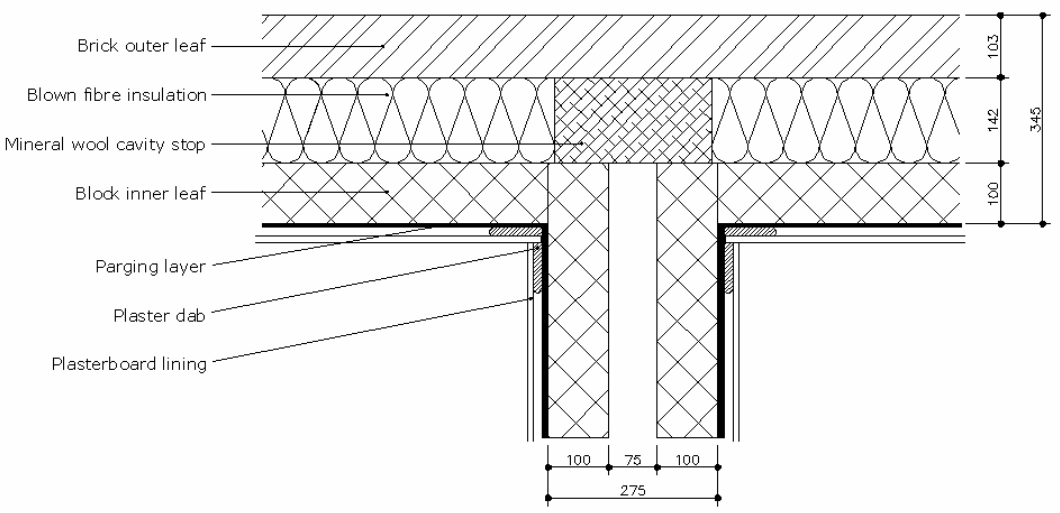

Figure 1 External and party wall construction for house E - Sketch plan section

2.2 Roof Space

The roofs of houses A and E were conventional trussed rafter constructions, insulated with 250 mm of cellulose fibre blown onto the loft floor. The roofs were covered with a low water vapour resistance underlay and interlocking tiles on wooden battens. This construction gives a nominal *U* value of 0.14 $Wm^{-2}K^{-1}$. Party walls rose through the unheated roof void, stopping a few centimetres below the roof membrane. The gap between the membrane and the top of the party wall was fire-stopped with mineral wool. The roof batten space was ventilated with a proprietary over-fascia vent at the eaves. The roof was fitted with a proprietary ridge vent, providing a continuous air path from the roof void to the outside.

2.3 Ground and intermediate floors

Ground floors were concrete slabs cast in-situ on 100 mm of closed cell plastic foam insulation, giving a *U* value of approximately 0.17 $Wm^{-2}K^{-1}$.

2.4 Windows and doors

Windows were double glazed in softwood frames with a nominal whole window *U* Value of just over 1.3 $Wm^{-2}K^{-1}$. The same glazing was used in doors, in addition to insulated opaque panels.

2.5 Dimensions of the co-heating test dwellings

Table 1 and Figures 2 and 3 summarise the form and dimensions of the co-heating test houses.

[17] In the UK, the regulations consist of a broadly framed, performance based, legal requirement supported by detailed technical guidance on compliance. Such guidance is provided by a system of approved documents issued by the Secretary of State. The current methodology for dwelling heat loss calculations is contained in the Standard Assessment Procedure 2005[(12)] which is invoked by regulation 17A and Approved Document L1A[(2)].

[18] The Building Regulations do limit the leakage of air from within each dwelling into the cavity though an overall limit on dwelling permeability.

Table 1 Summary of house form and dimensions

Developer	Plot No.	Form	Gross floor area (m^2)	Volume (m^3)	Plan depth (m)	Plan width (m)	Glazing ratio
Bryant	A	semi-detached, 2 storey, 3 bedroom	73	190	7.7	4.7	0.17
Redrow	E	mid-terrace, 3 storey, 3 bedroom	106	267	6.9	5.1	0.19

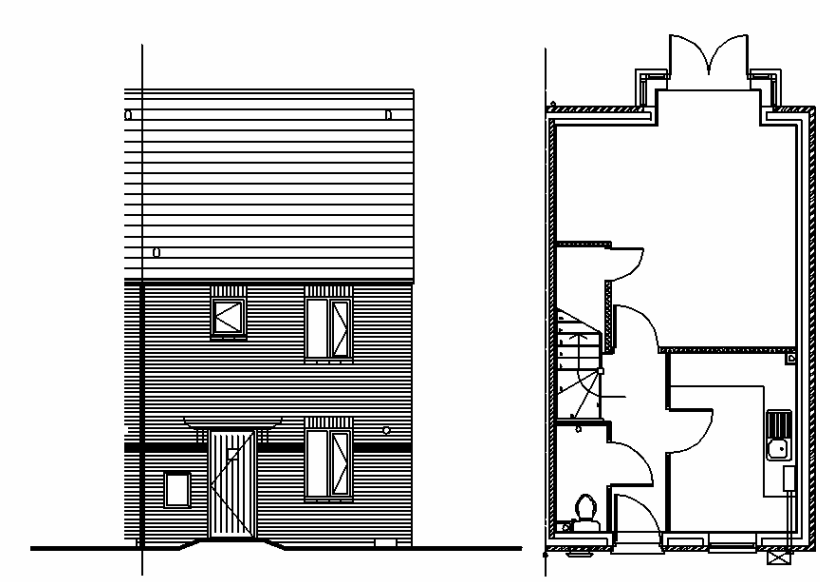

Figure 2 Plan and elevation drawings for house A

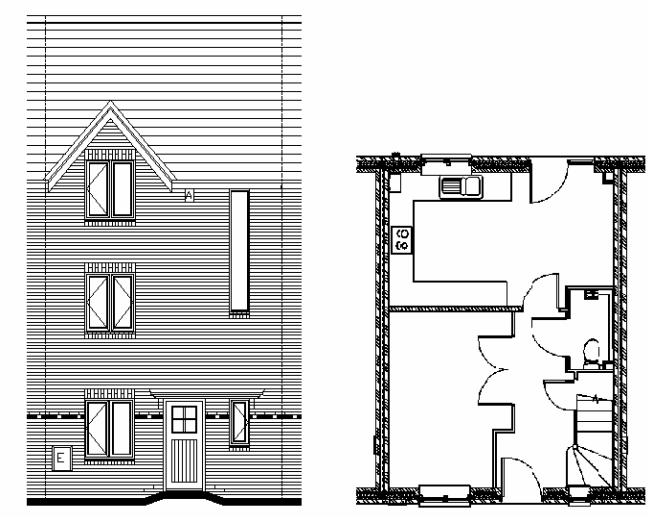

Figure 3 Plan and elevation drawings for house E

3 Methods of investigation

3.1 Co-heating test

A co-heating test involves heating the inside of a house to a constant temperature (typically 25 °C) over a period of at least a week using electrical resistance heaters. Correlation of electrical heat input with external temperature and insolation then allows estimation of the total heat loss coefficient and effective solar aperture. The procedure was originally described by Palmiter et al[13]. A detailed description of the

tests at Stamford Brook is presented by Wingfield et al[4]. A summary of the co-heating test rig is presented in Table 2. The weather station installation at Stamford Brook is described in Table 3. The weather station included instruments for the measurements of external temperature and solar insolation that were required for analysis of the co-heating test data.

Table 2 Co-heating test equipment specification - Dwellings

Component	Equipment Used	Equipment Specification
Datalogger	Eltek RX250 Receiver Logger	250 channel radio receiver logger Set at 10 minute logging interval
GSM Modem	Wavecom M1206B GSM Modem	-
Temperature Sensor	Eltek GC-10 Temp/RH Radio Transmitter	Minimum of 1 per floor
kWh Meter	Schlumberger SPA02	10 Wh pulse output 1 per floor
Pulse Transmitter	Eltek GS-62 Pulse Radio Transmitter	1 per kWh meter
Thermostat	Honeywell T4360B Thermostat	16A load capacity Mounted on a tripod at 1m 1 per kWh meter
Fan Heater	Delonghi THE332-3 3kW Fan Heater	3 kW max heat output 1 per floor
Circulation Fan	Prem-I-Air HPF-4500 Air Circulator	18" fan blade Minimum of 2 per floor

Table 3 Co-heating test equipment specification – Weather station

Weather Station Component	Equipment Used	Specification
Datalogger	Eltek RX250 Receiver Logger	250 channel radio receiver logger Set at 10 minute logging interval
GSM Modem	Wavecom M1206B GSM Modem	-
Temperature/Humidity Gauge	Rotronic Hygroclip S3 External Temperature/Humidity Sensor	Positioned at 2m on 4m mast Protected by Stephenson Radiation Screen
Temperature/Humidity Transmitter	Eltek GS-13 Hydroclip Radio Transmitter	-
Pyranometer	Kipp & Sonnen CM3 pyranometer	Vertical Orientation South Facing Positioned at 3m on 4m mast
Pyranometer Transmitter	Eltek GS-42 Voltage Radio Transmitter	Voltage Range 0-50 mV

3.2 Infra-red survey

A FLIR Systems Thermacam P65 model, with a 320x240 pixel array, a thermal sensitivity of 0.08 at 30 °C and spectral range of 7.5 -13 µm, was used to observe the surface temperatures of the main elements of both test houses during the co-heating tests. Imaging was carried out from both outside and inside the dwelling and also from inside the attic space.

3.3 Direct temperature measurements in party wall cavity

The temperature of the party wall cavity was measured with small datalogging temperature-humidity sensors attached to lengths of wire, pushed through the gap between the party wall and roof, and lowered down into the cavity to a predetermined level as described in section 4.4. The sensors were Tinytag Ultra TGU 1500 dual channel temperature humidity sensors manufactured by Gemini Dataloggers Ltd, with external dimensions 72 mm x 60 mm x 33 mm.

4 Results

4.1 Predicted heat loss coefficients

Ventilation rates n were estimated using a variant of the 1/20 rule-of-thumb:

$$n = 0.85 \,.\, q_{50}/20 \text{ (air changes h}^{-1}\text{)} \quad (1)$$

where 0.85 is an allowance for the protection provided by adjacent and nearby houses.

Air permeabilities were measured before and after the co-heating tests. The results are set out in Table 4.

Table 4 Measured air permeability in co-heating test houses

Plot No.	Permeability before ($m^3/(h.m^2)$ @ 50 Pa)	Permeability after ($m^3/(h.m^2)$ @ 50 Pa)	Increase in permeability ($m^3/(h.m^2)$ @ 50 Pa)	Consequent increase in heat loss coefficient (W/K)
A	3.3	4.2	0.9	0.6
E	5.3	5.9	0.6	0.8

Fabric heat loss coefficients were calculated from element areas and *U* values, junction lengths and linear thermal transmission coefficients. All heat loss coefficients[19] are summarised in Table 5.

Table 5 Estimated heat loss coefficients in co-heating test houses

Plot No.	Ventilation heat loss coefficient c_v (WK^{-1})	Fabric heat loss coefficient c_f (WK^{-1})	Linear thermal transmission included in c_f (WK^{-1})	Total heat loss coefficient $c_v + c_f$ (WK^{-1})
A	13.2	50.6	6.0	63.8
E	20.3	54.9	5.8	75.2

4.2 Predicted versus measured heat loss coefficients

The primary results of the co-heating tests are scatter plots of the heat input needed to maintain a constant internal temperature versus the inside-outside temperature difference. All quantities were averaged over successive 24 hour periods. Figures 4 and 5 show both uncorrected data and data corrected for solar radiation. The corrected daily mean heating power (an estimate of the daily mean heating power at zero insolation[20]) is given by:

$$Q' = Q - R.S \quad (2)$$

[19] The higher-than-normal inside-outside temperature difference during the co-heating tests implies that background ventilation rates and ventilation heat loss coefficients during these tests are likely to have exceeded those in the table. Calculations based on a semi-analytical model of air flow[(14)] suggest that the increase is of the order of 3 WK^{-1} (10%) for the two storey house A and 15 WK^{-1} (27%) for the 3 storey house E.

[20] Note that the correction is only used to improve the graphical presentation of the data. The heat loss coefficient is calculated directly from multiple regression of heating power against ΔT and S.

where R is the effective solar aperture calculated by multiple regressions of daily mean heating power Q against inside-outside temperature difference ΔT and insolation S, with regressions forced through the origin.

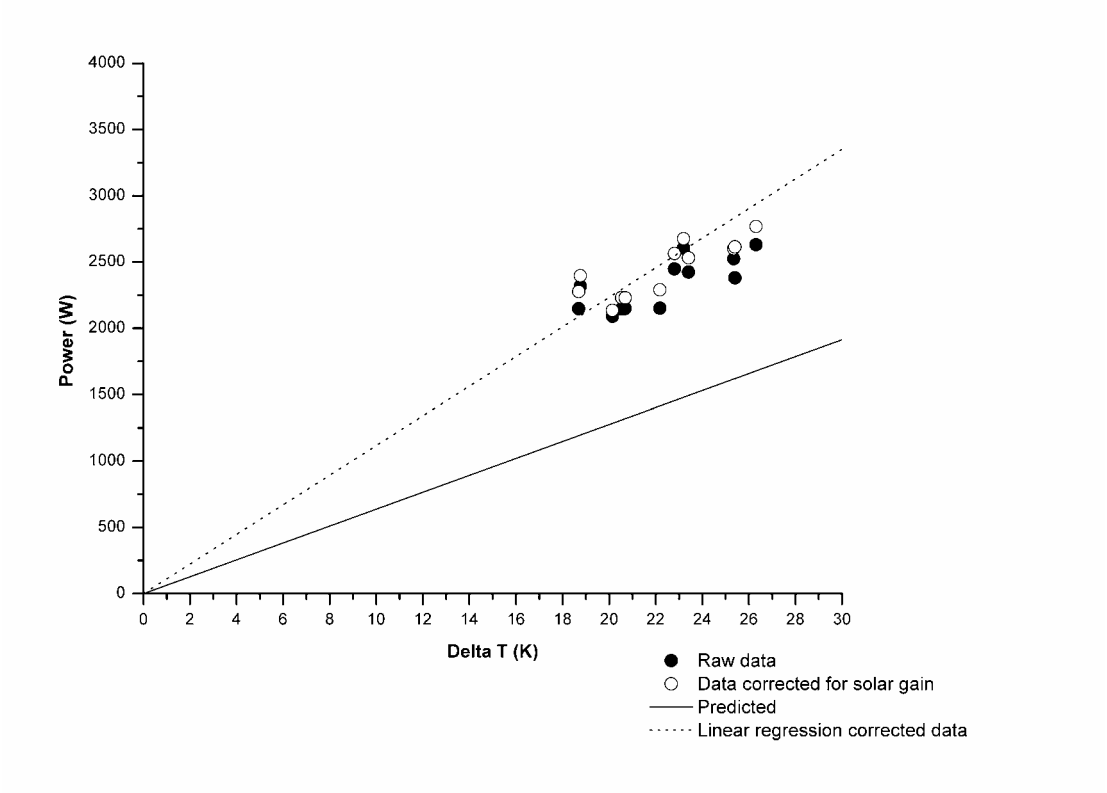

Figure 4 Scatter plot of heating power versus ΔT for house A (24 hour averages)

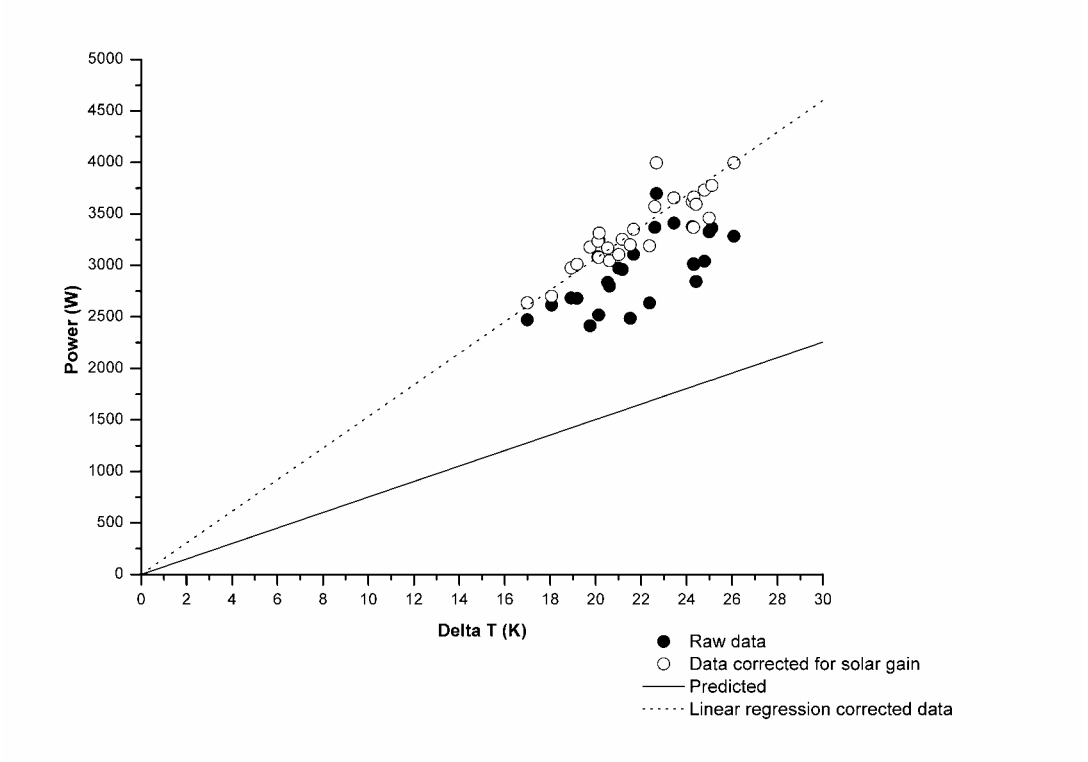

Figure 5 Scatter plot of heating power versus ΔT for house E (24 hour averages)

The results of these regressions are summarised in Table 6 below. It is apparent both from Figures 4 and 5 and from Table 6 that measured heat losses were higher than calculated. In the case of house E, the excess heat loss was between 1400-2000 W over the period shown.

Table 6 Comparison of predicted and measured heat loss coefficients

Plot No.	Predicted heat loss coefficient (WK^{-1})	Measured heat loss coefficient (WK^{-1})	Difference between predicted and measured (WK^{-1})
A	63.8	111.7 ± 5.9	47.9 (75%)
E	75.2	153.4 ± 3.3	78.2 (103%)

The calculated house-to-house *U* value of the party wall is 1.1 $Wm^{-2}K^{-1}$. With a temperature difference of approximately 5 K between house E and the adjacent dwellings, the predicted house-to-house heat flow would be of the order of 600 W. This is insufficient to explain the observed discrepancy between predicted and measured heat loss from house E during the co-heating test.

4.3 Surface temperatures of party walls in lofts

As noted earlier the first indication of anomalous behaviour in the test houses came from infra-red images of the party wall in house A. However, the clearest images were from house E. Some of these are shown below in Figures 6 and 7.

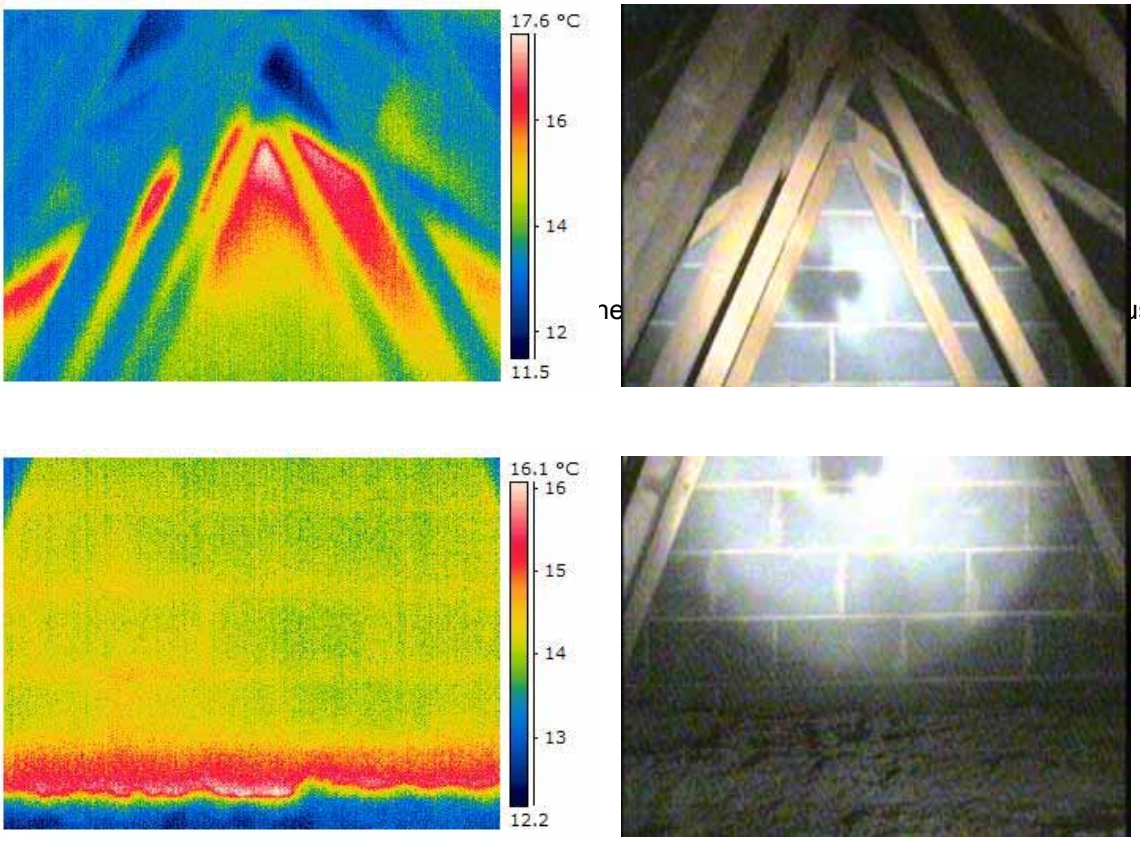

Figure 7 Infra-red and visible spectrum images of the bottom of party wall E-F taken in the loft of house E, with external temperature in the range 3-5ºC

The key features of these images are:

- the presence of a high temperature strip at the bottom of the wall, immediately above the insulation layer (Figure 7) – this is consistent with the thermal bridge between loft space and the room below, caused by the blockwork bypassing the insulation on the loft floor;

- surface temperatures in the range 13-14 ºC in the middle part of the triangle of blockwork – this was wholly unexpected;
- temperatures of around 17 ºC in the top metre or so of the wall – again wholly unexpected;
- the higher temperature of mortar joints compared with surrounding blockwork, seen particularly clearly in Figure 7.

Similar images were obtained for the other party wall in this loft (E-D).

4.4 Extended time series including loft and party wall cavity temperatures

The final broad category of empirical evidence is provided by extended time series data including temperatures in the loft void and in the party wall cavity. The main extended data set consists of the following measurements made at ten minute intervals over an 11 day period from 9 - 19 February inclusive:

- inside temperature;
- outside air temperature and insolation;
- the temperature in the loft void of test house E just above the insulation then at 1.0 m and1.5 m from the top of the insulation together with single point temperature in the loft of house F for 4 days from 16 to 19 February;
- temperatures in the cavity of the party wall separating houses E & D and E & F, at 0.5 m below insulation level and 1.0 m above.

Measurements were accompanied by further infra-red imaging. The daily mean temperatures over the 11 days are shown in Figure 8.

The data from the three temperature sensors in the loft of house E indicate temperature stratification, with a tendency to higher temperatures towards the top of the loft with a mean of 15.1 °C at 1.5 m above the ceiling, 12.7 °C at 1.0 m and 11.7 °C at 0.25 m. Over the eleven days the degree of stratification tended to decrease as the mean temperature in the loft increased.

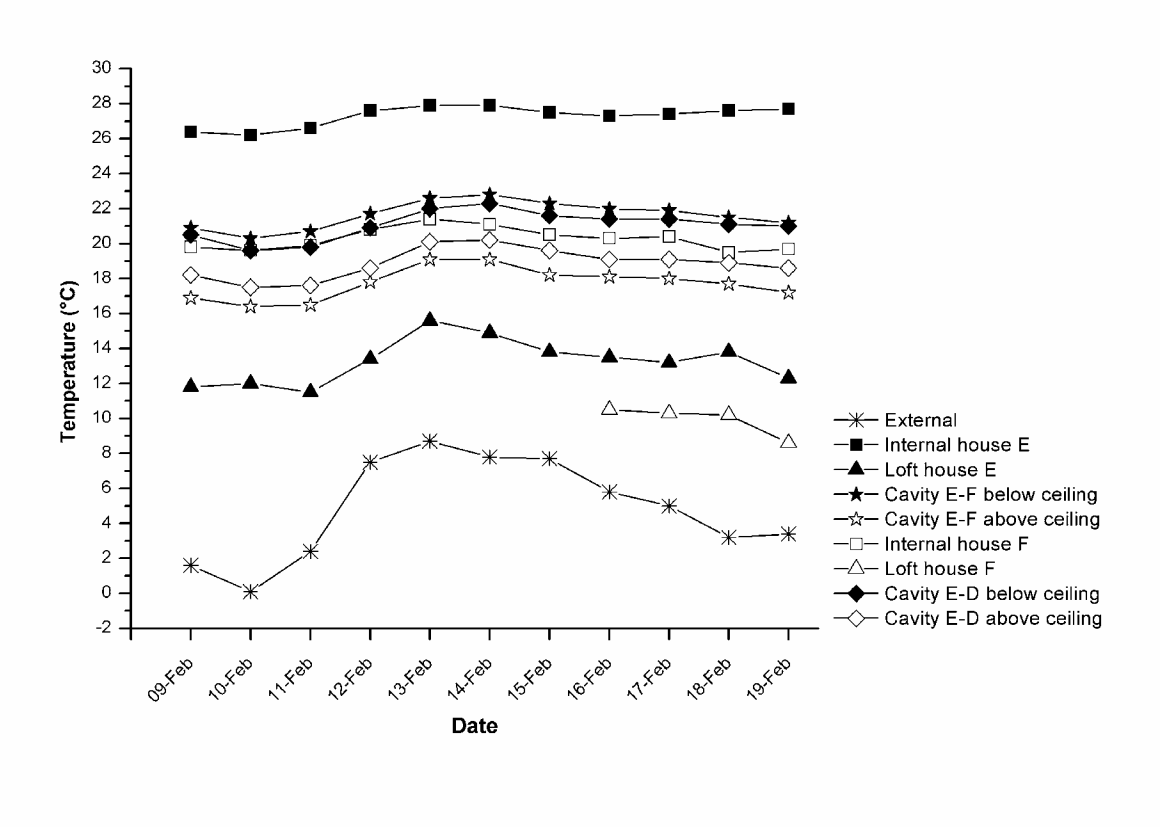

Figure 8 Extended temperature measurements in house E

The key features of these results are:

Temperatures generally were steady[9]. Loft temperature followed external air temperature closely and was largely unaffected by variation in insolation (e.g. 10 - 12 February).

Following stabilisation of the internal temperature at around 27 °C, the attic space was, on average between 8 K and 9 K warmer than the outside temperature over the test period (mean external temperature = 4.8 °C). This difference is larger, by a factor of around 8, than the 1.1 K that would be predicted on the basis of a simple model of heat transfer described below. It should be noted also that the mean loft temperature in house F for the four days at the end of the monitoring period (9.9 °C) was some 3 K lower than over the same four days in house E. This is consistent with the fact that house F is an end-of-terrace with only one party wall, while house E has two party walls.

The mean temperatures inside the attic party wall cavities ranged from some 21 °C below insulation level to 18 °C above the insulation level over the measurement period. The temperature difference between the cavity and the dwellings adjacent to house E would be associated with a heat flux of at most 500 W. House-to-house heat flux therefore accounts for less than one quarter of the difference between measured and predicted heat loss from house E and fails completely to explain the observed loft temperature excess.

The high temperatures and temperature gradient in the cavity are consistent with an upward flow of warm air, heating the loft space via conduction through the leaves of blockwork and by the movement of warm air through gaps in the blockwork and through the junction between the party wall and the roof. The observed temperatures are broadly in line with both the infra-red data (Figures 6 and 7) and a set of preliminary measurements taken in the party wall between dwellings E and F.

5 Analysis and discussion of possible physical mechanisms

The results set out above suggest that the roof insulation in the co-heating test houses was being bypassed by heat flowing up the cavities of the party walls. The purpose of this section of the paper is to analyse the data in more detail to see whether it supports the thermal bypass model.

5.1 Comparison of expected and measured temperatures in the loft

Figure 9 shows two simple models of heat flows between the inside and the outside of a dwelling through the loft.

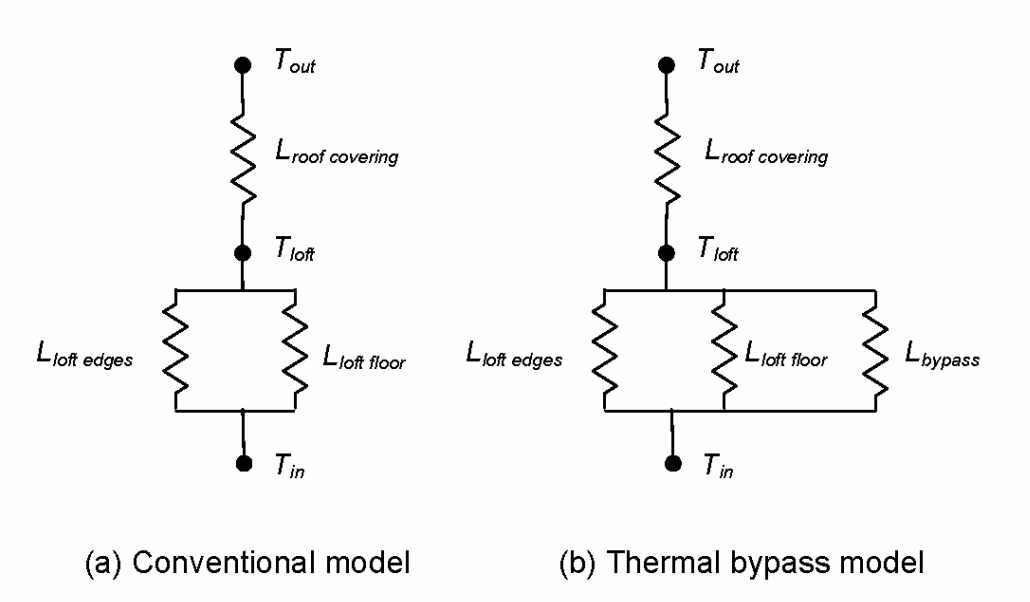

Figure 9 Simple models of heat flows through loft (assuming no heat transfer between dwellings)

Approximate values of the heat transfer coefficients are presented below:

$$L_{roof\ covering} = A_{roof} \,.\, h_{roof\ covering} \approx 35.2 \times 4.2 \approx 147 \qquad (3)$$

$$L_{loft\ floor} = A_{roof} \,.\, h_{loft\ floor} \approx 35.2 \times 0.14 \approx 5.0 \quad (4)$$

$$L_{loft\ edges} = 2 \,.\, (l_{eave} \,.\, \Psi_{eave} + l_{party\ wall} \,.\, \Psi_{party\ wall}) \approx 2 \times (6.9 \times 0.13 + 5.1 \times 0.023) \approx 1.9 \quad (5)$$

Solving the equation implied in Figure 9(a) for T_{loft} we get:

$$T_{loft} \approx T_{out} + (T_{in} - T_{out}) \,.\, (L_{loft\ floor} + L_{loft\ edges}) \,/\, L_{roof\ covering} \quad (6)$$

Using the values for house E (Equations 3, 4 and 5), the loft temperature can be estimated from equation 7.

$$T_{loft} \approx T_{out} + 0.05 \,.\, (T_{in} - T_{out}) \quad (7)$$

The implication of this analysis is that under the conditions during the eleven day period from 9 - 19 February illustrated in Figure 8 (mean T_{in} - T_{out} of 22.5 °C), we would expect the loft temperature to be within 1.1 K of the outside temperature. The fact that loft-outside temperature difference is almost eight times as great is clear evidence of one or more additional heat transfer mechanisms between the inside of the house and the loft. It is worth noting that the predicted loft temperature is strongly influenced by the assumed rate of heat transfer from the loft to outside, $h_{roof\ covering}$. Our estimate for this coefficient, which includes the resistance of the loft void, is taken from BS EN ISO 6946[15]. The actual value is unlikely to be smaller than this[21].

The size of the bypass coefficient L_{bypass} required to explain the observed loft temperature can be estimated. Firstly we will define the temperature difference ratio for the loft:

$$\phi_{loft} = (T_{loft} - T_{out}) \,/\, (T_{in} - T_{out}) \quad (8)$$

$$\phi_{loft} = \frac{1}{\frac{L_{roof\ covering}}{(L_{loft\ floor} + L_{loft\ edges} + L_{bypass})} + 1} \quad (9)$$

$$\phi_{loft} = \frac{(L_{loft\ floor} + L_{loft\ edges} + L_{bypass})}{(L_{loft\ floor} + L_{loft\ edges} + L_{bypass} + L_{roof\ covering})} \quad (10)$$

$$\phi_{loft} \,.\, (L_{loft\ floor} + L_{loft\ edges} + L_{bypass} + L_{roof\ covering}) = (L_{loft\ floor} + L_{loft\ edges} + L_{bypass}) \quad (11)$$

$$(1 - \phi_{loft}) \,.\, L_{bypass} = \phi_{loft} \,.\, (L_{loft\ floor} + L_{loft\ edges} + L_{roof\ covering}) - (L_{loft\ floor} + L_{loft\ edges}) \quad (12)$$

$$L_{bypass} = \frac{\phi_{loft} \,.\, (L_{loft\ floor} + L_{loft\ edges} + L_{roof\ covering}) - (L_{loft\ floor} + L_{loft\ edges})}{(1 - \phi_{loft})} \quad (13)$$

With the observed temperature difference ratio of approximately 0.44

$$L_{bypass} \approx 126 \quad (14)$$

Since the additional heat loss takes place through the roof covering, it is natural to express it as an effective *U* value for the roof. This effective *U* value is given by:

$$U_{roof\ effective} = \phi_{loft} \,.\, h_{roof\ covering} \approx 1.8 \ \mathrm{Wm^{-2}K^{-1}} \quad (15)$$

This is more than an order of magnitude larger than the notional *U* value and a factor of 9 higher than the combined loss through the loft floor and the thermal bridges associated with eaves and junctions between party walls and roof insulation. The additional heat loss increases the total heat loss coefficient of the house by:

$$A_{roof} \,.\, (U_{roof\ effective} - U_{roof\ notional}) \approx 60 \ \mathrm{WK^{-1}} \quad (16)$$

[21] In accordance with this standard, A_{roof} refers to the plan area of the roof.

This is of the same order as the observed discrepancy in the total heat loss coefficient for house E given in Table 6 (78 WK^{-1}).

It is possible to postulate three bypass mechanisms:

- air leaks through the loft floor;
- thermal bridging in addition to that already accounted for in relation to the eaves and party wall-ceiling junctions;
- heat transfer associated with the party wall.

In the case of the first possible mechanism; to account for the whole of the observed bypass coefficient via air leakage through the loft floor, the total flow of air between the upper storey and the loft would have to exceed the expected total background ventilation rate for the house by a factor in excess of 2. However, if half of the exfiltration from the dwelling passed though the roof, this would account for a quarter of the bypass coefficient. We consider it likely, though not certain, that the scale and possible concentration of air leakage paths that would be required to account for the local heating observed would have been detected with the infra-red camera. Similarly, if the second mechanism were to be significant, it is likely that unaccounted for conductive thermal bridging would be detected also in the infra-red images.

We strongly suspect that the first two possible heat loss mechanisms account for part of the observed loft temperature excess. But the empirical evidence for them is weak and indirect and they are unlikely to account for the whole of the excess. We therefore turn to evidence for heat transfer associated with the party wall.

5.2 Evidence for heat flow from the party wall into the loft

The observation (Figure 7) that temperature of mortar in the party wall in the loft space was higher than the temperature of the surrounding blockwork is direct qualitative evidence that the direction of heat flow is from the cavity into the attic. This is because the conductivity of the mortar is roughly 50% higher than that of medium density concrete blocks (0.9 compared with 0.5 $Wm^{-1}K^{-1}$). Based on the observed temperatures in the loft and party wall cavity and the calculated heat transfer coefficient through one leaf of blockwork, we estimate the total rate of conduction of heat into the loft space from both party wall cavities above the plane of the loft floor to be in the region of 50 WK^{-1}, where the driving temperature difference is given approximately by:

$$\tfrac{1}{4}\left(T_{in\,D} + 2.T_{in\,E} + T_{in\,F}\right) - T_{loft} \qquad (17)$$

where:

$T_{in\,D}$, $T_{in\,E}$ and $T_{in\,F}$ are the internal temperatures of houses D, E and F.

This accounts for approximately 40% of the observed bypass coefficient. We therefore seek an additional heat transfer mechanism from the party wall cavity into the loft.

5.3 Empirical evidence for air flow from the party wall cavity into the loft

Direct evidence for air flow over the top of the party wall and into the loft space is provided by the infra-red images of high surface temperatures in the loft void adjacent to the top of the party wall - these temperatures are close to the temperature of air in the upper part of the party wall cavity itself (Figure 6).

Indirect evidence for air movement up the party wall cavity is provided by:

- the fact that the air in the cavity below the plane of the loft floor is not in thermal equilibrium with the internal temperatures of the houses on either side – the temperature at this point is typically 2 K less than the mean of internal temperatures of the adjacent houses;
- the fact that, above the plane of the loft floor, temperatures in the party wall cavity tend to fall with increasing height;
- the observed stratification in the loft, with higher temperatures at the top, suggesting a warm air input into the loft void.

The presence of a gap connecting the top of the cavity directly to the loft void is crucial to this argument. It was not possible to measure the width of this gap directly, but it is clearly at least as wide as the Tinytag sensors (smallest dimension 33 mm) that were passed through it to measure temperatures in the cavity. Given that there is an equal gap on each side of the party wall, the total cross section of gap from the

cavity into the lofts on either side is not appreciably smaller than the width of the cavity itself. The air flow path at this point is only blocked by the mineral wool firestopping, which is not an effective air barrier[16]. Once the air reaches the top of the party wall cavity, it is likely that most passes into the loft void. The continuity of the roof membrane across the party wall will prevent direct leakage to outside.

The rate of fall of temperature in the upper part of the party wall cavity can be used to estimate the speed of air moving up the cavity. Here we assume that convective flows within the cavity are weak and that air flow in the cavity is uniformly upward. Temperature in the cavity will fall as heat is conducted through the blockwork into the lofts on either side of the wall. The upward speed of air in the cavity is then given by:

$$v = \frac{U_{cavity-loft}.\left(\left(T_{cavity} - T_{loft\ D}\right) + \left(T_{cavity} - T_{loft\ E}\right)\right)}{w_{cavity}.c_p.\rho.\frac{dT_{cavity}}{dz}} \qquad (18)$$

The rate of fall of temperature in the upper part of the party wall cavity, under the conditions of the co-heating test, is approximately 0.8 Km^{-1}. With $U_{cavity-loft} \approx 2.4$ $Wm^{-2}K^{-1}$

and

$w_{cavity} \approx 0.075$ m

we deduce that air moves up the party wall cavity at approximately 0.4 ms^{-1}.

The mass flow up each cavity is assumed to split equally between adjacent lofts. Where, as in house E, a house has two party walls, the total volume flow into the loft is in the order of $d.w_{cavity}.v \approx 0.15$ m^3s^{-1}, where d is the depth of the house plan, 6.9 m.

The accompanying heat flow is somewhat more difficult to estimate. The temperature of air flowing into the loft was measured, but the temperature of air flowing out of the loft was not. If we assume that the quantity that we have referred to as $T_{loft\ E}$ represents the temperature of outflowing air, then:

$$Q \approx c_p.\rho.d.w_{cavity}.v.\left(T_{cavity} - T_{loft}\right) \approx 820 \text{ W} \qquad (19)$$

The corresponding bypass heat transfer coefficient is given by:

$$\frac{Q}{\frac{1}{4}\left(T_{in\ D} + 2.T_{in\ E} + T_{in\ F}\right) - T_{loft}} \approx 78 \text{ WK}^{-1} \qquad (20)$$

Together with the 50 WK^{-1} derived earlier for conduction through the blockwork of the party walls into the loft, we have identified mechanisms that account for the whole of the 126 WK^{-1} bypass coefficient needed to explain the observed loft temperature excess. That most of this depends on air flow up the cavity requires us next to analyse the forces that might produce such a flow.

5.4 Analysis of bulk air movement in party wall cavity

The steadiness of the temperatures plotted in Figure 8 suggests that wind forces are not the primary driving force. The only other possibility is the stack pressure difference:

$$\Delta P_{stack} \approx \rho.g.H.\left(T_{cavity} - T_{out}\right)/\left(T_{out} + 273\right) \approx 4 - 6 \text{ Pa} \qquad (21)$$

The corresponding air flow path would be:

- infiltration through the outer leaf of the external wall into the external wall cavity;
- movement past the firestopping at the junction of external wall and party wall cavities, into the latter;
- movement up the party wall cavity;
- movement through the firestopping at the top of the party wall into the loft.

Each of these stages will generate a resistance to flow. The easiest to analyse is movement up the party wall. This is a 2-dimensional problem, but to make progress we will assume this flow to be 1 dimensional.

The ASHRAE Handbook[17] section 34 gives the pressure drop due to friction in a duct as:

$$\Delta P_f \approx \left(f.L/D_h\right).\tfrac{1}{2}\rho.v^2 \text{ Pa} \qquad (22)$$

where:

Re is the Reynold's number $\approx 66400.D_h.v$

f is the friction factor $\approx 0.11\left(\varepsilon/D_h + 68/\text{Re}\right)^{0.25}$ for the given range of Re

L is the length of the equivalent duct

ε is the absolute roughness

For flow in the party wall cavity

$D_h \approx 2.w_{cavity} = 0.15$ m

$L \approx H = 7.5$ m, and

$\varepsilon \approx 0.003$ m (a value quoted for concrete ducts[17]; f is relatively insensitive to ε).

On this basis, and with a flow speed of 0.4 ms^{-1}, the pressure drop in the party wall cavity is of the order of 0.2 Pa << ΔP_{stack} .

Resistances associated with the other parts of the system are likely to be higher than this, but are impossible to calculate with any confidence. Based on estimates of the permeability of masonry walls published by Lecompte[18], the pressure drop across the outer leaf and cavity of the external wall appears likely to be the largest, and could amount to 4 or 5 Pa.

If this is the case, then the party wall cavity operates as an isobaric plenum contributing around 2% to the total pressure drop across the system. This in turn implies that the neutral plane in the system is at the top of the party wall and that the pressure difference driving air into the party wall cavity varies approximately linearly with distance below the roof.

The length of the flow path in the party wall cavity from foundation to 2nd floor ceiling in house E is approximately 7.5 m. The corresponding transit time is in the region of 20 seconds. Assuming that air enters the party wall cavity at outside temperature and that the flow is one-dimensional, the temperature of air in the cavity will rise exponentially toward $\overline{T}_{in}$, the mean internal temperature of the adjacent houses:

$$T = \overline{T}_{in} - \left(\overline{T}_{in} - T_{out}\right).\exp\left(-t/\tau\right) \qquad (23)$$

and

$$\phi = 1 - \exp\left(-t/\tau\right) \qquad (24)$$

where:

$$\tau \approx \frac{w_{cavity}.\rho.c_p}{2.U_{house-cavity}} \qquad (25)$$

With $U_{house-cavity} \approx 2.1$ Wm^{-2}K^{-1}, $\tau \approx 22$ s. We would therefore expect the temperature difference ratio in the cavity just below the plane of the loft insulation to be in the region of 0.6. The observed temperature difference ratio is approximately 0.89.

5.5 Effective party wall *U* value

There are a number of different ways of stating the additional heat loss at Stamford Brook. We have already noted that the effective roof *U* value in house E is approximately 1.8 Wm^{-2}K^{-1}. Given that the main thermal bypass mechanism appears to be associated with the party walls, the additional heat loss can also usefully be expressed as an effective party wall *U* value. House E has an extra heat loss of some 60 WK^{-1} (Equation 16) and a total party wall area of 100 m^2 (counting both party walls). The effective single-sided party wall *U* value is therefore approximately 0.6 Wm^{-2}K^{-1}.

6 Relationship to earlier work

We have found three earlier pieces of work of relevance to this study. The first is a study of heat loss though insulated roofs reported by Anderson[19]. This study involved measurements of heat flow, temperatures and heat fluxes in the roof of a two storey terraced house. Part of the roof was insulated with 80 mm and part with 100 mm of glass fibre between joists. For the purposes of this paper, the key result was:

"…a satisfactory agreement between measured and predicted heat loss, indicating that the standard calculation procedure gives a *U* value which represents a realistic estimate of the actual performance of an insulated roof."

Measured *U* values were in most cases below predicted *U* values due to solar gain. The paper contains no indication of unusually high loft temperatures. Personal communication with Anderson indicates that the terrace was built in the 1970s, and that the party walls were constructed in cavity brick, changing to single brick above loft floor level. The apparent absence of a significant loft temperature excess would be consistent with this construction since the change to a solid wall would close the air bypass route.

The second is a study of experimental *U* values of house walls by Siviour[20]. Siviour measured heat flux through external and party walls using heat flux sensors. The resulting empirical *U* values for party walls ranged from 0.44 to "about 0.85 $Wm^{-2}K^{-1}$". The value measured at Stamford falls into the middle of this range. Siviour also noted that:

"The suggested reason for the heat loss through the party [and internal walls] is the movement of cold air in their cavities. Significant air movement between the loft and the cavity of one of the party walls through incomplete vertical movement joints was detected using a small hand-held smoke generator of the type used in airtightness testing."

The third is the study of energy conservation measures in the North Eastern USA at Twin Rivers[21,22]. This study reported a significant thermal bypass between basements and attics associated with the walls of terraced houses (row houses). These party walls were constructed in single leaf masonry, but the individual clinker blocks from which the party walls were constructed were hollow resulting in a series of continuous vertical slots. Despite partial blockage by mortar, these slots allowed air to flow from the basement into the attics of the houses. The party wall bypass conductance for a mid-terrace house (two party walls) was estimated as 74 WK^{-1} [21]. The Twin Rivers research team was able partially to block the party wall cavities in the plane of the roof insulation and demonstrate that this reduced attic temperatures and overall heat loss: the reduction in the party wall bypass conductance was estimated as 60%. The air flow path in these houses differed from that at Stamford Brook, in that it did not involve a connection with the external wall. Nevertheless the flow was stack driven and its effect on heat loss similar to that observed at Stamford Brook.

Recent investigations of actual *U* values in UK housing[23,24] have reported significant discrepancies between predicted and measured *U* values of external elements, but appear not to have investigated heat losses associated with cavity party walls.

7 Conclusions

This paper has presented empirical evidence of a significant additional heat loss mechanism in terraced and semi-detached housing of masonry construction in the UK. This evidence comes from measurements made in a field trial of otherwise highly insulated mass housing at Stamford Brook in the winter of 2005/6. At its simplest, the evidence consists of observations of high loft temperatures observed during co-heating tests in two houses at Stamford Brook. It is independent of the quality of our subsequent speculation on possible causal mechanisms and is therefore robust.

For the house which was examined in the greatest detail (house E, a three storey mid-terrace house with two cavity party walls), the effect would appear to add almost 60 WK^{-1} to the total heat loss coefficient. This is the largest single heat loss route in this house. It exceeds both the predicted fabric heat loss and the ventilation heat loss and exceeds the heat loss through the windows and doors by more than a factor of 2. The additional heat loss can be expressed as an effective roof *U* value. At 1.8 $Wm^{-2}K^{-1}$ this is more than ten times higher than the notional roof *U* value.

We conclude that the roof insulation is being bypassed by one or more heat transfer mechanisms. The evidence clearly indicates that most of the bypassing is associated with the party walls. The additional heat loss can therefore usefully be expressed as an effective party wall *U* value. The effective single-sided party wall *U* value is approximately 0.6 $Wm^{-2}K^{-1}$ - more than twice the calculated external wall *U* value in these houses. Direct measurements of air speeds in the party wall cavity were not made, but a

variety of indirect evidence and analysis indicates that most of the bypass heat flow is associated with stack driven air movement in the party wall cavities.

An obvious implication of this result is that heat loss from terraced houses at Stamford Brook is significantly higher than for detached houses of the same basic design. We do not know what proportion of the UK housing stock is affected by this mechanism, because the construction of masonry party walls has varied over the years. Party walls in the solid-walled stock are invariably of solid construction. Even in cavity walled construction, until the 1960s, it was not uncommon for party walls in loft spaces and gables to be solid. It is clear that the relative importance of the effect is greatest in dwellings built to the most recent energy performance standards which have resulted in significant reductions in fabric heat loss compared to the housing stock as a whole.

The most reliable estimates of stock mean internal temperature in UK dwellings are based on estimates of delivered energy input, space heating system efficiency and utilisation of free heat gains over the heating season are due to Shorrock & Utley[25]. Errors in specific heat loss will therefore have led to overestimates of mean internal temperature in house types with cavity party walls. Semi-detached dwellings are the easiest group to analyse in this respect, since most have been built since the advent of party wall construction. Shorrock's & Utley's estimate of the mean heat loss of this group in 2001 was 276 WK^{-1}, and their estimate of the stock mean heating season internal temperature was 19 ºC. Assuming that each such dwelling had 40 m^2 of cavity party wall with an effective *U* value of 0.6 $Wm^{-2}K^{-1}$, the internal temperature in this group will have been overestimated by approximately 0.8 ºC. This is not so large a source of error that it would have been detected by comparison with spot measurements of internal temperature or with the limited stock of continuously monitored dwelling temperatures. It may, however, be significant in the context of arguments about trends in internal temperatures in UK housing.

It would be straightforward to prevent bypassing of roof insulation by party walls: for example by filling the cavity of the party wall with mineral fibre, or by inserting a flexible membrane or plastic sleeved cavity closer across the cavity in the plane of the roof insulation. Before widespread implementation, it would be crucial to confirm empirically the efficacy of such measures and their impacts on buildability and acoustic performance.

The identification and approximate quantification of this heat loss mechanism has emerged shortly after the publication of the 2006 amendment to Part L of the Building Regulations and its supporting documentation. In the UK context it is therefore fortunate that we can see no need to amend the new regulations. Amendment is however likely to be required in BS EN ISO 6946[6], the SAP 2005[12], the BR 443 conventions for calculating *U* values[26], the conventions used in the calculation of the Dwelling CO_2 Emission Rate[2,12] and in supporting documentation for the system of accredited construction details that forms part of the wider regulatory framework for building energy performance in the UK.

The most important remaining scientific questions relate, in our view, to the nature of the air flow in the external wall and party wall cavities. We have estimated the speed of air flow in the cavity based on measured temperatures and on the assumption that flow is uniform, and have discounted the possibility of one or more convective loops within cavity. A full understanding of the observed phenomena requires direct simultaneous measurement of temperature and flow fields in both cavities. It is anticipated that the further work at Stamford Brook scheduled for the winter of 2006/07 will help to clarify these and other important issues.

Acknowledgements

The authors acknowledge the support of their partners in the Stamford Brook Project, National Trust, Redrow Homes, Bryant Homes/Taylor Woodrow, Vent Axia, CITB, NHBC and the Concrete Block Association. The authors particularly acknowledge the positive cooperation of both developers and the forbearance and goodwill of the occupants of the dwellings adjacent to the test houses throughout the work described here. The authors also acknowledge the cooperation of the Bartlett School of Graduate Studies, led by Prof Tadj Oreszczyn, which resulted in the loan, at short notice, of a high resolution infra-red camera.

The Stamford Brook project is funded by the project partners and the DTI and DCLG under the Partners in Innovation Programme (Contract CI 39-3-663)

References

1 Lowe RJ & Bell M. *Evaluating the Impact of an Enhanced Energy Performance Standard on Load-Bearing Masonry Domestic Construction, Partners in Innovation CI 39/3/663, Project Implementation Plan*. Leeds: Centre for the Built Environment, Leeds Metropolitan University, 2002.

2 ODPM. *Building Regulations Approved Document L1A: Conservation of Fuel and Power in New Dwellings*. London: ODPM, 2006. http://www.odpm.gov.uk/ (accessed 31 May 2006).

3 Lowe RJ & Bell M. *A Trial of Dwelling Energy Performance Standards for 2008: Prototype standards for energy and ventilation performance*. Leeds: Centre for the Built Environment Leeds Metropolitan University, 2001.

4 Wingfield J, Bell M, Bell JM & Lowe RJ. *Evaluating the Impact of an Enhanced Energy Performance Standard on Load-Bearing Masonry Domestic Construction, Partners in Innovation CI 39/3/663, Interim Report Number 5 – Post Construction Testing and Envelope Performance*. Leeds: Centre for the Built Environment, Leeds Metropolitan University, 2006.

5 Roberts D, Bell M & Lowe RJ. *Evaluating the Impact of an Enhanced Energy Performance Standard on Load-Bearing Masonry Construction, Partners in Innovation CI 39/3/663, Interim Report No 2 – Design Process*, Leeds: Centre for the Built Environment, Leeds Metropolitan University, 2004.

6 Roberts D, Andersson M, Lowe RJ, Bell M & Wingfield J. *Evaluating the Impact of an Enhanced Energy Performance Standard on Load-Bearing Masonry Domestic Construction, Partners in Innovation CI 39/3/663, Interim Report Number 4 – Construction Process*. Leeds: Centre for the Built Environment, Leeds Metropolitan University, 2005.

7 Roberts D, Johnston D & Isle JA. A Novel Approach to Achieving Airtightness in Drylined Load-bearing Masonry Dwellings, *Building Services, Engineering, Research & Technology* 2005; 26 (1): 63-69.

8 Stephen RK. *Airtightness in UK dwellings*, IP 1/00. Watford: BRE, 2000.

9 Grigg P. *Assessment of energy efficiency impact of Building Regulations compliance*, Client Report 219683. Watford: BRE, 2004.

10 OPDM. *Building Regulations Approved Document E: Resistance to the Passage of Sound*. London: ODPM, 2003. http://www.odpm.gov.uk/ (accessed 31 May 2006).

11 ODPM. *Building Regulations Approved Document L1: Conservation of Fuel and Power in Dwellings*. London: ODPM, 2002.

12 DEFRA. *SAP 2005; The Government's Standard Assessment Procedure for Energy Rating of Dwellings - 2005 edition*. Watford: BRE (Published on behalf of the Department for Environment Food and Rural Affairs), 2005.

13 Palmiter LS, Hamilton LB & Holtz MJ. *Low cost performance evaluation of passive solar buildings*, SERI/RR 63-223. Golden, Colorado: Solar Energy Research Institute, 1979.

14 Lowe RJ. Ventilation strategy, energy use and CO_2 emissions in dwellings - a theoretical approach. *Building Services, Engineering, Research & Technology* 2000; 21 (3): 181-187.

15 BS EN ISO 6946: 1997 *Building components and building elements – Thermal resistance and thermal transmittance – Calculation method*.

16 Carlsson B, Elmroth A & Engvall P. *Air Tightness and Thermal Insulation - Building Design Solutions*. Stockholm: Byggforskningrådet (Swedish Council for Building Research), 1980.

17 *2001 ASHRAE Handbook: Fundamentals*. Atlanta GA: ASHRAE.

18 Lecompte JGN. Airtightness of masonry walls. In: *Proceedings 8th AIVC Conference, Überlingen, DBR*. AIVC, September 1987.

19 Anderson BR. Measurements of the heat loss through an insulated roof. *Building Services Engineering Research & Technology* 1981; 2 (2): 65-72.

20 Siviour JB. Experimental *U*-values of Some House Walls. *Building Services, Engineering, Research & Technology* 1994; 15 (1): 35-36.

21 Socolow R ed. *Saving Energy in the Home: Princeton's Experiments at Twin Rivers*. Cambridge MA: Ballinger, 1978.

22 Harrje DT, Dutt GS & Beyea JE. Locating and eliminating obscure but major energy losses in residential housing. *ASHRAE Transactions* 1979; 85 (2): 521-534.

23 Doran S. *Field investigations of the thermal performance (U-values) of construction elements – as built*, BRE Report 78132. Watford: BRE, 2000.

24 Doran S. *Improving the thermal performance of buildings in practice*, BRE Client Report 222392. Watford: BRE, 2005.

25 Shorrock LD & Utley JI. *Domestic Energy Factfile 2003*, BR457. Watford: BRE, 2003.

26 Anderson BR. *Conventions for U-value calculations*, BR 443, 2nd edition. Watford: BRE, 2006.

Appendix 2 - Co-heating Test Specification

Technical Note - Second Phase Co-heating Test Specification

Sept 2006, Jez Wingfield, Leeds Metropolitan University

1. Introduction

Two further co-heating tests at Stamford Brook are planned for the winter of 2006-2007. This note details the test specification.

2. Test Dwellings

The following plots have been selected for the co-heating tests:

Table 1 - Designated Second Phase Co-heating Test Dwellings

Developer	Plot Numbers	Developer House Type	Dwelling Form	Gross Floor Area (m^2)
Bryant	116, 117	Chatsworth	2-storey Semi-detached	73
Redrow	110, 111	Mendip	3-storey End-terrace (111) Mid-terrace (110)	141

For the initial co-heating tests carried out during the winter of 2005-2006, internal temperature control was limited to the test house only. For the second phase tests the intention is to control the temperature in two adjacent dwellings (a pair from each developer) to enable us to control heat flow across the party wall. One house from each pair of dwellings will be nominated as the “test dwelling”. In the case of the terraced houses plots 110 and 111 the test house will be the end terrace plot 111. The plot adjacent to the test dwelling will be nominated as the “access dwelling” and will house the datalogger and will also be used to access the cavity wall for temperature and air flow measurements.

A cavity sock will be installed horizontally in the party wall between the two adjacent dwellings at the level of the ceiling insulation during construction. The co-heating tests will be carried with and without the cavity sock in position. In order to facilitate easy removal of the cavity sock, several blocks in the party wall in the attic of the “access dwelling” will be constructed with minimum mortar application so that they can be more easily removed to access the cavity sock. A trial installation of a horizontal cavity sock has already been undertaken on a party wall of a Bryant dwelling (between plots 128 &129). No significant problems were reported by the site team during installation. A photograph of the installation is shown in Figure 1.

Figure 1 - Trial Installation of Horizontal Cavity Sock in Party Wall

3. Co-heating Test Equipment

Both the test dwelling and access dwelling will be heated by one 3kW electric fan heater per floor. Each floor will also be equipped by two 18” circulation fans. The total power consumption for the fan heater and circulation fans on each floor will be measured using a pulsed kWh meter with a pulse resolution of 10Wh per pulse.

The temperature of each floor will be separately controlled by an in-line 16A thermostat linked to each fan heater. The nominal target temperature during the co-heating test will be set at 25°C.

Two or more temperature/humidity sensors will be positioned on each floor of both the test dwelling and access dwelling and two temperature sensors will also be placed in the attic of both test dwelling and access dwelling.

The temperature/humidity readings and kWh pulse outputs will be transmitted to a wireless datalogger located in the access dwelling. Data will be logged at an interval of 10 minutes.

4. Party Wall Cavity Temperature Measurement

We have purchased four Eltek thermocouple transmitters to enable us to continuously measure the temperature within the party wall cavity. Each transmitter has inputs for 4 type-K thermocouple probes, giving a total capacity of 16 temperature locations. We have also purchased 16 type-K thermocouple

wires with a length of 5 metres each to allow some flexibility in the location of the temperature probes. The temperature probes will be placed into the centre of the party wall cavity through a series of holes of 10mm diameter which will be drilled into the party wall from the access dwelling side. The proposed location of the 16 temperature sensors and 4 transmitters for the two different dwelling types is shown in the following diagrams.

Figure 2 - Party Wall Cavity Thermocouple Locations - Chatsworth Type

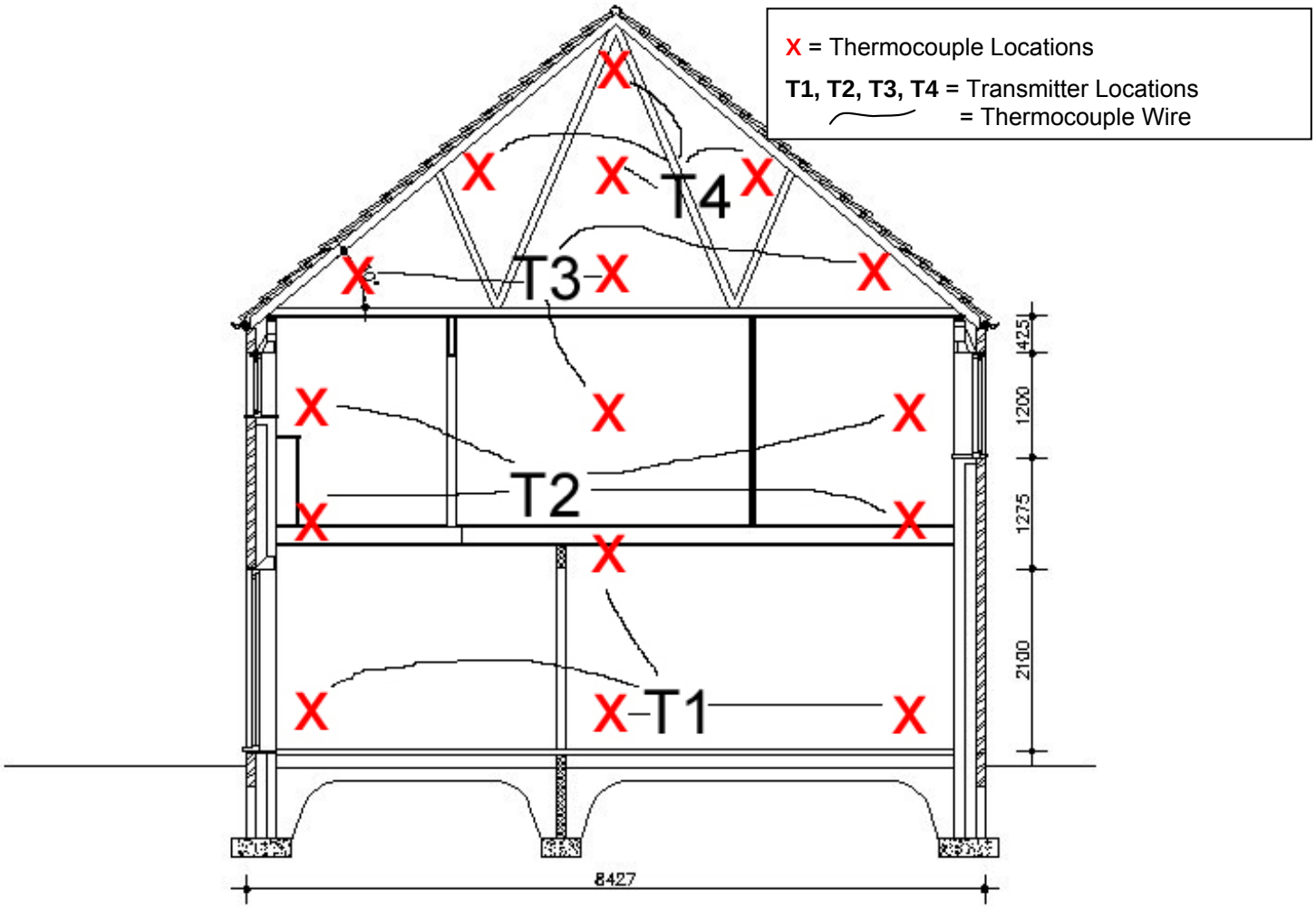

Figure 3 - Party Wall Cavity Thermocouple Locations - Mendip Type

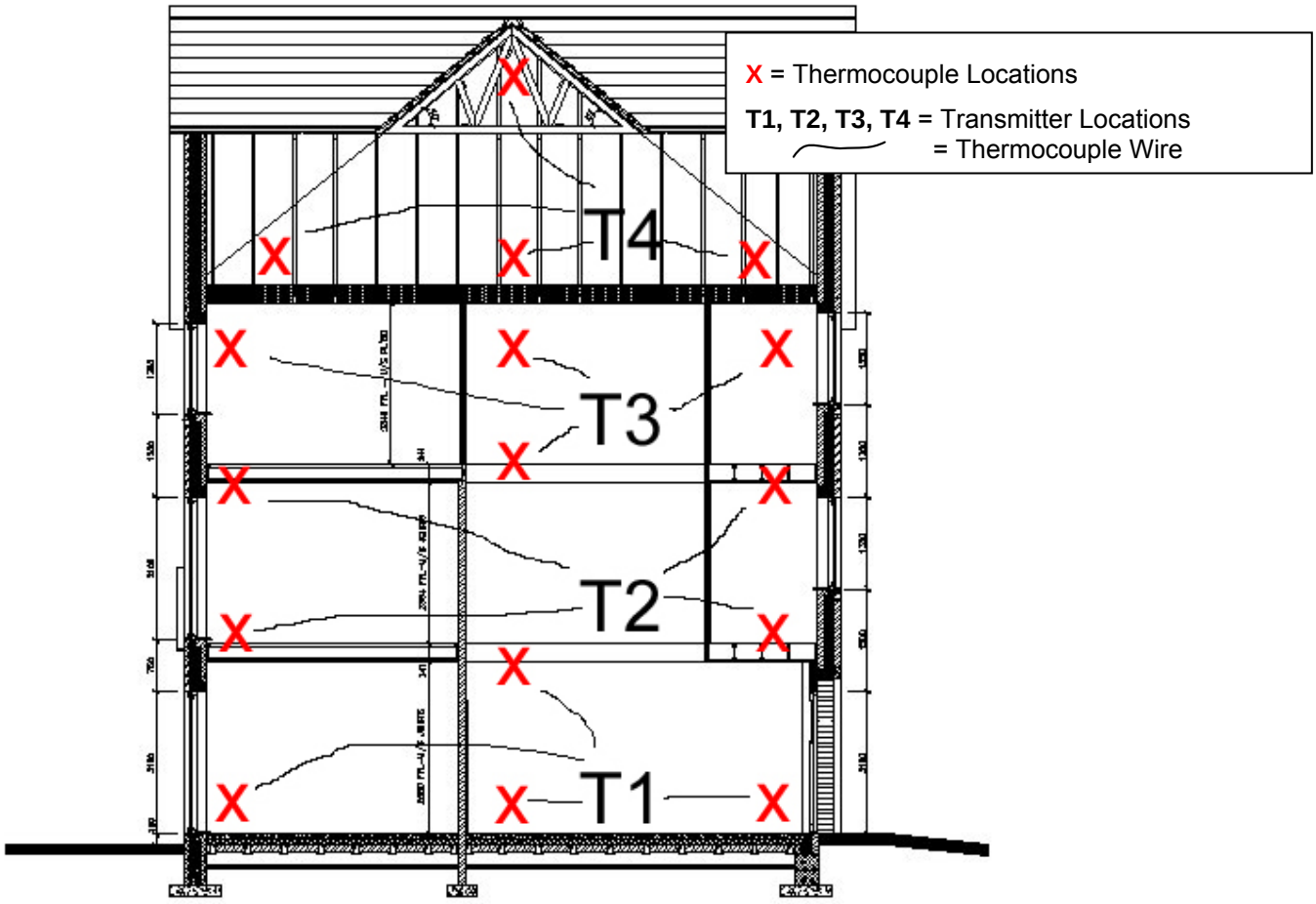

If we notice any significant anomalies in the first test, it may be appropriate to move the location of some of the sensors for the second test.

5. Cavity Air Flow Measurements

Measurements of air flow within the party wall cavity will be taken using a hand-held hot bulb anemometer probe (Air Flow Developments TA35 anemometer). The measurements will be taken via the holes made for the thermocouple sensors. The thermocouple sensors will be removed temporarily during the flow measurements.

The flow measurements will be made in both horizontal and vertical axes by adjusting the direction of the flow orifice on the sensor head.

Flow measurements will be made before commencement of the co-heating test and at regular intervals during the test. In particular tests will be carried out with and without the party wall cavity sock in position.

The external wind speed and wind direction will be recorded on the same days as the cavity air flow measurements.

6. Thermal Camera

An infrared thermal camera will be used to record surface temperatures of the party wall during the co-heating test for both pairs of dwellings. This will be done both with the cavity sock in position and when the cavity sock has been removed. It is proposed to again borrow the FLIR infrared camera from UCL. However, if this is not available at the relevant times then we will hire a suitable camera. We will also inspect the external fabric of all four dwellings during the co-heating tests for continuity of thermal insulation.

7. Airtightness Tests

Pressure tests will be conducted on the test dwelling and access dwelling for both pairs of houses. These will be conducted before and after the co-heating tests. If time allows we may also conduct an inter-dwelling leakage test on one or both pairs.

8. Acoustic Tests

In order to ascertain the effect of the party wall cavity sock on acoustic transmission between the adjacent dwellings, airborne acoustic tests will be conducted on the two sets of dwellings. These will be done with and without the cavity sock in position at the top of the party wall. These tests will be conducted by Leeds Met personnel in accordance with Part E protocols.

9. Weather Station

The external temperature used to calculate the internal-external temperature difference (Delta-T) will be obtained from the Leeds Met weather station at Stamford Brook.

The solar insolation data that will be used to correct the measured heat loss coefficients for solar gain will be obtained from the two pyranometers on the Leeds Met weather station. One of these pyranometers will be orientated vertically and south facing. The second pyranometer will also be orientated vertically but will be rotated to face in the same direction as the main façade of the dwellings undergoing the co-heating test at the time.

10. Observation of Construction Process

Occasional site visits will be made to observe the construction of the test dwellings. These visits will be recorded photographically. The two Bryant plots 116 and 117 are already substantially complete, so we will not have a full record of the construction of these dwellings.

11. Proposed Test Timescales

The proposed test schedule is given in Table 2. This may be subject to change due to changes in the build programme. However, the main limitation on the test programme is the external temperature. In order to maintain a suitable Delta-T it is imperative that co-heating tests on both pairs of dwellings are complete before the middle of March before the mean external temperature gets too high. There is some flexibility in the length of the co-heating tests themselves - but this is very much dependent upon the length of time it takes for the internal temperatures to stabilise at the start of each test.

Table 2 - Proposed Second Phase Co-heating Test Schedule

Target Start Date	Target End Date	Test Dwellings	Test Description
1 Dec 06	1 Dec 06	Bryant 116-117	Pressure Test - Pre-coheating Acoustic Test - Cavity Sock In
4 Dec 06	19 Dec 06	Bryant 116-117	Co-heating Test - Cavity Sock In
20 Dec 06	20 Dec 06	Bryant 116-117	Remove Cavity Sock
21 Dec 06	11 Jan 07	Bryant 116-117	Co-heating Test - Cavity Sock Out
12 Jan 07	12 Jan 07	Bryant 116-117	Pressure Test - Post-coheating Acoustic Test - Cavity Sock Out
29 Jan 07	29 Jan 07	Redrow 110-111	Pressure Test - Pre-coheating Acoustic Test - Cavity Sock In
30 Jan 07	16 Feb 07	Redrow 110-111	Co-heating Test - Cavity Sock In
19 Feb 07	19 Feb 07	Redrow 110-111	Remove Cavity Sock
20 Feb 07	12 Mar 07	Redrow 110-111	Co-heating Test - Cavity Sock Out
13 Mar 07	13 Mar 07	Redrow 110-111	Pressure Test - Post-coheating Acoustic Test - Cavity Sock Out

Appendix 3 - Detailed Description of Co-heating Test Procedure

1 The co-heating test involved heating the inside of each dwelling to a set temperature (typically around 25°C) over a period of at least a week using electrical resistance heaters. The heat loss in W/K could then be determined by measuring the daily electrical energy used to maintain the inside temperature relative to the daily mean difference between the internal and external temperature (delta-T). In order to minimise contributions from other heat loss or heat gain mechanisms during the test, all electrical and heating systems inside the dwelling were turned off (e.g. boiler, heating system, fridge, lights, ventilation fan, etc) and all ventilation system vents and other openings were closed (windows, doors, trickle vents, extract vents, cooker hood etc). In order to maintain an even temperature profile throughout the dwelling, circulation fans were used to mix the internal air. The energy used by the fans was also included in the calculations of energy used to maintain internal temperature. In order to maximise the delta-T value, the co-heating tests were carried out in winter when the external temperatures are lower.

2 During the tests, access to the test dwellings was restricted to a minimum. Where visits were necessary to adjust thermostats or check equipment, these were kept as short as possible and care was taken not to leave outside doors open for longer than necessary and lights were not turned on.

Co-heating Test Equipment and Instrumentation

3 The test equipment and instrumentation used for the co-heating tests at Stamford Brook are listed in Table A1. The Eltek wireless datalogging system allowed for flexibility in the placement of temperature sensors and kWh meters without the need for extensive wiring. Each floor of the test dwelling was equipped with one pulse output kWh meter and a 16A electromechanical in-line thermostat and wireless pulse transmitter. This was done to minimise the load on the electrical system and to allow for temperature control of each floor as a zone. On each floor, the fan heater and circulation fans were connected to the kWh meter via a 4-gang extension lead. Each kWh meter was connected to a mains socket via an RCD socket adapter.

Table A1 - Co-heating Test Equipment Specification

Component	Equipment Used	Equipment Specification
Datalogger	Eltek RX250 Receiver Logger	250 channel radio receiver logger Set at 10 minute logging interval
GSM Modem	Wavecom M1206B GSM Modem	
Temperature Sensor	Eltek GC-10 Temp/RH Radio Transmitter	Minimum of 1 per floor with additional sensors in Attic Space
kWh Meter	Schlumberger SPA02 or Electrex CD1	10 Wh pulse output 1 per floor
Pulse Transmitter	Eltek GS-62 Pulse Radio Transmitter	1 per kWh meter
Thermostat	Honeywell T4360B Thermostat or Sunvic TLM 2253 Thermostat	16A load capacity Mounted on a tripod at 1m above floor level 1 per kWh meter
Fan Heater	Delonghi THE332-3 3kW Fan Heater or Dimplex DLB503 3kW Fan Heater	3 kW max heat output 1 per floor
Circulation Fan	Prem-I-Air HPF-4500 Air Circulator	18” fan blade 2 per floor
Thermocouple	Type K Thermocouple (5m long)	16 thermocouples in party wall cavity
Thermocouple Transmitter	Eltek GS-24 Type K/T Thermocouple Radio Transmitter	4 thermocouples per transmitter

4 In addition to the equipment listed in Table A1, the co-heating test required the collection of external weather data. These were obtained from the Leeds Met weather station located on site at Stamford Brook. The weather measurements needed for the co-heating test were the external temperature and the vertical south facing solar insolation. The external temperature/humidity sensor and pyranometer fitted to the Leeds Met weather station are listed in Table A2. The weather station data were also collected by an Eltek wireless datalogger system.

Table A2 - Leeds Met Weather Station Equipment Specification

Weather Station Component	Equipment Used	Specification
Datalogger	Eltek RX250 Receiver Logger	250 channel radio receiver logger Set at 10 minute logging interval
GSM Modem	Wavecom M1206B GSM Modem	
Temperature/Humidity Gauge	Rotronic Hygroclip S3 External Temperature/Humidity Sensor	Positioned at 2m on 4m mast Protected by Stephenson Radiation Screen
Temperature/Humidity Transmitter	Eltek GS-13 Hydroclip Radio Transmitter	
Pyranometer	2 x Kipp & Sonnen CM3 pyranometers	Vertical Orientation South Facing Positioned at 3m on 4m mast Average taken of readings from the 2 pyranometers
Pyranometer Transmitter	2 x Eltek GS-42 Voltage Radio Transmitter	Voltage Range 0-50mV
Anemometer	Vector Instruments AN1 Anemometer	Wind speed is the mean speed in m/s over the 10 minute logging period
Anemometer Transmitter	Eltek GS-62 Pulse Radio Transmitter	Positioned at 4m on 4m mast

5 The co-heating test equipment is illustrated in Figure A1. This photograph shows the fan heater, kWh meter, pulse transmitter, thermostat and one of the circulation fans in position on the ground floor of one of the test plots.

Figure A1 - Co-heating Equipment on Location in Room in Test Dwelling at Stamford Brook

Testing Procedure

6 The test procedure used for the co-heating tests was as follows:

c) All electrical systems not used during the test were switched off (at the mains switch where applicable). These included the fridge, freezer, heating controls, oven, ventilation fans, cooker hood and all lights.

d) All ventilation extracts or inlets were either closed or sealed with plastic film. These included trickle vents in windows and mechanical extract system vents. It was not necessary to seal the cooker extracts as these were recirculating systems with no external extract.

e) All heating systems such as the gas boiler and immersion tank were turned off.

f) All external openings such as windows, doors and loft hatches were inspected to ensure that they were tightly closed.

g) All traps in sinks, baths, toilets and showers were filled with water.

h) All internal doors were wedged open. These included doors to the cylinder cupboard and built-in wardrobes and cupboards.

i) Each floor in the test dwelling was fitted with a kWh meter which was plugged into a mains socket. For health and safety reasons, the mains circuit was protected with a plug-in RCD socket adapter. The pulse output of the kWh meter was connected to the input of a pulse radio transmitter. A fan heater was connected to the kWh meter via an in-line thermostat mounted on a tripod wired directly to the output of the kWh meter and located centrally on the floor. Two circulation fans per floor were also connected to the extension lead output of the kWh meter and located at appropriate positions in the dwelling to provide good mixing of the internal air.

j) The thermostat on each floor was set initially at between 25°C and 27°C.

k) Between one and two temperature/humidity sensors were positioned on each floor, out of direct sunlight and out of direct line of the fan heater.

l) For the first couple of days of the test, the logged temperatures were observed to ensure that the internal temperatures recorded by all the sensors were increasing to the set point. Once the set point had been reached, observation continued to determine the stability and spread of internal temperature. Where necessary the thermostats on the different floors were adjusted to give an even temperature throughout the dwelling. Where the internal temperatures had drifted slightly from the set point but were stable and even, the test was allowed to continue at the different set point as stability was more important than the actual temperature.

m) Internal temperatures, kWh pulse and external weather data were logged at 10 minute intervals and were downloaded from the loggers by GSM modem on a regular basis.

Appendix 4 - Plan & Elevation Drawings of Co-heating Test Dwellings

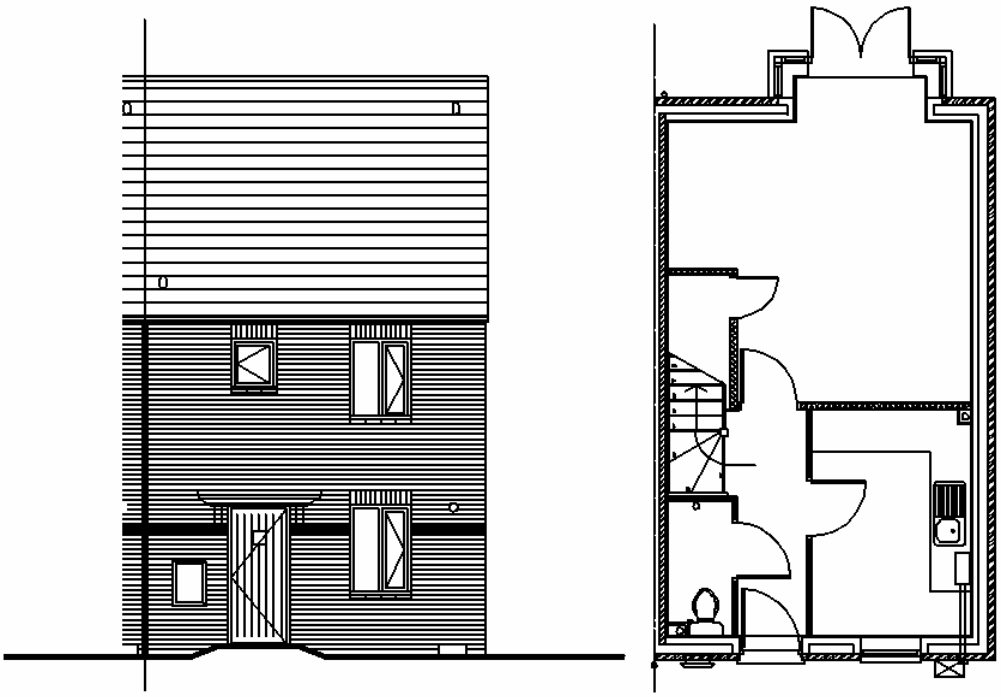

Plan and Elevation - Bryant Chatsworth House Type

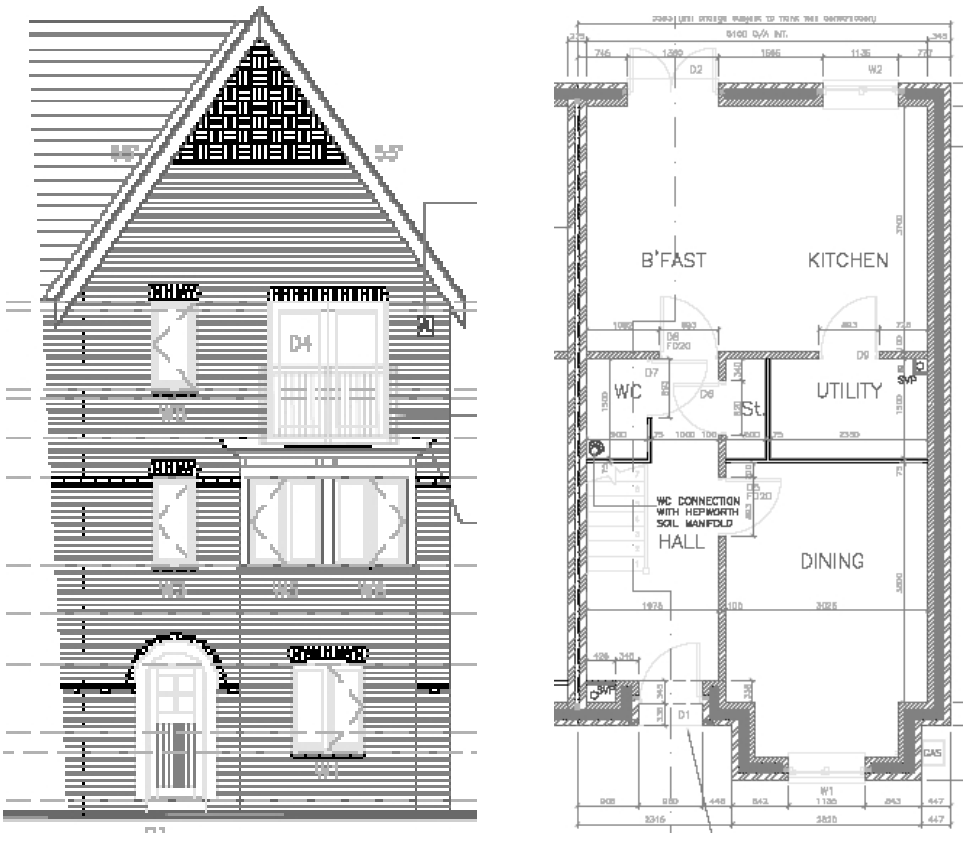

Plan & Elevation - Redrow Mendip House Type